Intelligent Cane Robot for Human Walking Assistance

Pei DI

Intelligent Cane Robot for Human Walking Assistance

Department of Micro-Nano Engineering System

Nagoya University

Pei DI

2013.01.20

Acknowledgements

I am so lucky man that many people help me to accomplish my Ph.D. thesis both in life and research aspects. Firstly I would to express my highest consideration and respect to my motherland-China. This work could never be accomplished without the support of Global COE (Center of Excellent) who supported the scholarship in my Ph.D. course and the COI (Center of Innovation) who also support my and give me a change to continue my research in Nagoya University as a postdoctoral fellow.

One of the important people in my life is Professor Toshio FUKUDA; his is my supervisor from 2008 as I was a master course student. He lead me into the research field of robotics. His sagacious instructions and encouragement making this work possible. Although he retired last years, he try to find time to have meeting to give us a lot of valuable comments. Associate Professor Kosuke SEKIYAMA is another supervisor who lead my work from 2008 till now. I will never forget his rigorous scientific approach.

I would like to express my gratitude to all members of Ph.D. thesis review committee: Professor Fumihito ARAI, Department of Micro-Nano Systems Engineering. Professor Goro OBINATA, School of Engineering Dept. of Mechanical Science and Engineering, and Center for Cooperative Research in Advanced Science and Technology in Nagoya University, Professor Yoji YAMADA of Mechanical Science and Engineering, Graduate School of Engineering, Nagoya University, and Professor Kazuya TAKEDA, Graduate School of Information Science.

Particular thanks to my friend- Associate Professor Jian HUANG of Department of Control Science and Engineering, Huazhong University of Science and Technology. We work together for almost 6 years. He give me many valuable suggestions for improving my research as a mentor. My workmates- Dr. Fei CHEN, Dr. Baiqing SUN, Dr. Hironobu SASAKI and Professor Takayuki MATSUNO, I respect them for cooperation and their remarkable research. In the past 4 years, my team partner Shotaro NAKAGAWA worked with me, his hard-working and meticulous research attitude impressed me.

I appreciate to Assistance Professor Masahiro NAKAJIMA for helping me not only for

research but also in daily life; Associate Professor Yasuhisa HASEGAWA of Department of Intelligent Interaction Technologies at University of Tsukuba, Dr. Zhenhai ZHANG of School of Astronautics Science and Technology at Beijing Institute of Technology for their valuable advices. I thank Professor Tzyh Jong Tarn, and Professor Ning Xi for their valuable comments in the seminar.

I wish to express my appreciation to all of the previous and present faculty and staff members; secretaries- Ms. Akiko TANAKA, Ms. Ai URAGAMI and former secretary Ms. Michiko SHIGEMATSU; Technical assistant, Mr. Hideo MATSUURA, his wonderful skill and support has helped me a lot to take out ideal experiments by fabricating experimental parts. My special thanks to I am also grateful my friends Zhan YANG, Zhenghuan YIN, Xiaojie ZHUANG, Yajing SHEN, Zhiguo Lu, Chaoyang SHI, Chengzhi HU, Tao YUE, Jaehoon JUNG, Huaping WANG, Tao SUN, Zeyang LIU, Yifeng CAI, Pengfei WANG and all the members of laboratory for their support and discussion.

Finally, I wish to express my deep appreciation to my family for their understanding and support. My special thanks to my beloved wife-Jiwen YU who encourage me with love and bright smile. With her company, I accomplished this thesis and finished my study in Nagoya University.

Contents

Acknowledgements iii

Contents vii

List of Figures xii

List of Tables xiii

1 Introduction 1

1.1 Background . . . 2

1.1.1 Aging Society . . . 2

1.1.2 Society Problems . . . 12

1.1.3 Needs of Nursing-Care Robot . . . 13

1.2 Related Works . . . 14

1.3 Motivation . . . 32

1.3.1 Applicable Targets . . . 34

1.3.2 How to define nursing-care level . . . 34

1.3.3 Concepts and Contents . . . 38

1.4 Organization of Thesis . . . 41

2 Human Walking Intention Estimation 45

2.1 Omni-Directional Type Cane Robot . . . 46

2.2 Modeling and Estimation of Human Walking Intention . . . 48

2.2.1 Intentional Direction (ITD) and Its State Model . . . 48

2.2.2 Observation Model of ITD Based on Human-Robot Interaction Force 53

2.3 Walking Intention Based Admittance Control . . . 57

2.4 Experiments . . . 60

2.4.1 Investigating Observation Noise . . . 62

2.4.2 Experiment on Flat Ground . . . 63
2.4.3 Experiment on Slope . . . 66
2.4.4 Experiment on Subject Imitating the Handicapped . . . 66
2.4.5 Experimental Comparison Study . . . 68
2.5 Summary . . . 71

3 Optimized Motion Control for Easing Muscular Fatigue 75
3.1 Introduction . . . 75
3.2 System Configuration . . . 76
3.2.1 Cane Robot with Sensor Group . . . 76
3.2.2 On-shoe Load Sensor . . . 77
3.3 Motion Control Based on Walking Pattern Characteristics of Elderly . . . 79
3.3.1 How to use a cane . . . 80
3.3.2 Proposed algorithm for controlling intelligent cane . . . 82
3.3.3 Experiment Conditions . . . 84
3.3.4 Experiment Result . . . 84
3.4 Summary . . . 86

4 Fall Detection 87
4.1 Introduction . . . 87
4.2 Fall Detection based on Sensor Fusion (*Prototype II*) . . . 88
4.2.1 System Configuration of Cane Robot (*Prototype II*) . . . 89
4.2.2 Data acquisition algorithms . . . 91
4.2.3 Fall Model and Fall Detection . . . 93
4.2.4 Fall Detection . . . 96
4.2.5 Experiments . . . 96
4.2.6 Experiments of Normal Walking . . . 96
4.2.7 Experiment of Fall Detection . . . 97
4.2.8 Summary . . . 97
4.3 Fall Detection based on the ZMP Stability Theory . . . 97
4.3.1 Intelligent Cane Robot System . . . 101
4.3.2 Definitions of stability and instability statuses of human-cane system 103
4.3.3 Sensor configuration . . . 105
4.3.4 Falling detection method based on Fuzzy theory . . . 106
4.3.5 Experiment study . . . 108
4.4 Summary . . . 110

5 Fall Prevention **111**
5.1 Introduction . . . 111
5.2 Fall Prevention for the Elderly (*Prototype III*) . . . 111
5.2.1 Mechanism of cane robot . . . 111
5.2.2 Control Architecture . . . 114
5.2.3 Walking model of human operator . . . 114
5.3 Static Tip-Over Stability Analysis for the Cane Robot (*Prototype IV*) . . . 117
5.3.1 Real-time Posture and Motion Control . . . 118
5.3.2 Simulation for maximum tolerant thrust . . . 124
5.4 Fall and Overturn Prevention Control for Human-Cane Robotic System (*Prototype V*) . . . 127
5.4.1 Introduction . . . 127
5.4.2 Dynamic Model of Human-Cane Robotic System . . . 131
5.4.3 Fall and Overturn Prevention Impedance Control . . . 136
5.4.4 Simulation and Experiment Result . . . 138
5.4.5 Summary and Discussion . . . 139
5.4.6 Summary . . . 139

6 Conclusion and Future Work **143**
6.1 Conclusion . . . 143
6.2 Future Work . . . 144

Bibliography **147**

List of Figures

1.1 An aging world . . . 1
1.2 Current countries with the oldest population in the world. . . . 3
1.3 Current countries with the youngest population in the world. . . . 3
1.4 Median age by country, 2005. . . . 4
1.5 Proportion of elderly population by country(Aged 65 years and over). . . . 5
1.6 Percent of population aged 65 or older, 2050. . . . 7
1.7 Population aging in Japan (1,000 people, %). . . . 8
1.8 Life expectancy at birth . . . 8
1.9 Population pyramids of Japan 1950, 2000, 2050. . . . 9
1.10 Total fertility trajectories of the world and major development groups, 1950-2050. . . . 10
1.11 Declining fertilities in Japan(1947−2008). . . . 11
1.12 Total fertility rates: international comparison(2006−2008). . . . 12
1.13 The 4−2−1 family. . . . 13
1.14 The classification of nursing-care robots. . . . 15
1.15 Cane, Crutches. . . . 17
1.16 Wheelchair. . . . 18
1.17 Track, Trolley. . . . 19
1.18 The elderly works on his balance on the parallel bars with help. . . . 20
1.19 Treadmill Training. . . . 21
1.20 Suspension Device. . . . 23
1.21 Smart Cane. . . . 24
1.22 Smart Walker. . . . 25
1.23 Exoskeleton. . . . 27
1.24 Gait Training. . . . 29
1.25 Mobility Training Device. . . . 31
1.26 Limbs Rehabilitation. . . . 33

1.27 Compared with related works. . . . 35
1.28 The definition of nursing-care levels. . . . 36
1.29 Flowchart to determine the level of SIDE. . . . 38
1.30 To classify the nursing-care level by measuring SIDE, . . . 39
1.31 Research contents of intelligent cane robot - Safety. . . . 40
1.32 Research contents of intelligent cane robot - Assistance. . . . 42
1.33 Research contents of intelligent cane robot - Usability. . . . 42
1.34 Structure of thesis. . . . 43

2.1 Omni-directional type cane robot prototype III. . . . 47
2.2 Concept of intelligent cane robot. . . . 48
2.3 Coordinate system definition of the cane robot. . . . 50
2.4 Quantitative representation of the intentional direction (ITD). . . . 50
2.5 Transition diagram of possible move modes. . . . 51
2.6 Typical turning around move mode. . . . 52
2.7 Static force analysis of the upper part of stick above the force sensor. . . . 54
2.8 The principle of IBAC scheme. . . . 57
2.9 Coordinate frame I based on the ITD. . . . 58
2.10 Resultant driven force. . . . 59
2.11 Control diagram of the whole system. . . . 60
2.12 Three experiment situations. . . . 61
2.13 The covariance of noise when a person moves straight. . . . 62
2.14 Experiment 1 on the flat ground (I→IIa→IIb→I). . . . 64
2.15 Experiment 2 on the flat ground (I→IIa→IIb→I). . . . 65
2.16 Experiments on slope. . . . 68
2.17 Experiments when imitating a handicapped. . . . 69
2.18 Two walking mode series used in the comparison study. . . . 70
2.19 Comparisons of experiment results using the IBAC strategy and the CAC strategy. . . . 72

3.1 Intelligent cane robot prototype IV. . . . 76
3.2 On-shoe load sensor with motion sensor . . . 77
3.3 Experimental results of *FlexiForce* sensor . . . 79
3.4 Performance of *FlexiForce* sensor . . . 80
3.5 How to select and hold a cane. . . . 81
3.6 How to walk with a cane . . . 82

3.7 Proposed flowchart to reduce load applied to affected leg 83
3.8 Experiment of case 2 85
3.9 Velocity of cane robot 85
3.10 Load on user's leg and cane 86

4.1 Prototype of the omni-directional type cane robot. 90
4.2 The control diagram of the intelligent cane system. 90
4.3 Tracking head position using CCD camera. 91
4.4 Tracking leg's positions using LRF. 92
4.5 Walking state is monitored simultaneously by camera and LRF. 93
4.6 Normal walking and possible falling states. 94
4.7 Walking states represented in 2D top view. 95
4.8 Tracking head and legs position. 95
4.9 The original fused position data. 98
4.10 The computed feature distance d of both subjects. 99
4.11 The possibility distributions of feature distance d of both subjects. 100
4.12 Experimental result of fall detection. 101
4.13 Intelligent cane robot prototype IV. 102
4.14 On-shoe load sensor system. 103
4.15 The human-in-the-loop system block diagram. 104
4.16 The simplified link model of human walking. 105
4.17 Sensory data required in ZMP calculation. 106
4.18 (a) Normal walking and possible falling states. 107
4.19 (b) Point positions of different falling cases. 107
4.20 The feature $(\Delta x, \Delta y)^T$ of fall detection. 107
4.21 Trajectories, data histograms, probability and possibility distributions of "normal walking". 109
4.22 The membership degree function of "normal walking". 109
4.23 Fall detection experiment. 110

5.1 Omni-directional type cane robot.(*Prototype III*) 112
5.2 Coordinate frame I based on the ITD. 113
5.3 Kinematics of Omni-wheel robot. 114
5.4 The hierarchial control structure. 115
5.5 Absolute coordinate and bearing coordinate. 116
5.6 Definition of cane robot coordinate system {1} 118

5.7 Coordinate systems definition. 120
5.8 Force analysis of intelligent cane robot. 122
5.9 Structure of omni-wheel robot. 124
5.10 Fall direction of cane robot. 125
5.11 The simulation result of case *I* and case *II*. 126
5.12 Simplified link model of human-cane robotic system. 130
5.13 Model and dynamics analysis of human-cane robotic system. 134
5.14 The human-cane robot system.. 135
5.15 The fall prevention procedure. 137
5.16 Control diagram of cane robot system. 138
5.17 Simulation results of fall prevention. 141

6.1 Research contents for the intelligent cane robot 145

List of Tables

1.1 Countries with the highest shares of 60^{+} population in 2011 and 2050. . . . 6
1.2 Classification of SIDE 37

2.1 Possible Walking Modes 51
2.2 Comparison of *D(CANE,ITD)* using different control strategies 71

3.1 Experimental result of on-shoe load sensor 78
3.2 Comparative experiment results for ITD and CGP 84

Chapter 1

Introduction

The world is facing challenges of rapid aging population(see **Fig.** 1.1). Elderly people suffer from low levels of physical strength due to muscle weakness, which affects their motion ability significantly. Restricted movement lowers the performance of most activities of daily living (ADLs). In addition, the growing elderly population causes the shortage of young people for nursing care. Therefore, walking-aid robots find their application in the nursing and therapy field for these mobility impaired people.

Figure 1.1: An aging world

Illustration by Daniel Horowitz
http://www.businessweek.com/articles/2013-02-07/an-aging-population-may-be-what-the-world-needs

This thesis summarized the research activities in the past 3 years. Practically, this project was started from 2008 and it is my great honour to join the team from the beginning when I was a master student in Nagoya University. In the past 5 years 4 prototypes of cane robot have been developed with different functions. The cane robot becomes smaller and smaller, more and more useful and safe. Many functions was proposed e.g., walking assistance, falling detection and prevention.

1.1 Background

1.1.1 Aging Society

Population aging is taking place in most of countries in the world. There are two factors underlying this trend: [1]

- **Increasing Aging Population:** In most parts of the world, people are living significantly longer lives than in previous decades(see **Fig. 1.2**). For the world as a whole, life expectancy increased by two decades since 1950 (from 48 years in 1950-1955 to 68 years in 2005-2010). During the current half century, the UN Population Division projects global life expectancy to rise further to 76 years.
  As more people live longer, retirement, pensions and other social benefits tend to extend over longer periods of time. This makes it necessary for social security systems to change substantially in order to remain effective. Increasing longevity can also result in rising medical costs and increasing demands for health services, since older people are typically more vulnerable to chronic diseases.

- **Declining Birthrate:** The worlds total fertility rate fell from 5 children per women in 1950 to roughly 2.5 today, and is projected to drop further to about 2.2 by 2050. As families have fewer children, the elderly share of the population naturally increases. These low birth countries contain over 40% of the worlds population, including every country in Western Europe, China, Japan, Russia, Poland, and Canada, to name just a few. Birth rates in many other countries, including the United States, Mexico, and Iran, are only a little above the level necessary to replace the number of deaths. In 1970 the average woman on the planet gave birth to 4.7 children in her lifetime. By 2011 that number had dropped to 2.5. Even in the worlds most fecund region, sub-Saharan Africa, the fertility rate fell from 6.7 to 4.9 between 1980 and 2010 and births among women under 20 dropped 20% in the first decade of the new millennium(see **Fig. 1.3**).

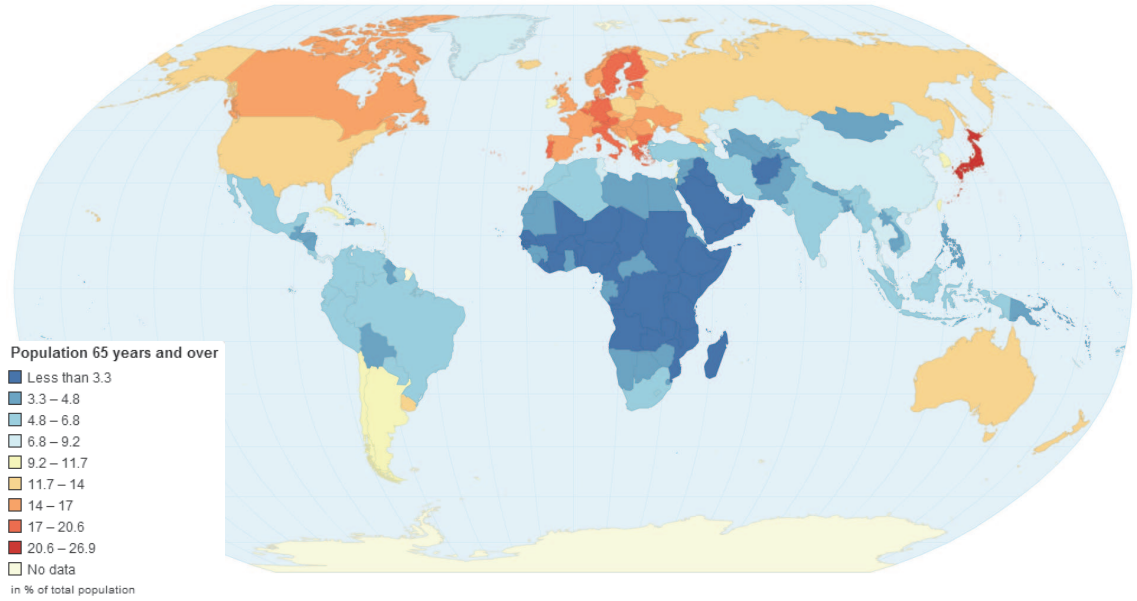

Figure 1.2: Current countries with the oldest population in the world.

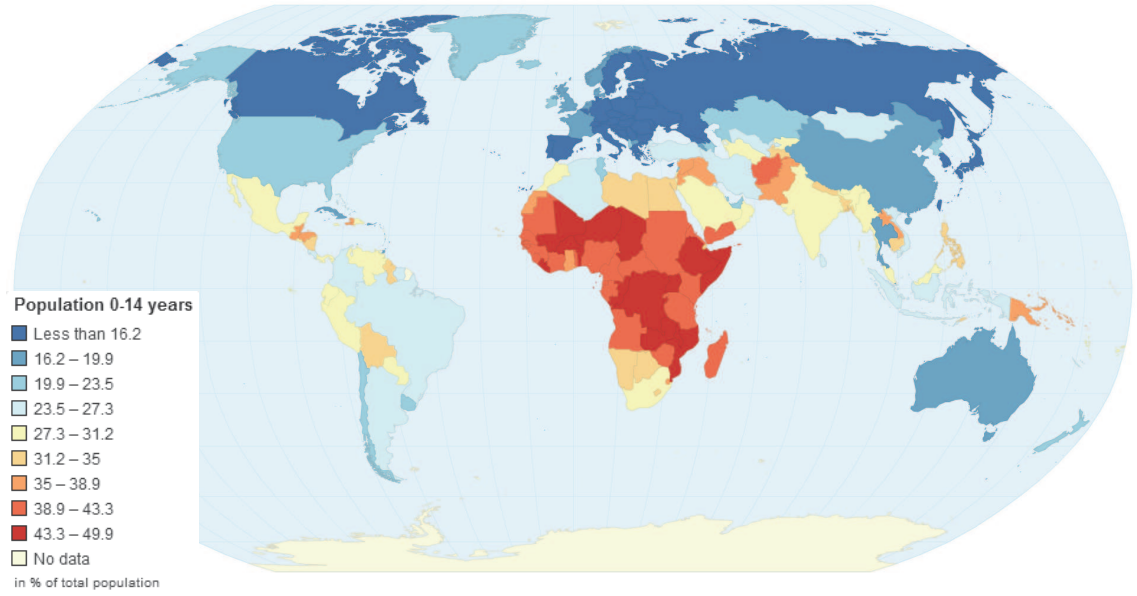

Figure 1.3: Current countries with the youngest population in the world.

The combination of falling birthrates and longer life expectancies also means the world is rapidly adding wrinkles. In 1980 the median age was 23; by 2050, according to the UN, it will be 38. In 1970 about half of the worlds population was younger than 20; by 2011 that

figure had dropped to a little more than one-third, and the UN predicts it will be closer to one-quarter by mid-century. Meanwhile, the number of people older than 65 increased from 5 percent to 9 percent between 1970 and 2011 and will climb to 20 percent by 2050. Despite the global population being about 2 billion higher, the absolute number of young people at mid-century will be no larger than today. The global elderly will have increased from 648 million to 1.9 billion.

Increasing Aging Population

1. ***Definition of the Elderly*:** Most developed world countries have accepted the chronological age of 65 years as a definition of 'elderly' or older person [2], but like many westernized concepts, this does not adapt well to the situation in Africa. While this definition is somewhat arbitrary, it is many times associated with the age at which one can begin to receive pension benefits. For this thesis, we will use 65 years of age and older as the general definition of an elderly person.

2. ***World Population Ageing*:** As many people know, the world is aging so fast that it is leading us into uncharted demographic waters. Most countries are not prepared to support their swelling numbers of elderly people(see **Fig. 1.4**).

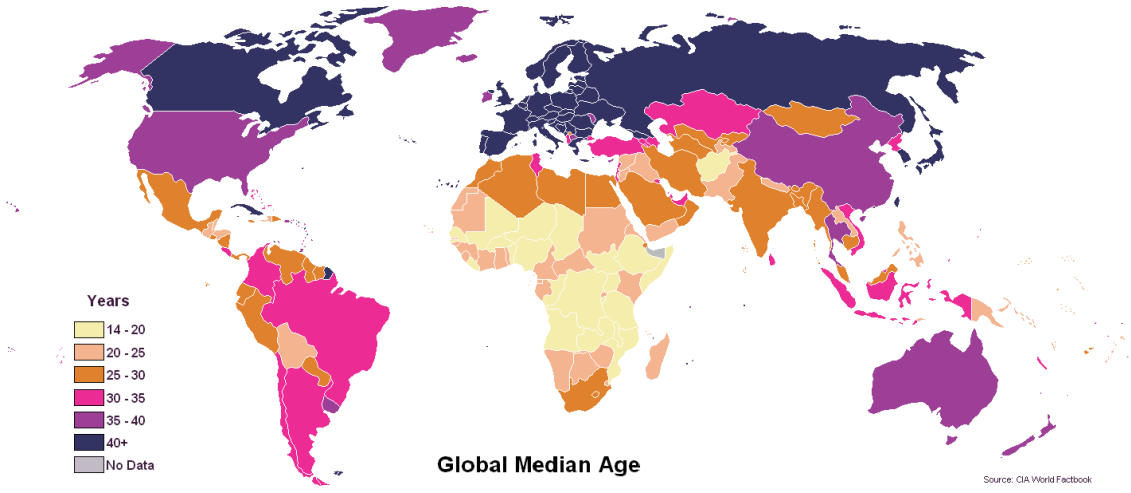

Figure 1.4: Median age by country, 2005.

Source: The World Factbook, Central Intelligence Agency. Data last updated on April 2, 2009.
https://www.cia.gov/library/publications/the-world-factbook/fields/2177.html
http://en.wikipedia.org/wiki/List_of_countries_by_median_age#cite_note-1

There will be higher absolute numbers of elderly people, a larger share of elderly,

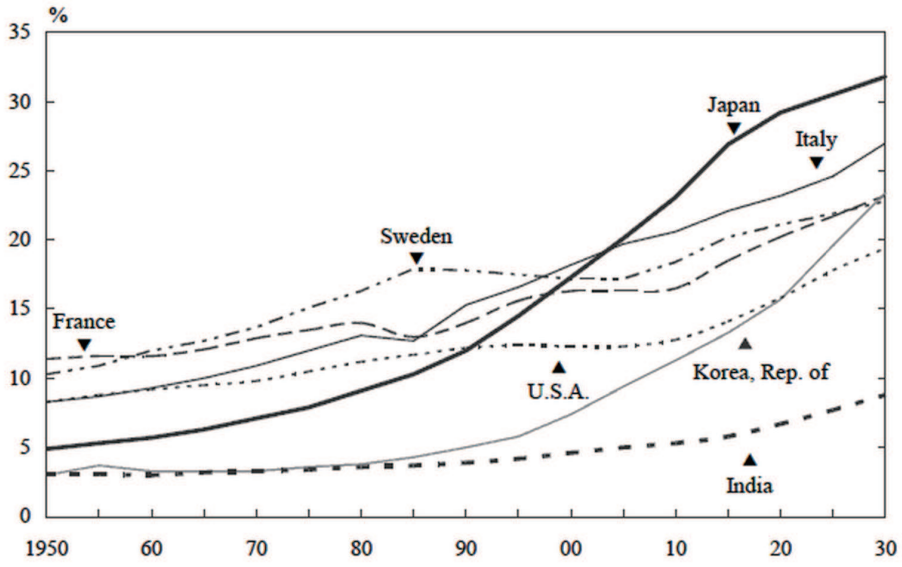

Figure 1.5: Proportion of elderly population by country(Aged 65 years and over).

longer healthy life expectancies, and relatively fewer numbers of working age people. There are alarmist views - both popular and serious - in circulation regarding what these changes might mean for business and economic performance.

Initially experienced by the more developed countries, the process has recently become apparent in much of the developing world as well. For the near future, virtually all countries will face population ageing, although at varying levels of intensity and in different time frames.(**Fig.** 1.5)

Although population aging is occurring in both developed and developing countries, **Table** 1.1 shows that the 10 countries with the highest shares of 60^+ population in 2011 are all in the developed world (or are countries in transition, such as Bulgaria and Croatia). The picture will change by 2050, when perhaps most notably Cuba will enter the list − and Finland and Sweden, for example, will no longer be on it. Most remarkably, the UN projects that in 2050 there will be 42 countries with higher shares of 60^+ population than Japan has now.

Populations are aging even faster in the developing world, as fertility rates there have declined more rapidly and more recently than in the developed world. Asia and Latin America and the Caribbean are the world's fastest aging regions, with the percent of elderly in both regions projected to double between 2000 and 2050 (see **Fig.** 1.6). Even sub-Saharan Africa, which has the smallest proportion of elderly and which is

Table 1.1: Countries with the highest shares of 60^+ population in 2011 and 2050.

2011		2050	
Japan	31	Japan	42
Italy	27	Portugal	40
Germany	26	Bosnia and Herzegovina	40
Finland	25	Cuba	39
Sweden	25	Republic of Korea	39
Bulgaria	25	Italy	38
Greece	25	Spain	38
Portugal	24	Singapore	38
Belgium	24	Germany	38
Croatia	24	Switzerland	37

Source: United Nations Population Division (2011).

aging slower than any other region, is projected to see the absolute size of its older population grow by 2.3 times between 2000 and 2050.

But less developed countrieswhich have much lower levels of economic development and access to adequate health care than more developed countrieswill be hard-pressed to meet the challenges of more elderly people, especially as traditional family support systems for the elderly are breaking down. Policymakers in the developing world need to invest soon in formal systems of old-age support to be able to meet these challenges in the coming decades.

3. ***Population Ageing in Japan*:** Japan, struggling to deal with a falling birth rate and an aging population, said people 65 or older accounted for 21 percent of the total population in 2005, the world's highest elderly ratio, surpassing Italy's 20 percent ratio. The ratio of people 15 or younger in the total population was the world's lowest, at 13.6 percent, surpassing Bulgaria's 13.8 percent, the report said. Japan is setting the pace among the aging societies of the world. People aged 65 and over now make up over one-fifth of the population and in twenty years will reach one-third.

   The total Japanese population as of 2008 is 127.69 million (62.25 million men and

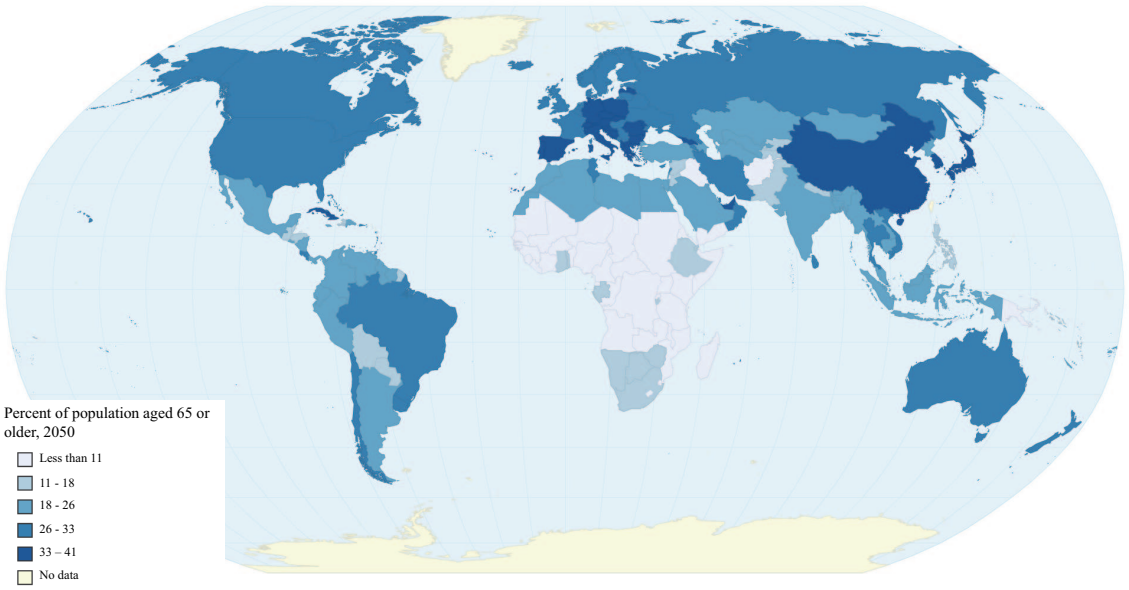

Figure 1.6: Percent of population aged 65 or older, 2050.

65.44 million women); about 28.22 million are aged 65 and over and 13.22 million are 75 and over. Older Japanese (aged 65 and over) represent 22.1% of the population, and people aged 75 and over represent 10.4%(see **Fig.** 1.7).

One reason for the growth of the elderly population is that people now live longer(see **Fig.** 1.8). Japan has one of the highest life expectancies in the world with average life expectancy at 79.2 years for men and 86.0 years for women.

The Ministry of Health, Labour and Welfare, Japan investigated the vital statistics by 2011. We can find that the shape of population pyramid is changing into a shuttle. It means more and more elderly need the young people i.e. the productive population to nurse care of them. In the next generation, the radical transformation of the Japanese population structure is dramatically shown in **Fig.** 1.9 for 1950, 2000 and 2050. Japan went from being quite a young nation, to a middle-aged nation, to a remarkably old nation. The rapid growth in the 65^{+} is almost over. From 1980 to 2005 the number of elderly people more than doubled, but the rate of increase will moderate sharply from about 2010. However, the old-age share of the population will continue to go up because the total population is shrinking.

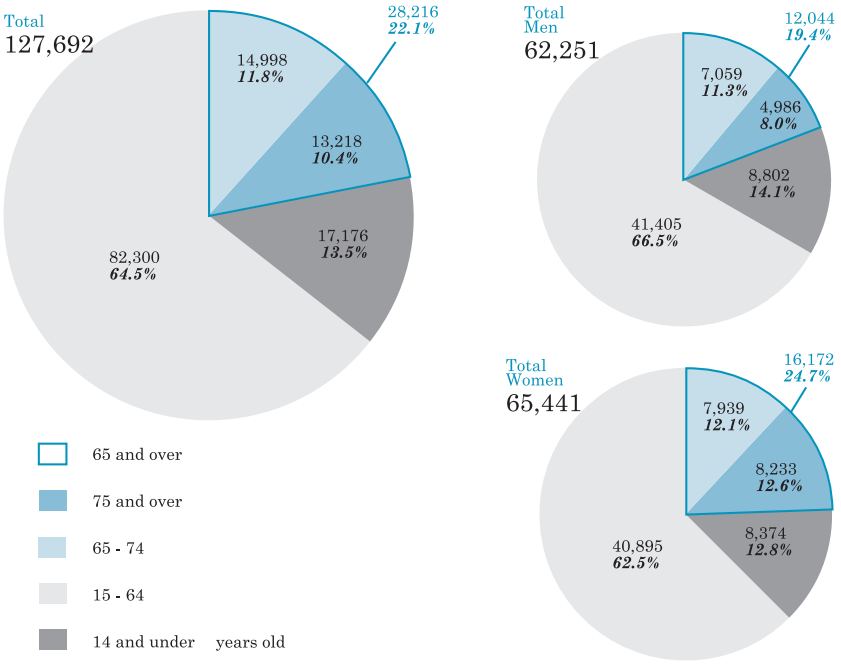

Ministry of Internal Affairs and Communications, *Population Estimates,* 2008

Figure 1.7: Population aging in Japan (1,000 people, %).
http://www.ilcjapan.org/agingE/doc/POJ_2010_1.pdf

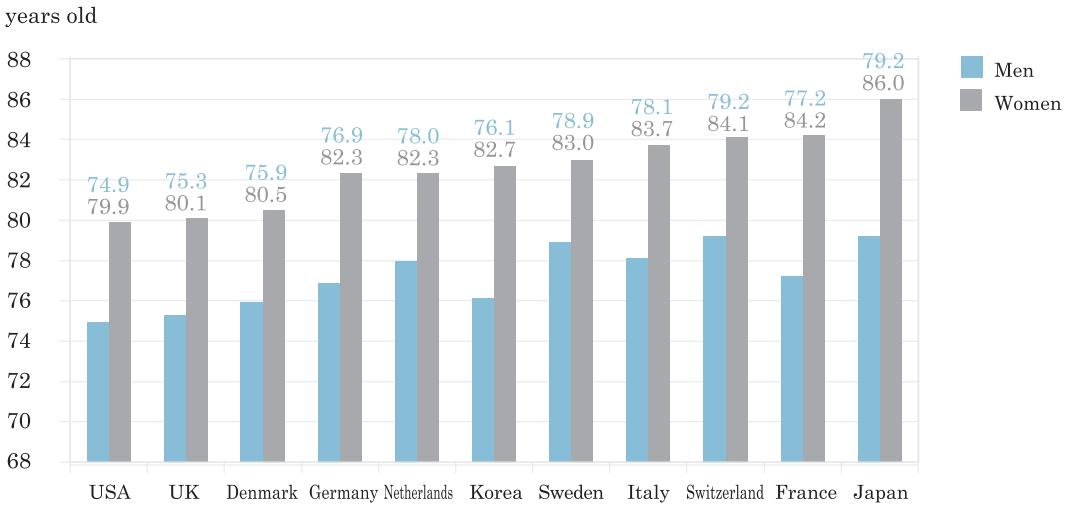

UN, *Demographic Yearbook,* 2007

Figure 1.8: Life expectancy at birth

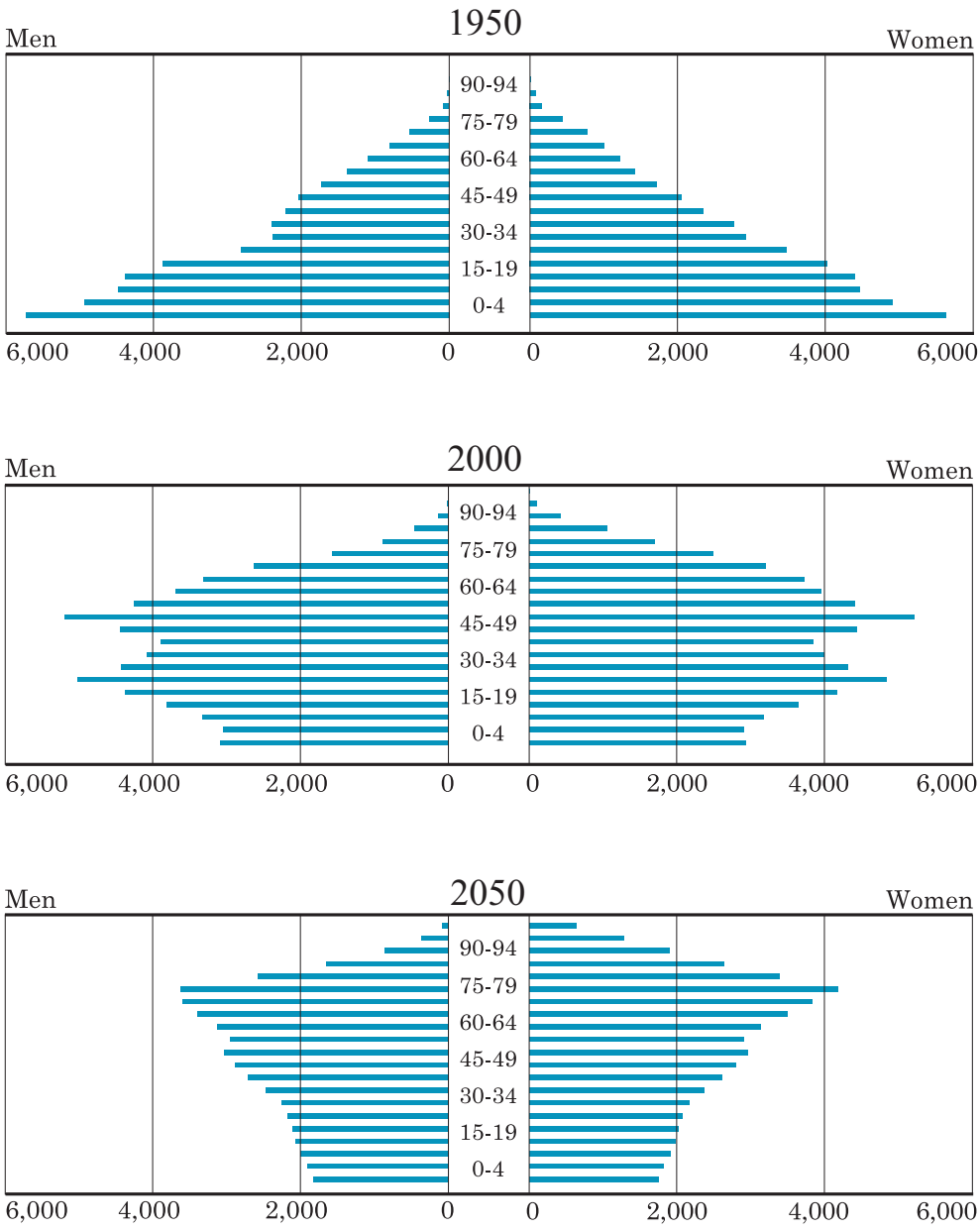

Figure 1.9: Population pyramids of Japan 1950, 2000, 2050.

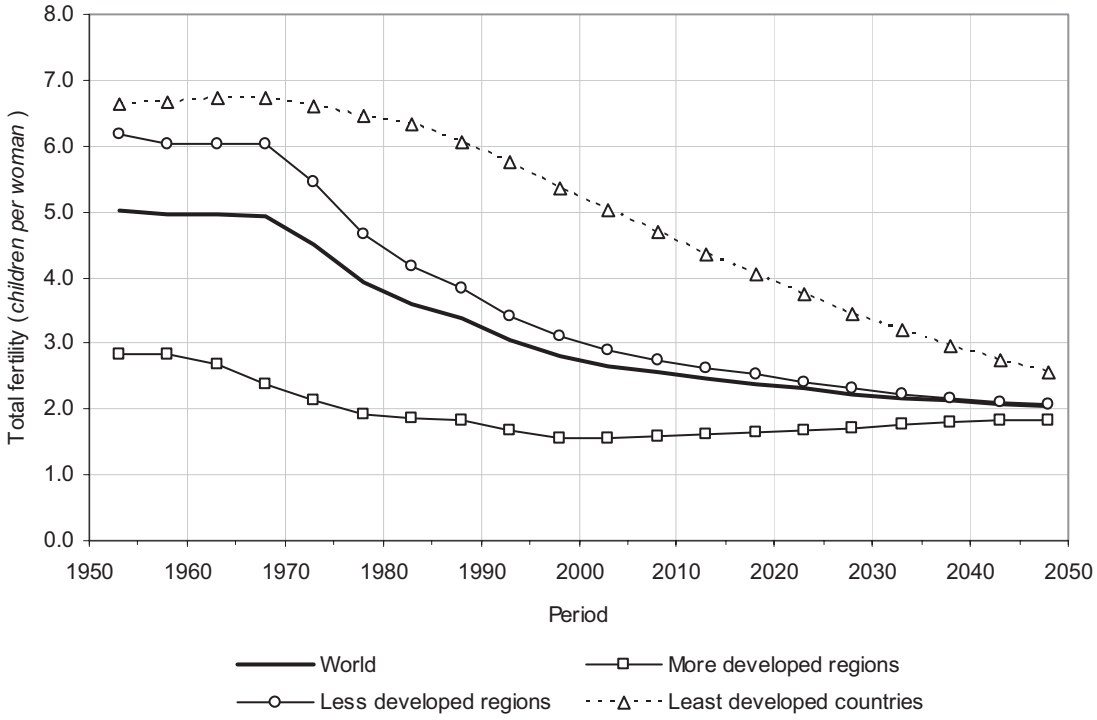

Figure 1.10: Total fertility trajectories of the world and major development groups, 1950-2050.

Declining Birthrate

1. ***Falling of Total Fertility in World*:** According to the 2004 Revision, total fertilitythat is, the average number of children a woman would bear if fertility rates remained unchanged during her lifetimewas 2.65 children per woman in 2000-2005 at the world level. This average masks the heterogeneity of fertility levels among countries.(**Fig. 1.10**)

   In 2005, the 65 countries where total fertility was below replacement level accounted for 43 per cent of the world's population, or 2.8 billion people, whereas the countries with fertility at or above replacement level had 3.6 billion persons in 2005, or 57 per cent of the total. Because of their low fertility and the expectation that it will not rise markedly in the future, the countries with below-replacement fertility are projected to have only a slightly larger population in 2050 than today (2.9 billion people). In contrast, the countries whose fertility is currently above replacement level are expected to experience a marked population increase, reaching 6.1 billion by 2050

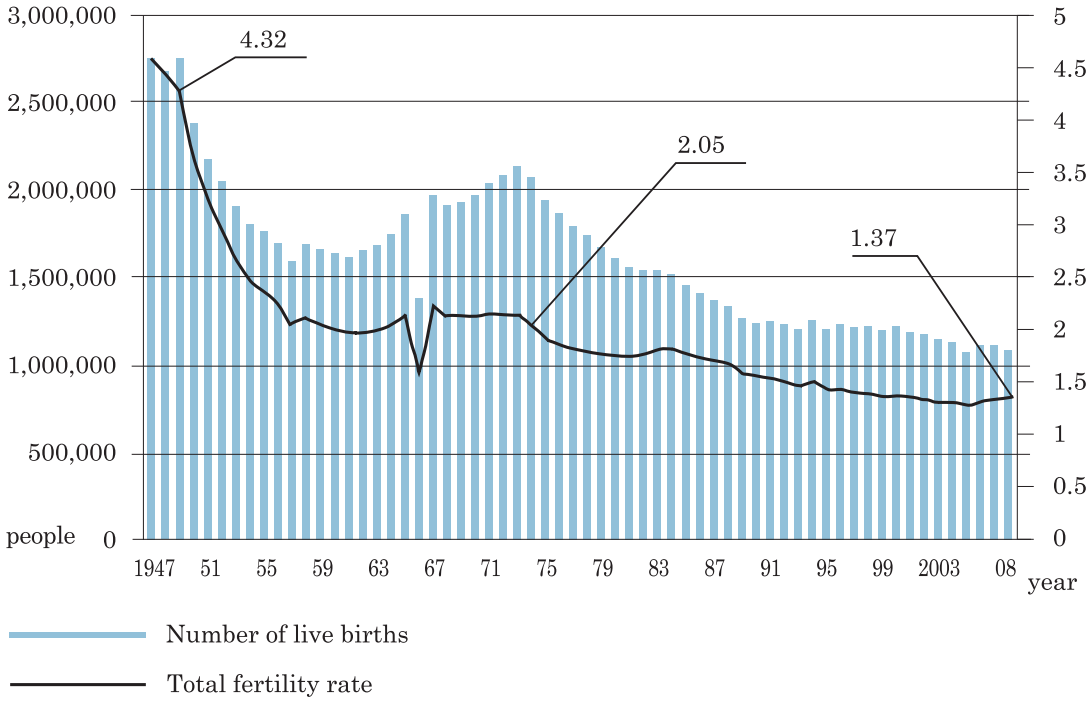

Ministry of Health, Labour and Welfare, *Vital Statistics*, 2008

Figure 1.11: Declining fertilities in Japan(1947−2008).

and accounting then for 68 per cent of the global population.

Although most developing countries are already far advanced in the transition from high to low fertility, 17 still had fertility levels of 6 children per woman or higher in 2000-2005 and for 15 of them there is either no recent evidence about fertility trends or the available evidence does not indicate the onset of a fertility reduction. Although the fertility of those 17 countries is projected to decline after 2010 at a pace of about one child per decade, none is expected to reach 2.1 children per woman by 2050 in the medium variant. As a result of those trends, their population is expected to rise from 250 million in mid-2005 to 791 million in 2050.

2. ***Falling of Total Fertility in Japan*:**The primary reason for the rapidity of aging in Japan is the declining number of births. The total fertility rate(TFR) had been over 4.30 in the late 1940s, when the baby-boom generation was born, but in 1974 it declined to 2.05, which is the replacement fertility rate, and continued to fall to 1.37 in 2008. The primary reasons for this trend are fewer and later marriages, and fewer births among married couples.(**Fig. 1.11**)

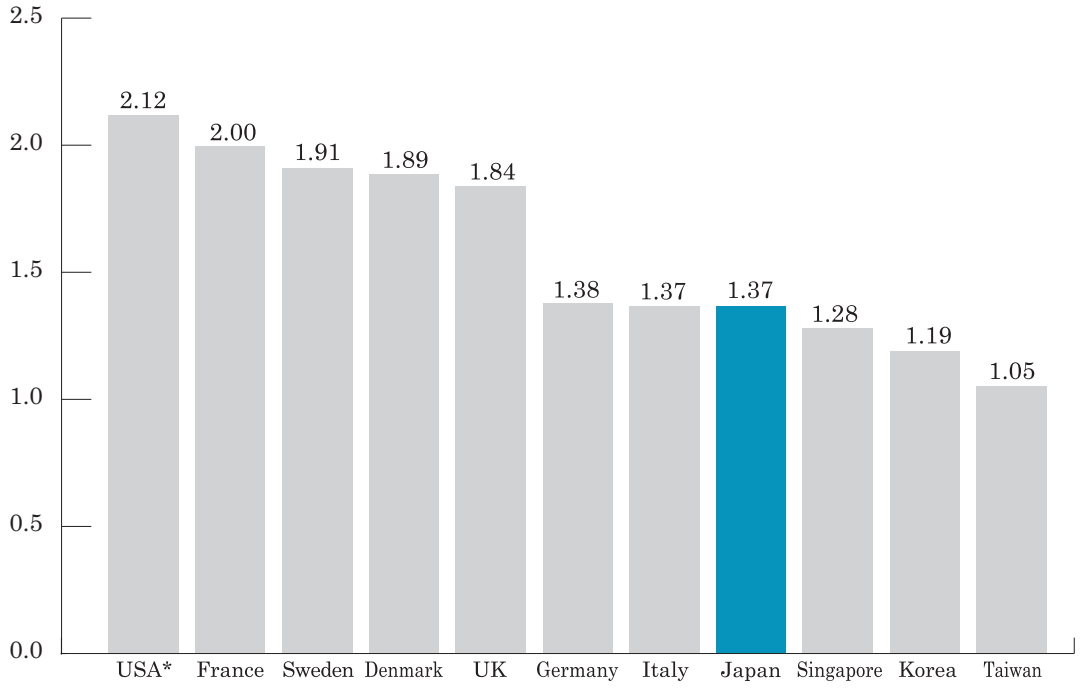

Figure 1.12: Total fertility rates: international comparison(2006−2008).

In comparison with other countries, Japan;s TFR is lower than in the US, France and the Scandinavian countries, and similar to the in Germany and Italy. TFRs in Korea, Taiwan and Singapore are currently lower than in Japan.(**Fig. 1.12**)

The government has initiated several programs to raise birth rates, but so far they have been ineffectual. In any case, even if the fertility rate were to rise, the number of women able to have babies will be declining rapidly once the "secondary baby boom"(aged 25-29 in 2000) passes out of its fertile years.

1.1.2 Society Problems

Burden of Nursing Care

In the late 1970s and early 1980s, the government advocated a "later, longer, fewer" lifestyle, encouraging people to marry later, have wide gaps between children and fewer children overall. It also instated the controversial one-child policy. These were attempts to curb population growth in a bid to help modernise the economy.

Women are having fewer children, but having a smaller generation follow a boom generation - and longer life expectancies - means that by 2050, it is expected that for every 100

Figure 1.13: The 4−2−1 family.
http://www.bbc.co.uk/news/world-asia-19630110

people aged 20-64, there will be 45 people aged over 65, compared with about 15 today.

Only children from single-child parents face what is known as the 4-2-1 (**Fig. 1.13**) phenomenon: when the child reaches working age, he or she could have to care for two parents and four grandparents in retirement.

Form 1950, many of the countries with high birth rates and a life expectancy of about 44 years. When children of the one-child generation reach their 30s or 40s, there is a good chance their parents and grandparents will be alive and need some form of care.

The elderly people regarded as senior citizens draw attention because of their weakest and problematic living conditions. It is an important responsibility of democratic welfare state to solve the problems of aging and take care of elderly people.

1.1.3 Needs of Nursing-Care Robot

In an aging society it is extremely important to develop devices, which can support and assist the elderly in their daily life, since their mobility degrades with age. This situation requires a great medical care, incurs large costs and can be fatal in some cases. The elderly tend to have cognitive impairments and experience more serious falls but there is strong evidence that daily exercise may result on fall prevention and postural stability. So, it becomes more and more relevant to find ways and tools to compensate, to improve or to restore and to enhance this mobility.

On the other hand, living in the nurse home can partly relieve the stress of nursing

elderly, and the centralized management can enhance the efficiency and quality. Still, more and more increasing elder population cause the shortage of young people to nurse them. In most of nursing home, However, this therapy requires the involvement of two or three therapists to assist patients in walking, holding their lower limbs to control movement. Thus, a substantial commitment and effort on the part of therapists is required.

1.2 Related Works

For the elderly, there are three issues: mobility, mental and cognitive disabilities. In this thesis, the mainly work is focusing on the assistance of motor function. In daily life, the walking is one of the most important human activities.

In the past several decades researchers have been addressing the needs of persons with mobility disabilities through alternative or augmentative devices. These solutions are selected based on the degree of disability of the user. Mainly, the nursing devices are classified into two types:

- ***Manual*:** The manual devices support the user passively without power. The people need to operate it by himself. The ingenious mechanical design and single function is the characteristic of these kind of devices.

- ***Automatic*:** The automatic nursing-care machines with numbers of sensor and actuators can provide more effective support to the user. More smart and more reliable functions are the reasons that people tent to buy it, even it much expensive then the manual one.

Moreover, these kind of assistive device can be classified into mobile and fixed type which is defined as follow:

- ***Mobile*:** Devices or machines which move passively or actively are defined as a mobile type. This type of assistive device can help people and provide sufficient support during walking. They are designed for patients who with different physical disabilities.

- ***Fixed*:** In consideration of the safety, many nursing and rehabilitation machines are designed in large-scale and fixed on the ground. The stability of these assistive device is depend on the size. The bigger one can get the robust stability but at the cost of losing the mobility.

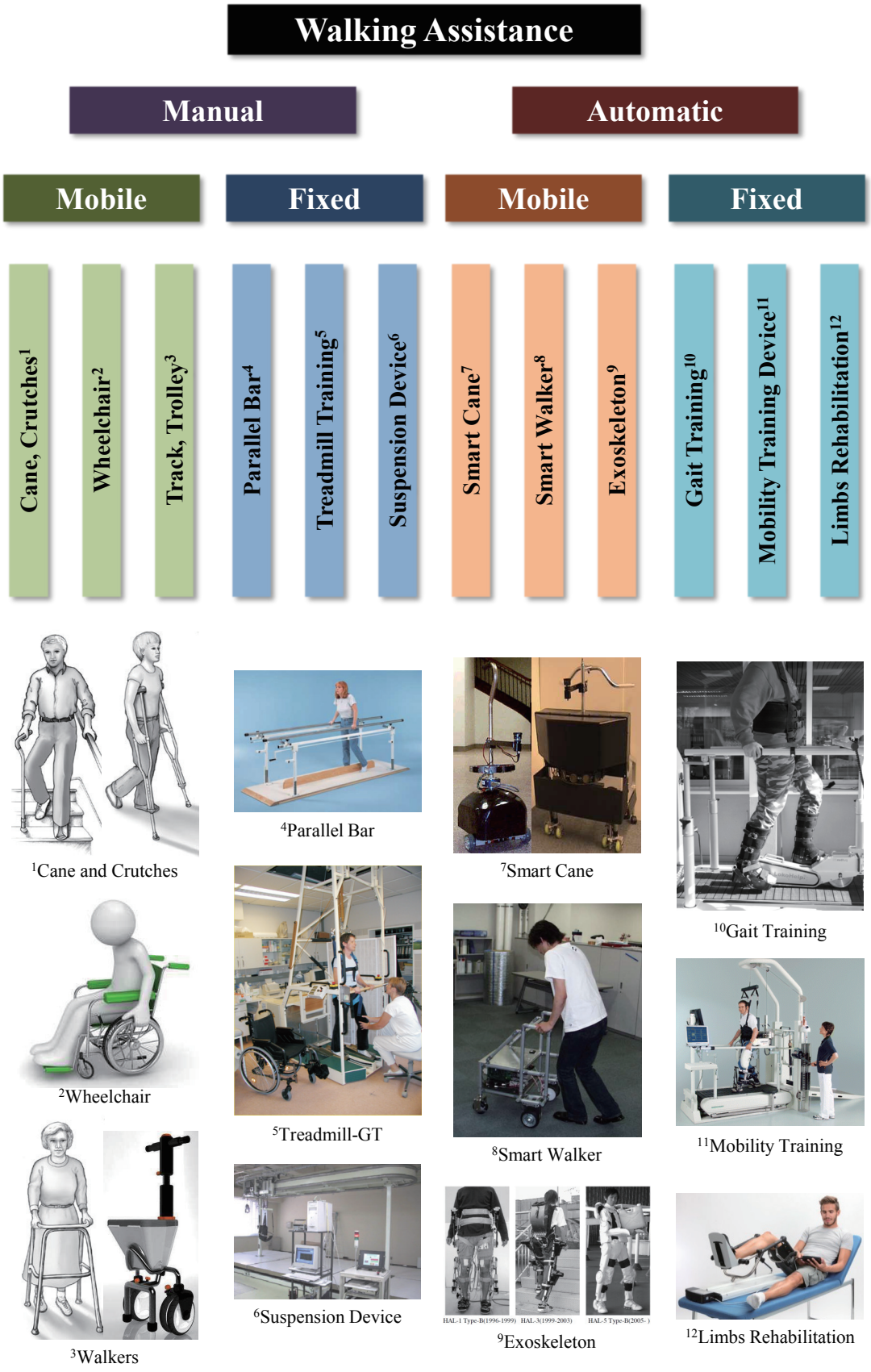

Figure 1.14: The classification of nursing-care robots.

In the following paragraph, we discuss the use, usage, advantages and deficiencies of 12 representative nursing devices: we classified all the devices into 4 groups, mobile or fixed manual devices and mobile or fixed automatic devices. For each group 3 distinguished examples are discussed.

1. Cane, Crutch: It is helpful to use a Cane if people have a small problem with balance or instability, some weakness in leg or stroke, an injury, or pain. [3–5] For elderly, a single point cane may also help them to keep living independently

Canes widen a person's base of support, thereby providing increased balance.(**See Fig. 1.15**). While canes have traditionally been used only for balance and not weight bearing, modified designs permit various degrees of weight bearing through the cane. A cane typically is used when only one upper extremity is required for balance or bearing weight. Some modified cane designs include offset, multiple-legged, and walk canes. There is limited research comparing the efficacy of different types of canes; one study indicated no advantage of multiple-legged canes over standard canes for assistance with standing balance [6]

J. A. Ashton-Miller et al. test the hypothesis that use of a cane in the nondominant hand during challenging balance tasks would significantly decrease loss of balance in patients with peripheral neuropathy while transferring from bipedal to unipedal stance on an unsteady surface. Use of a cane by peripheral neuropathy (PN) patients significantly reduced their risk of losing balance on unstable surfaces, especially under low-light conditions. [7]

The top of cane should reach to the crease in wrist when people stand up straight. The elbow should bend a bit when people hold cane. Hold the cane in the hand opposite the side that needs support. The cane and injured leg swing and strike the ground at the same time. To start, position cane about one small stride ahead and step off on the injured leg. Finish the step with the normal leg.

If an injury or surgical procedure requires to keep weight off the leg or foot, people may have to use a crutch [8]. The top of the crutch should reach between 1 and 1.5 inches below armpits while people stand up straight. The handgrips of the crutch should be even with the top of the hip line. The elbows should bend a bit when people use the handgrips. Hold the top of the crutch tightly to people sides, and use the hands to absorb the weight. Don't let the tops of the crutches press into armpits.

The advantages of cane and crutches are the light weight and its popular price. People can use them in their daily life. But the supportability is insufficient. [9]

2. Wheelchair: A wheelchair is a chair with wheels, designed to be a replacement for walking [**?**, 10–12]. Someone who is paralyzed and unable to use his legs for walking can sit in a wheelchair and use it to move around. There are manual wheelchairs for people

(A) Standard wooden cane, which must be custom fitted for length.

(B) Standard aluminum cane. The length is adjustable.

(C) Standard aluminum cane. The length is adjustable.

(D) Multiple-legged, or "quad cane".

(E) Walk cane. Walk canes are best for patients requiring continuous weight bearing using only one hand.

(F) Axillary crutch. This crutch requires considerable strength to use and is generally used on a temporary basis.

(D) Forearm crutch. This device also is known as the Canadian crutch or Lofstrand crutch.

Figure 1.15: Cane, Crutches.

(A) Conventional rigid frame manual wheel chair for assisting people walking

(B) Quick-adjust wheelchair axle. Position of axle changed in vertical and horizontal directions with turn of knob

(C) The NavChair Assistive Wheelchair Navigation System

(D) Robotic wheelchair MAid, traveling in the concourse of a railway station

Figure 1.16: Wheelchair.

who can use their hands and arms to push the wheels. Often there are handles behind the seat for someone else to do the pushing.(**Fig. 1.16 - (A)**)

A person who can walk but has difficulty keeping balance might have to reduce the distance and amount of time spent walking, or risk injury from falling down. One advantage of using a wheelchair is that a person with balance issues can continue doing regular activities. He can go shopping or clear snow from the driveway without worrying about getting hurt. [13] When a person breaks the leg, knee or ankle, the doctor will advise against putting weight and stress on it while the bone mends. Sometimes people can get

Figure 1.17: Track, Trolley.
http://www.trendhunter.com/trends/mp-walker

around on crutches, but using them for long periods may be too painful or exhausting. When both legs are broken, crutches are not an option. A wheelchair gives people the advantage of being able to move around for as long and as far as she likes. But the use of a wheelchair is limited by the step or doorsill.(**Fig. 1.16 - (B)**)

Levine et al. [14] developed a wheelchair navigation system to reduce the cognitive and physical requirements of operating a power wheelchair for people with wide ranging impairments that limit their access to powered mobility.(**Fig. 1.16 - (C)**)

Automatic navigation is one of the major research issues in robotic wheelchair, since mobility assist is the fundamental function of a wheelchair. Prassler et al. [15] developed robotic wheelchair MAid (Mobility Aid for Elderly and Disabled People) to support and transport senior users with limited motion skills and to provide them with a certain amount of autonomy and independence. As shown in **Fig. 1.16 - (D)**, in a test, MAid could travel autonomously in the concourse of a railway station through crowded people.

3. Track, Trolley: The trolley-type walker(see **Fig. 1.17**) is a mobility solution for people who have total knee or hip joint replacement surgery. In this case, people need more help with balance and walking than using a crutches or a cane. A pickup walker with four wheels or solid prongs on the bottom may give people the most stability. The walker keeps all or some of user's weight off of the lower body, and the arms support some of the weight. The top of walker should match the crease in user's wrist when stand up straight. As strength and endurance get better, people may gradually be able to carry more weight

Figure 1.18: The elderly works on his balance on the parallel bars with help.

in the legs. [16]

4. Parallel Bar: The most basic mobility-training devices are the parallel bars(**Fig. 1.18**). Their objective is to help people regain their strength, balance, range of motion, independence and to recover from some injuries, and other debilitating conditions. Patients are required to repeat concise movements that work more than one joint and muscle. Parallel bars are also used for ambulatory exercises to improve a patients ability to walk independently or with assistance. [17, 18]

Rehabilitation therapists use parallel bars for coordination exercises. These task-oriented procedures help people with balance and coordination problems, typically resulting from strokes or brain trauma. Patients are required to repeat concise movements that work more than one joint and muscle.

Even if a patient can walk, they may find it extremely difficult without proper rehabilitative therapy. Some injuries, such as those to the brain or spine, commonly effect motor skills and may cause spasms. Gait training can help patients regain their normal ambulatory motion.

Therapy parallel bars are also used for general conditioning exercises. This rehabilitative therapy combines range-of-motion, muscle-strengthening, and ambulatory exercises to counteract effects from being in a wheelchair for a sustained period of time or from prolonged bed rest and immobilization. General conditioning exercises are used to increase heart and lung function as well assist in restoring necessary blood flow.

5. Treadmill Training: The Treadmill devices(**Fig. 1.19**) which address patients who have neurological disorders manipulate the legs, according to the kinematics provided by each mechanism and the speed desired. [19–22] However, they need to be permanently

(A) GlideTrak Unweighted Treadmill Training System

(B) Gait training device with medicinal slow treadmill

(C) Electromechanical Gait Trainer GT with movable footplates.

Figure 1.19: Treadmill Training.

installed in a room. They require that patients have to be moved from their beds to that room to experience the robotic rehabilitation. Unfortunately, depending on the healthy state of the patients, it may not always be possible to move the patient out of his bed to start the rehabilitation therapy. Additionally, waiting may imply destruction of cortical tissues, and less possibilities of recovering these neural functionalities. [23]

6. Suspension Device: The suspension training system(**Fig. 1.20 - (a)**) is the training device that tries to obtain the effect similar to the walk training. A train patient hangs and is supported to the hanging system and walks the force plate top. Hanging it up power is controlled on the basis of the information from the force plates. This system can give the most effective load to a training person, by adjusting to the real time while hangs in accordance with the recovery degree of a train patient. It becomes possible to evaluate the training effect on the basis of the data that was obtained from force plate. [24]

In [25] a automatic suspension device (REHABOT) suspends the patient's body in a standing position allowing the patient to walk around the circular handrail without forward propulsion. Reduction of body weight is accurately maintained automatically while safely supporting the patient. There are three advantages for the suspension device; first one is that it may be used for patients with open wounds or cardiac problems, or patients using prostheses or orthoses, second, preparation and walking practice are simpler both for patients and staff than the therapeutic pool and walking trolley, third, running costs are lower than the therapeutic pool. Its drawbacks are that the initial cost is relatively high,

only one patient can be trained at a time, and the effect of warm water is missing.(See **Fig. 1.20 - (b)**) The automatic suspension device enables gait training even for patients who have open wounds, percutaneous fixation, prostheses, orthoses, etc. The preparation before the walking practice with the device is simpler than for the therapeutic pool for both patients and staff. Staff costs using the device also are low. The running cost of the device is merely the cost of electricity.

M. Peshkin et al. proposed KineAssist.(See **Fig. 1.20 - (c)**) It is a robotic device for gait and balance training. The needs of user led to focus on increasing the level of challenge to a patient's ability to maintain balance during gait training, and also on maintaining direct involvement of a physical therapist (rather than attempting robotic replacement.) The KineAssist provides partial body weight support and postural torques on the torso; allows many axes of motion of the trunk as well as of the pelvis; leaves the patient's legs accessible to a physical therapist during walking; servo-follows a patient's walking motions overground in forward, rotation, and sidestepping directions; and catches a patient who begins to fall. [26]

7. Smart Cane: Generally, there are two type of smart cane robot for assisting the people walking who suffered from visual [27–33] or motion function handicap [34–40]. The need for effective and interactive assistive mobility devices is becoming more prevalent every year. In more specific situations, the Smart Walkers can be used to monitor some health parameters of the user. This health information is used to keep a medical history of the user or inform through a wireless communication network a health center or the medical staff in case an emergency situation is detected. The PAMM Smart Walker(as shown in **Fig. 1.21 - (a)**) focuses specifically on the users needs in an elderly-nursing facility It provides greater support for walking; monitors the health of the user (e.g. electrocardiogram), and it informs the user about his scheduled of tasks (e.g. taking medications). These functions were developed so that the elderly people can live more independently.

8. Smart Walker: Smart Walkers(**Fig. 1.22**) have emerged with the same structure as the conventional ones but they include additional robotic and electronic components, that promote a better assistance to gait, especially considering navigation, gait monitoring, and partial body weight support. However, some of these devices became too complex to use. When designing a walker, we need to take into account not only the users disabilities in locomotion but also the fact that many of these users have additional deficiencies at cognitive and sensory levels. For instance, elderly people usually present slower behavior and are not familiar with mechatronic devices. Further, walkers should be designed to continually evaluate and correct their actions based on their perception of the needs of the

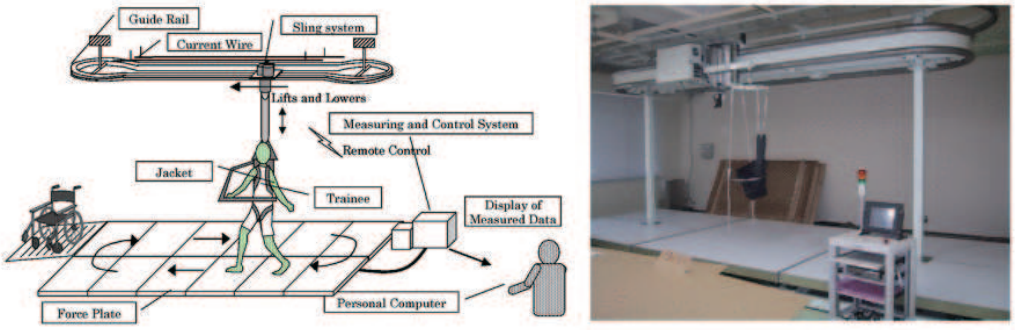

(a) System diagram of the suspension device.

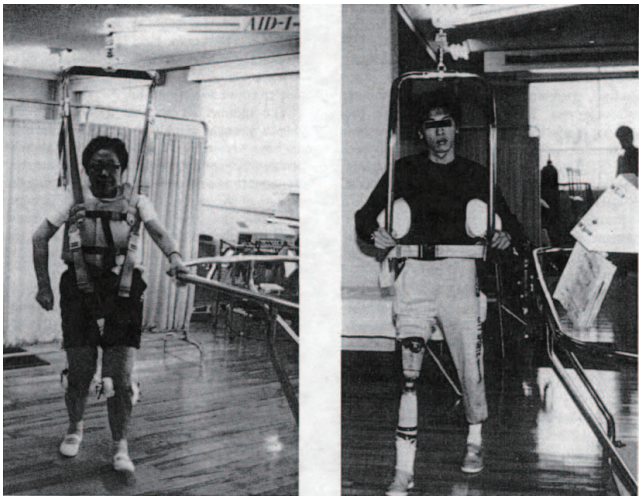

(b) Automatic suspension device (REHABOT).

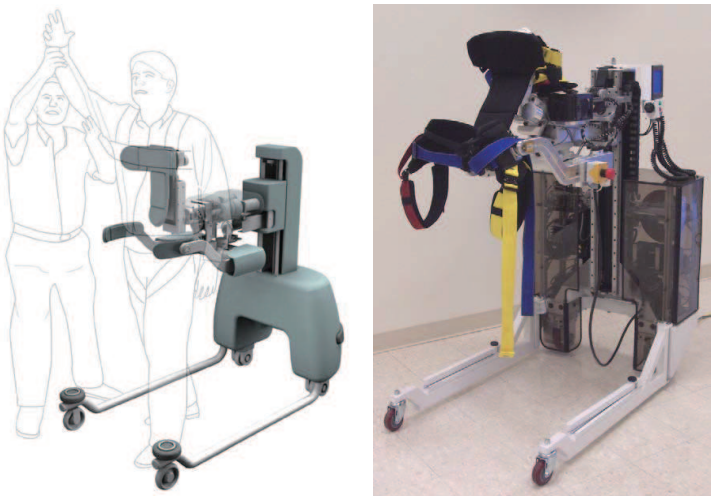

(c) A physical therapist works with a patient on balance exercises(KineAssist).

Figure 1.20: Suspension Device.

(a) Smart Walker and Smart Cane

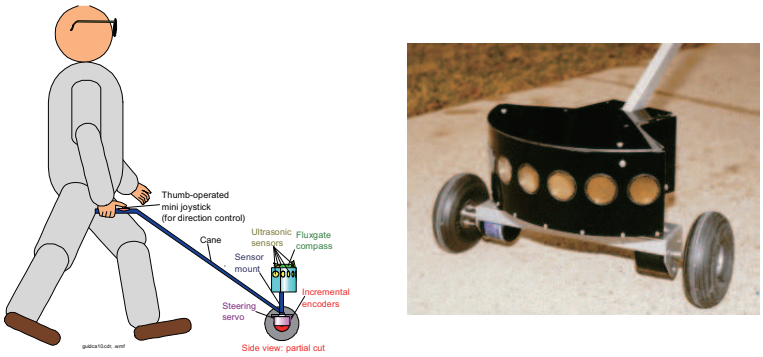

(b) The GuideCane for assisting blind person walking

(c) Dr. Cang Ye is working to develop a "smart cane" that will help visually impaired people travel more easily and safely. [41]

(d) Sebastian Ritzler developed a smart cane that with the help of electronics, become more like a guide dog than a cane. [42]

Figure 1.21: Smart Cane.

(a) RT Walker.

(b) Smart Walker: A tool for promoting mobility in elderly adults. [47]

Figure 1.22: Smart Walker.

user. Also, the walkers need to be used during the daily routines of the user, such as, go to the bathroom, elevator, etc. Therefore, they have to be completely accepted by the user in their daily life. [43–46]

Smart Walkers can also be classified according to their capability to assist user navigation and localization in structured environments and outdoors. These Smart Walkers are very important to people that have cognitive issues and problems related to memory and orientation. Some Smart Walkers are programmed to follow predetermined paths inside clinical environments or to achieve a certain location on a map of a house or medical facility. Other devices are capable of creating maps of an unknown environment or localization in a map using markers placed on the surroundings. Smart Walkers may also be able to communicate bidirectionally with the user through a visual interface or voice commands, receiving directions from the user, or informing him about the present localization in a map and the environment conditions, e.g. obstacles.

A new intelligent walker based on passive robotics that assists the elderly, handicapped people, and the blind who have difficulty in walking. A prototype of the Robot Technology Walker (RT Walker: **Fig. 1.22 - (a)**), a passive intelligent walker that uses servo brakes

was proposed. This system is intrinsically safe for humans, as it cannot move unintentionally, i.e., it has no driving actuators. In addition, the RT Walker provides a number of navigational features, including good maneuverability, by appropriately controlling the torque of servo brakes based on RT. [48–53]

9. Exoskeleton: The exoskeleton devices i.e. self-ported devices are carried by the user either to improve function of movable parts of the body (orthoses) or to substitute a lost member(**Fig. 1.23**). Between these two, orthoses are the ones that present an intense physical and cognitive interaction with the user, and are intended to offset the loss of mechanical function and work together with the movements of the patient. Orthoses allow the patient to perform a wide range of locomotor tasks on the ground, compared with the other mobility-training devices. Their function is to mechanically compensate or enhance functionally of the damaged member, acting in parallel with it. [54–56] Orthoses can be active or passive. Active orthoses bring the necessary energy to enable the movement by applying actuators or motors. This type of orthoses use actuators or motors. As examples we have the HAL-5 (Hybrid Assistive Limb) [57]. This principle takes advantage from the gravity force to balance the gait of the patient.(see **Fig. 1.23 - (a)**)

These devices are intended to restore mobility to people with severe walking impairments. By enabling wheelchair users to stand, walk, and climb stairs, these devices deliver dignity, health, inclusion, and self-esteem.

Slipping into a robotic exoskeleton that could enhance strength or even serve as a prosthetic limb is a highly appealing concept and contrary to popular belief, exoskeletons that aim to impart superhuman strength are not new and can be traced back to 1965. It was then that, with funding from the US Department of Defence, General Electric developed the prototype Hardiman (Human Augmentation Research and Development Investigation, see **Fig. 1.23 - (b)**) which was intended to allow the wearer to lift loads of up to 1,500 lb (682 kg). However, by 1970 only one arm had been made to work and although it could lift 750 lbs (341 kg) and responded according to specification, it weighed three-quarters of a ton. [58]

Military uses feature prominently among proposed exoskeleton applications and the US Army is showing great interest in the technology. With funding from the American Defense Advanced Research Projects Agency (DARPA), Sarcos, a Raytheon company, has been developing a robotic suit since 2000 which is aimed at the “soldier of tomorrow”, at its research facility in Salt Lake City, Utah. The exoskeleton is essentially a wearable robot (see **Fig. 1.23 - (c)**) that amplifies the wearers strength and endurance, allowing them, for example, to lift 200 lb loads repeatedly without tiring. [59]

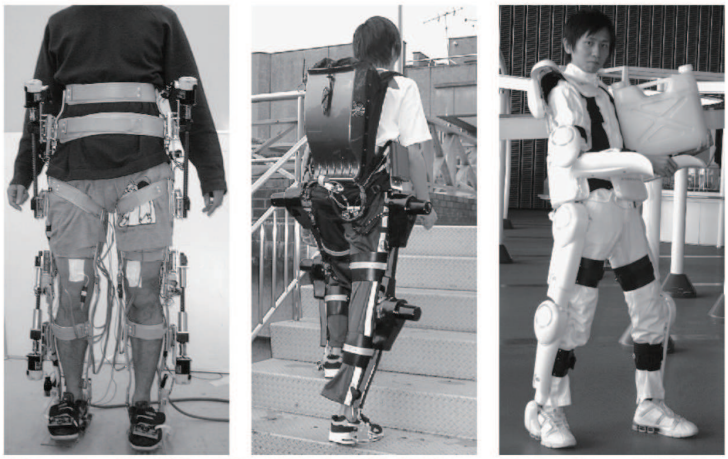

(a) Robot Suit HAL

(b) The Hardiman exoskeleton prototype, developed in the 1960s by General Electric.

(c) The Raytheon/Sarcos exoskeleton being worn

(d) Prototype exoskeleton aimed at assisting agricultural workers

(e) MITs prototype lower-body exoskeleton

Figure 1.23: Exoskeleton.

Accordingly, robotic devices are viewed as a critical technology which will allow the elderly to retain their independence and maintain an active lifestyle. An example is work at the Tokyo University of Agriculture and Technology. This exoskeleton is intended to assist less-able farmers with physically demanding tasks such as uprooting crops, tilling the soil and pruning trees (see **Fig. 1.23 - (d)**), which is particularly important, as almost half of Japans agricultural workers are now aged 65 or over. It presently weighs 25 kg and features 16 sensors which monitor the users movements.

Similar DARPA-funded work is underway by the Biomechatronics Group at Massachusetts Institute of Technology's (MIT) renowned Media Lab. This aims to develop exoskeletons which would reduce the burden for soldiers and others who carry heavy packs and equipment but unlike the Sarcos design, this is a lower leg device rather than an entire suit (see **Fig. 1.23 - (e)**). The prototype weighs about 11.8 kg and is powered by a 48V battery pack.

10. Gait Training Device: Robotic mobility-training devices can be further divided into three different type of devices, according to the patients' pathologies, as follows: treadmill-training devices, ambulatory training devices and feet-manipulator training devices.(See **Fig. 1.24**

The feet-manipulator training devices, which are based on holding the patients feet to a robotic manipulator. This manipulator supports and gently leads the patients in the continuous practice of walking situations. The wheelchair-bound patient is attached to a steel frame in a type of harness, their feet on plates whose trajectories can be fully programmed and imitate everyday walking situations: walking on a level, tripping, slipping or climbing up and down stairs.(See **Fig. 1.24 - (a)**) Reacquiring these abilities is essential for mobility in everyday life. The objective is to copy these movements as naturally as possible. As a result of these artificial feet movements the slack muscles between the toes and the hips are forced into action again. These devices address patients who have neurological disorders. [60]

Gait training of stroke survivors is crucial to facilitate neuromuscular plasticity needed for improvements in functional walking ability. Sai K. Banala et al. investigated the robot assisted gait training (RAGT) for stroke survivors using active leg exoskeleton (ALEX) and a force-field controller, which uses assist-as-needed paradigm rehabilitation.(See **Fig. 1.24 - (b)**) The force-field controller achieves this paradigm by effectively applying forces at the ankle of the subject through actuators on the hip and knee joints. [61]

Pneumatic gait training robot(See **Fig. 1.24 - (c)**): pelvic assist manipulator (PAM) and pneumatically operated gait orthosis (POGO). Each side of PAM is composed of 3

(a) Patient engaged in treadmill training with the LokoHelp device.

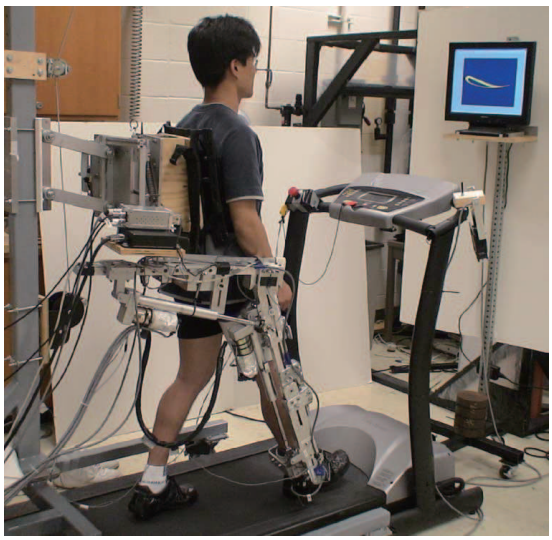

(b) Active leg exoskeleton(ALEX).

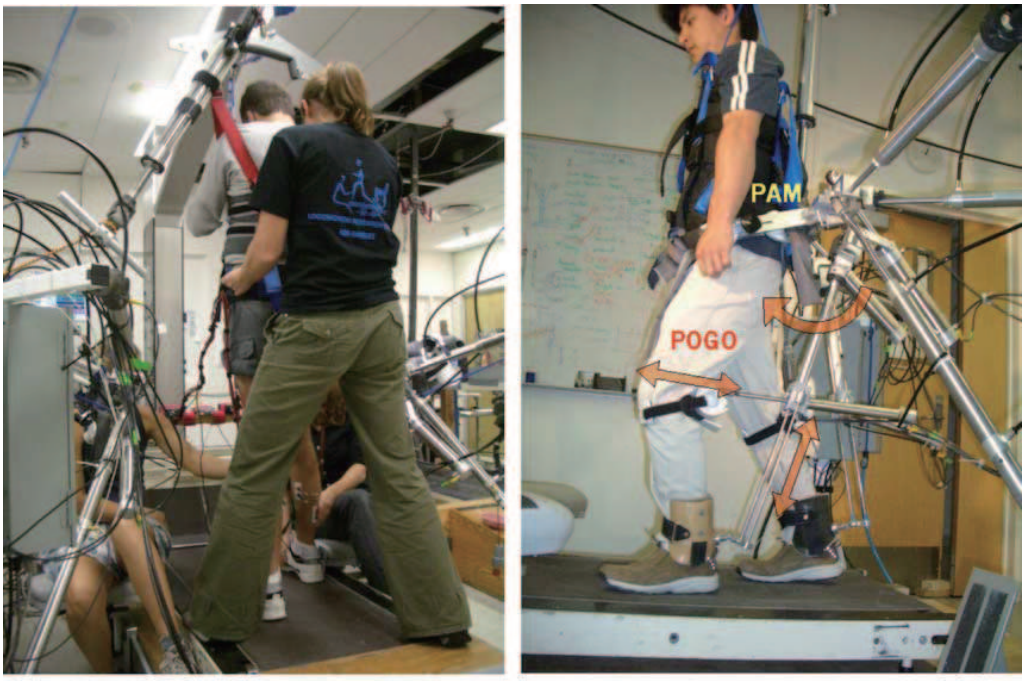

(c) Body-weight-supported gait training following neurologic injury.

Figure 1.24: Gait Training.

pneumatic actuators that attach to belt worn by subject; 3 cylinders form tripod. Lines of action of left side cylinders are labeled with arrows. Each side of POGO is composed of 2 pneumatic cylinders and telescoping rail that extends from PAM belt to cuff on lower shank. Telescoping action of rail is shown with dashed arrow. Knee cylinder is mounted midway down rail and pushes on hamstrings tendon and pulls on patella tendon (arrow at knee shows line of action). Hip cylinder (visible in middle of PAM) rotates rail and thus flexes leg by pushing on achilles tendon or extends hip by pulling on tibialis anterior tendon (curved arrow shows motion of rail that results from actuation of hip cylinder). Subject also wears harness connected to force-controlled body-weight support system (not visible). [62]

11. Mobility Training Device: The mobility training device, which apply a treadmill while training. Some examples use a partial bodyweight support, assisting patients to re-learn walking movements through repetition and task-oriented training. The main aim is to eliminate the need of the patients to deal with balance during the gait, focusing their concentration on the lower limb movements. Additionally, the body-weight support relieves the patient from his own load. The treadmill-based training devices have been the most common method for mobility training.(See **Fig. 1.25**)

Their target users are patients who suffer from musculoskeletal or neurological disorders (muscular dystrophy, amputees, multiple sclerosis, spinal cord injury, lower extremity joint pain). One of the most debilitating aspects for musculoskeletal or neurological disorders is the loss of the ability to ambulate. Gait restoration is an integral part of rehabilitation of brain lesion patients. Modern concepts favour a task-specific repetitive approach, i.e. who wants to regain walking has to walk, while tone-inhibiting and gait preparatory manoeuvres had dominated therapy before. Following the first mobilization out of the bed, the wheelchair-bound patient should have the possibility to practise complex gait cycles as soon as possible. Steps in this direction were treadmill training with partial body weight support and most recently gait machines enabling the repetitive training of even surface gait and even of stair climbing. [63](See **Fig. 1.25 - (a)**)

The HapticWalker accomplishes the paradigm for optimal training, because it is the first gait rehabilitation device which is not restricted to training of walking on even ground.(See **Fig. 1.25 - (b)**) In contrast to all treadmill bound machines, it enables the patient to train arbitrary gait trajectories and daily life walking situations. It is also distinct from the small number of haptic foot device prototypes, which have been built by groups in the USA [64, 65] and Japan [66, 67] for healthy subjects (e.g. virtual soldier training). Unlike these machines, which are designed to provide contact between foot and footplate

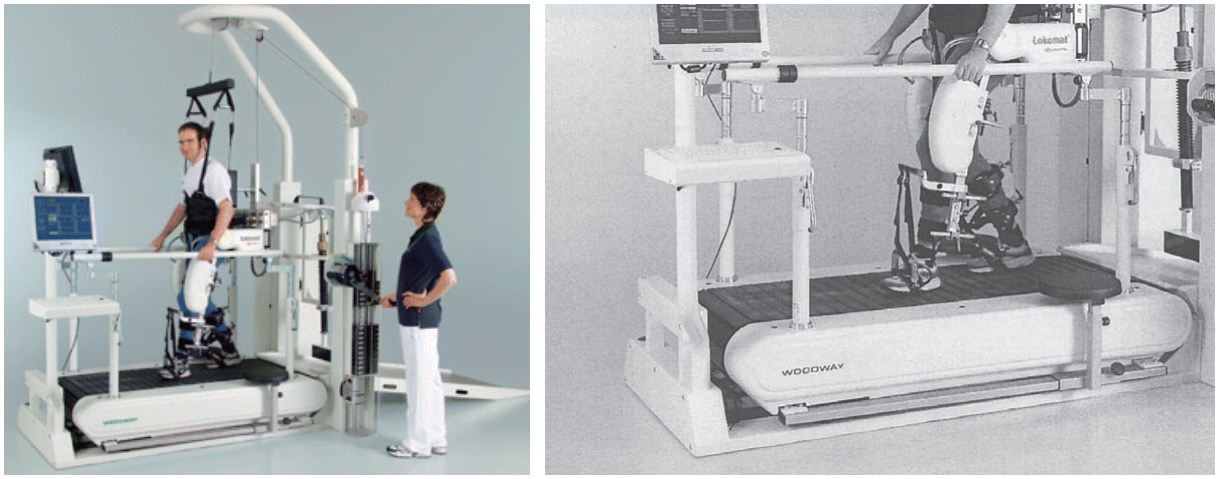

(a) The driven-gait orthosis (DGO).

(b) HapticWalker with Spinal cord injury(SCI) patient and physiotherapist.

Figure 1.25: Mobility Training Device.

only during stance phase, the HapticWalker comprises a translatory and rotatory footplate workspace needed for permanent foot attachment along arbitrary walking trajectories during all phases of gait. This is an essential feature for gait rehabilitation machines. A group at Rutgers University [68] recently built a small walking simulator tested with permanent foot attachment based on two small Stuart platforms. Those motion platforms, which are also called hexapod platforms, are based on a parallel kinematics principle and often used for flight simulators. The workspace and dynamic range of the small Stewart platforms the group designed are very limited and do not allow for natural walking profiles. [69]

12. Limbs Rehabilitation: The limbs rehabilitation devices manipulate the legs [70], according to the kinematics provided by each mechanism and the speed desired. However, they need to be permanently installed in a room. They require that patients have to be moved from their beds to that room to experience the robotic rehabilitation. Unfortunately, depending on the healthy state of the patients, it may not always be possible to move the patient out of his bed to start the rehabilitation therapy. Additionally, waiting may imply destruction of cortical tissues, and less possibilities of recovering these neural functionalities.(**Fig. 1.26 - (a)**)

The limbs rehabilitation system is a robotic device dedicated to the recovery of walking skills in stroke patients during the acute phase, when they are on bed, not yet able to keep a safe upright posture and walking. The system has been designed in order to provide, as soon as possible, rehabilitation therapy, thus avoiding as much as possible further damages of the cortical tissues due to their non-use, and to facilitate neural function recovery with repetitive exercise. Stroke involves several modifications on walking performance due to the damages occurred in the Central Nervous System. Adaptive plasticity and favorable recovery could result from an early, intensive and task oriented neuro-motor rehabilitation aimed at preventing abnormal posture, training muscle performance and allowing re-learning of motor skills. To this aim, a new robotic platform, called NEUROBike [71–73], is presented. It has been designed in order to overcome limits of the commercial rehabilitative robots.(**Fig. 1.26 - (b)**)

1.3 Motivation

As mentioned above, many kinds of nursing-care robots have been developed to aid people walking. For different needs, some of them are big in size or heavy in weight, in that case it can achieve the robust stability but at the cost of losing the mobility. In another hand, many small size walker robots gain the mobility advantage, but they cannot provide

(a) A low-limb rehabilitation device.

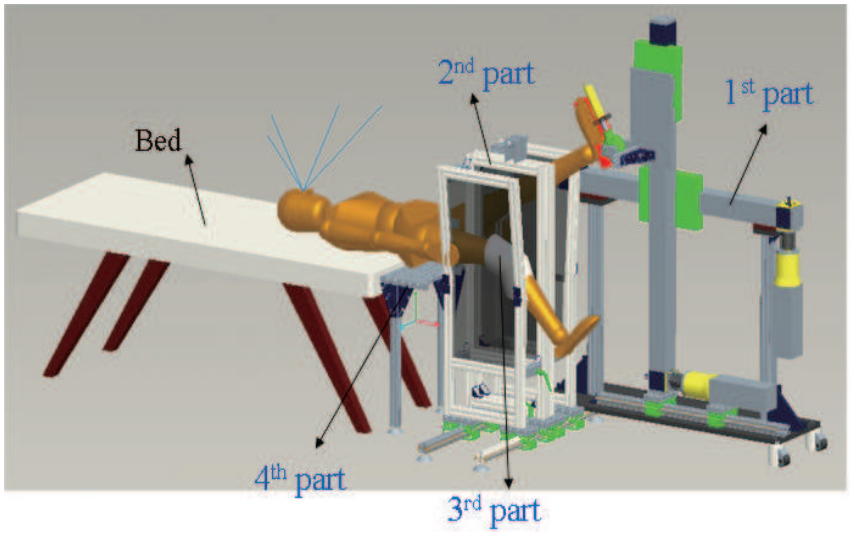

(b) Overall structure of NEUROBike.

Figure 1.26: Limbs Rehabilitation.

enough support while the user is losing his balance. The compared result with related works shows that the mobility is inversely proportional to stability(see 1.27)

Therefore, in our study we are aiming to develop a downsized nursing-care robot to assist people walking with both high mobility and trustable stability. Even the too much light weight lead to the overturn issue, by controlling the motion of robot, the falling moment can be counteracted.

1.3.1 Applicable Targets

In Japan where the aging of the population has been advancing at a rate which is unprecedented in world history the issue of long-term care for the elderly is one of the most important issues facing citizens, along with the issues of medical care and pensions. The spouses or children of elderly people have traditionally provided long-term care. Ministry of health, labor and welfare, Japan defined the nursing-care levels as shown in **Fig. 1.28**. The elderly in the "Support Level 1,2" and "Care Level 1" are not so weak, they can walk by themselves and live an independent life.

As the most basically motion functions- 'standing', 'sitting up', 'standing on one leg' and 'walking' abilities are use to define the user nursing-care levels. More additional judgement conditions which are including the mental and cognitive factors are proposed to classify the elderly into different levels.

For the support level 1. the people are competent to live with themselves. Although they are slower in motion or response then they were young, but they almost can live without any assistance or support. For the support level 2 and care level 1, people have different degrees of disability e.g. the muscle weakness or geriatric diseases which lead the elderly can not live an independent life. Most people in there levels have problems with walking. Because the lower limb function degradation, they are in a high risk of falling. Therefore, many kinds of walking assistance device are used to help them walking. Because the support limitation of our cane robot, people who are identified in the care level 2 and more higher levels can not only user the cane robot for nursing-care. Particularly, for the care level 4 and 5, people can not walking any more, in other words, they are bedridden.

1.3.2 How to define nursing-care level

For assisting the elderly safe and effective, firstly we needs define the user group. In [74], a study of the standing test for imbalance and disequilibrium(SIDE) was proposed to classify the nursing-care level. Postural control ability was decided based on whether the subject

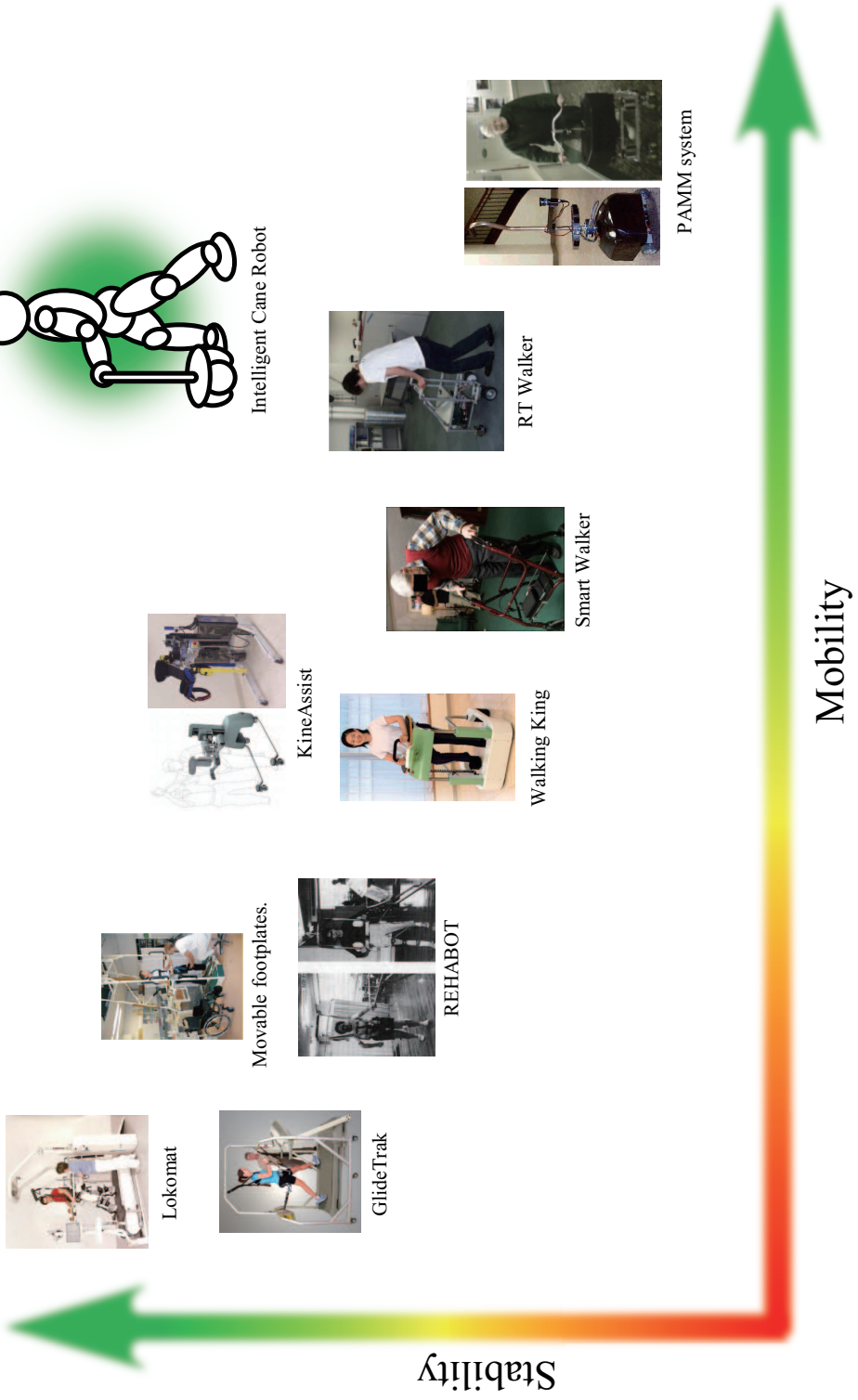

Figure 1.27: Compared with related works.

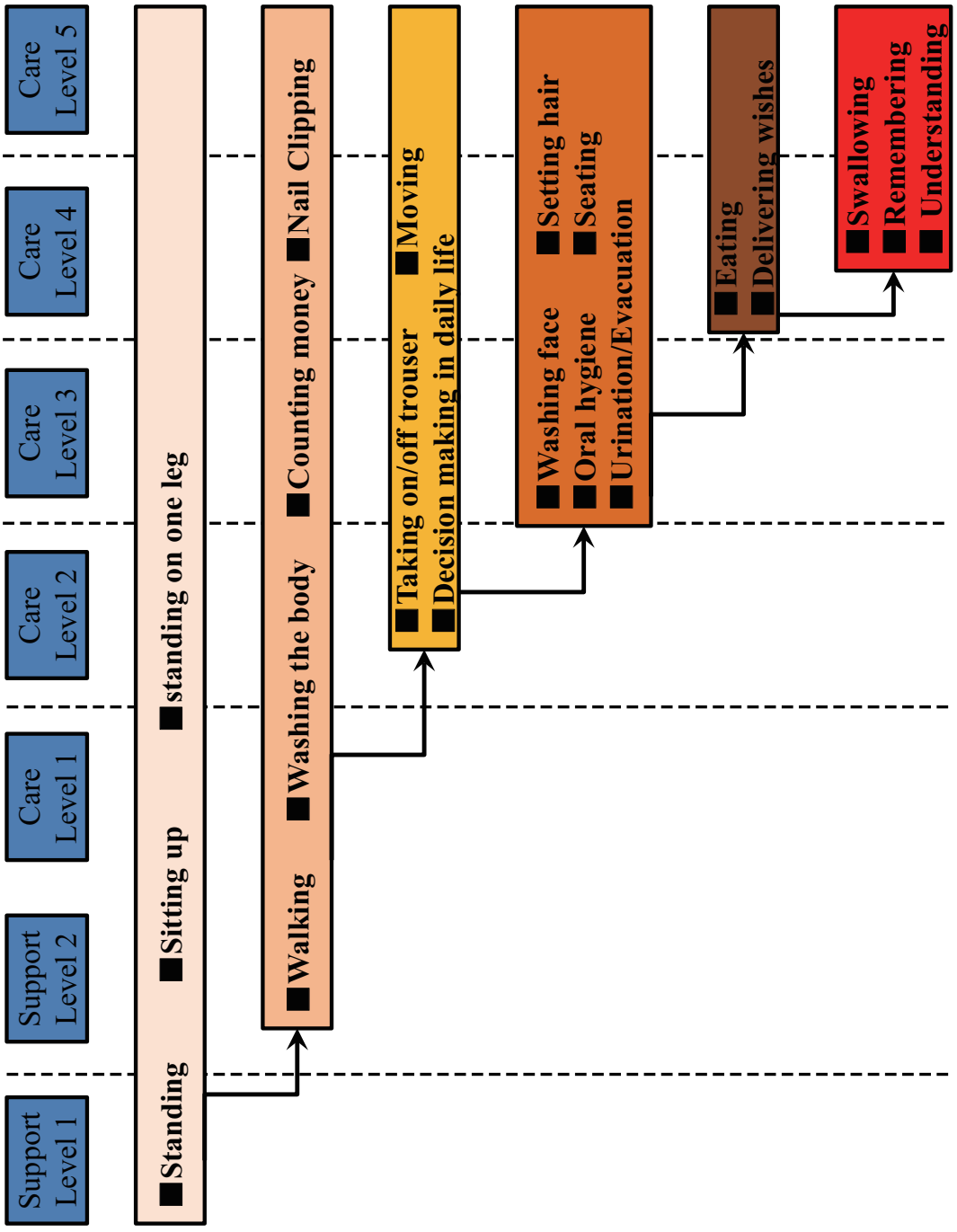

Figure 1.28: The definition of nursing-care levels.

Table 1.2: Classification of SIDE

	WB	NB	TS	OF
Level 0	×	×	×	×
Level 1	$5s^-$	×	×	×
Level 2a	◯	$5s^+$	$5s^-$	×
Level 2b	◯	◯	$5s^+$	×
Level 3	◯	◯	◯	$30s^-$
Level 4	◯	◯	◯	$30s^+$

could maintain a sequence of postures adopted in each level. The sequence of postures was wide-base, narrow-base, tandem stance, and one-foot stance, respectively (**Fig. 1.29**).

The levels are arranged in order of difficulty; more levels should not be included once a subject loses balance at a certain leveland requires assistance. As the level of difficulty in the test increases, the risk of falling increases. Level 0: a standing position with a wide base cannot be maintained by a patient without assistance. Supports provided by grasping something or being assisted by caregiver are always required to maintain a standing position. Level 1: a standing position with a wide base can be maintained without assistance, but standing with a narrow base cannot be maintained for more than 5 s. Balance is lost in a standing position with a narrow base, which involves bringing the legs close together such that feet are in contact with each other medially at both the heel and forefoot. Level 2a: a standing position with a narrow base can be maintained by a patient for more than 5 s, but a tandem standing position cannot be maintained for more than 5 s with either leg position.The tandem standing position involves standing with the heel of one foot placed at the toe of the other foot, in a straight line (either foot may be in the front). Level 2b: a tandem standing position can be maintained by a patient for more than 5 s with one, but not the other, leg in the leading position. Level 3: a tandem standing position can be maintained with either leg in the front for more than 5 s, but standing on one leg is difficult to maintain for more than 30 s with either leg. Level 4: a position of standing on one leg can be maintained for more than 30 s with any one leg. (see **TABLE. 1.2**)

WB: standing with a wide base. **NB**: standing with a narrow base. **TS**: tandem standing. **OF**: standing on one foot

Center of pressure (COP) was measured using a on-shoe load sensor(see **Fig. 1.30**). At first, practice trials were provided so subjects could become familiar with the measure-

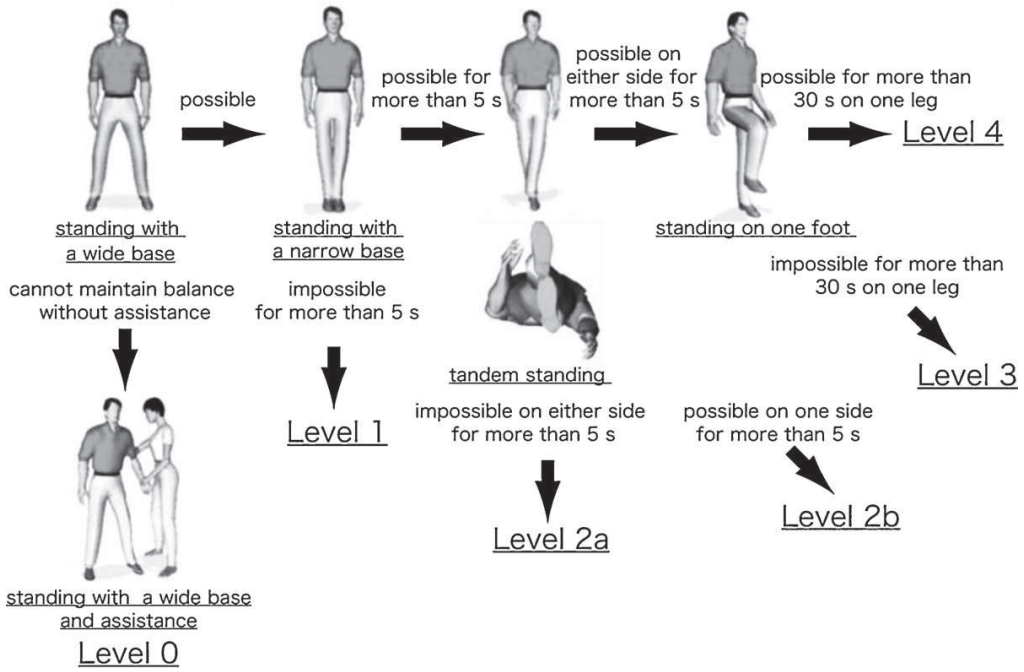

Figure 1.29: Flowchart to determine the level of SIDE.

ments. After subjects stabilized themselves with the on-shoe load sensor, COP trajectories were collected for 30s at a sampling rate of 10fps in each trial. Subjects stood wearing the on-shoe load system with eyes open and arms at their sides. We did not use a visual target or muffle distracting noises, as SIDE is usually performed at the bedside or in a gym under ordinary hospital circumstances.

Subjects were asked to stand under four stance conditions: wide-base; narrow-base; tandem; and one-foot. Subjects stood with feet 20 cm apart and parallel to each other in the wide-base stance. During the narrow-base stance, subjects stood with feet touching each other at the medial sides. Subjects stood with one leg in front of the other with heel and toe touching in the tandem stance on the longitudinal axis of the force-plate, to ensure that both feet were on a straight line. During the one-foot stance, subjects stood with one foot on the longitudinal axis of the force-plate and the other leg not touching the plate or ground outside the plate.

1.3.3 Concepts and Contents

There are three main topics of this research, the ‘Safety’, ‘Assistance’ and ‘Usability’. In the past 5 years, 5 prototypes of cane robot have been development to realize different

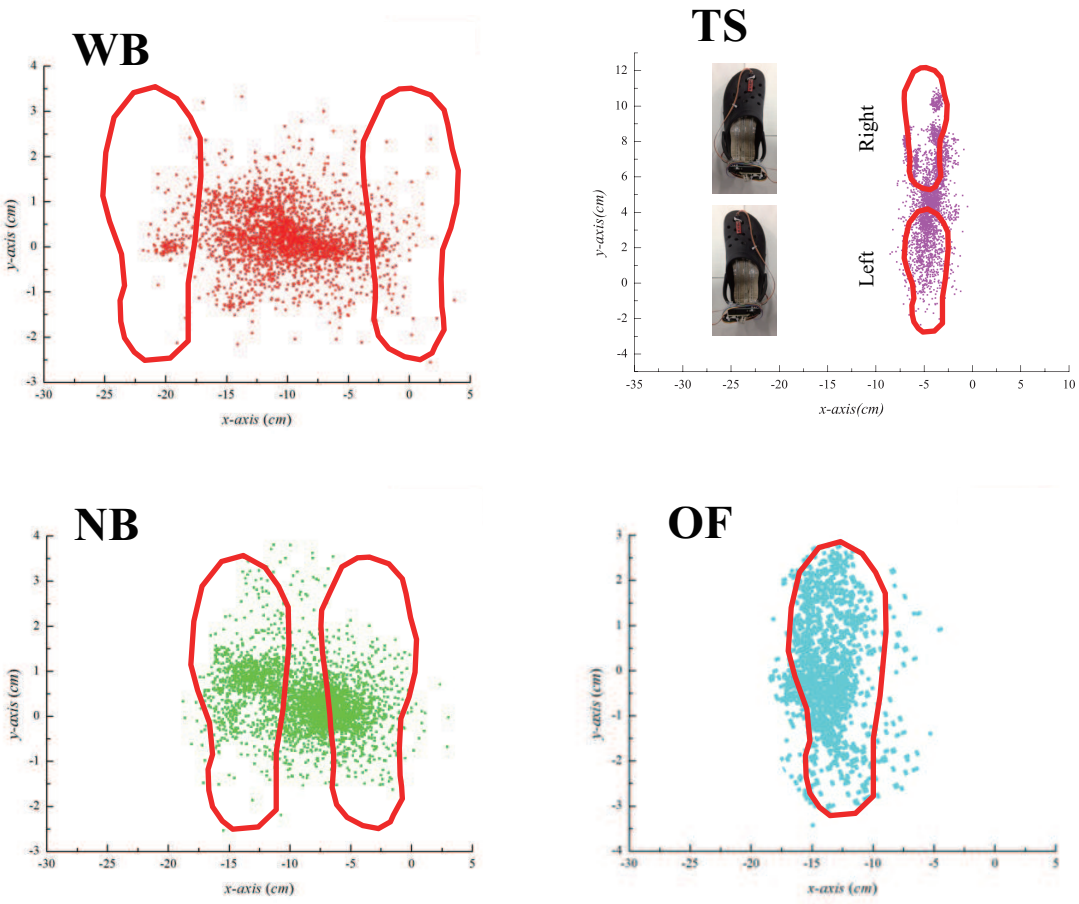

Figure 1.30: To classify the nursing-care level by measuring SIDE,

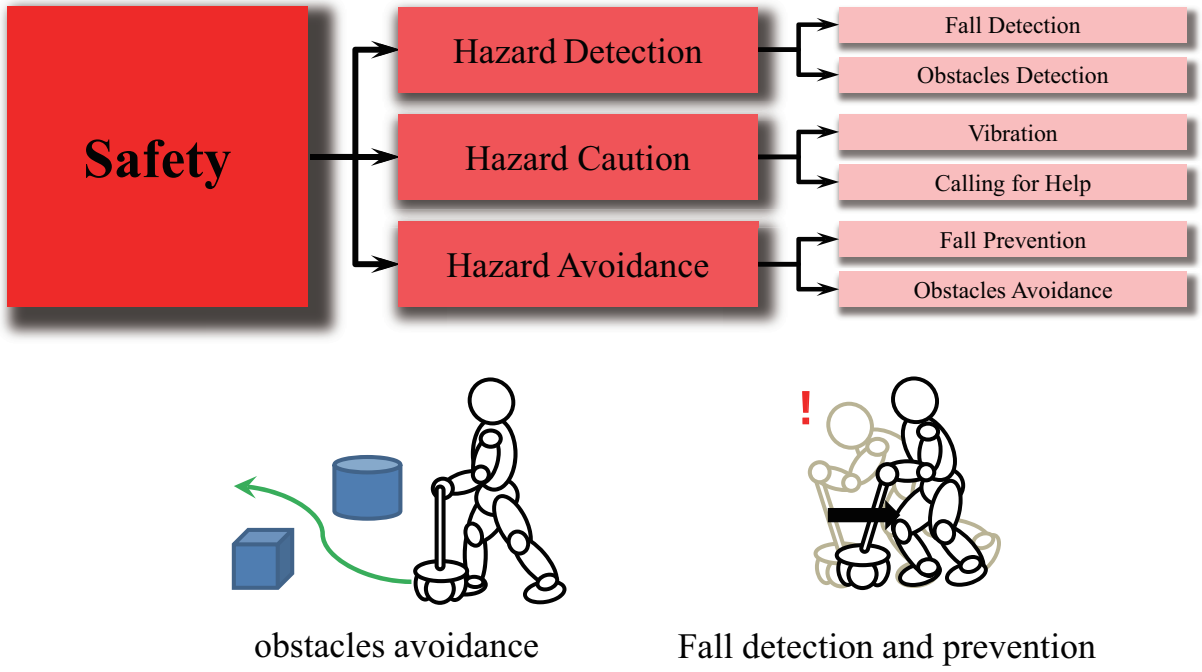

Figure 1.31: Research contents of intelligent cane robot - Safety.

functions. The cane robot becomes more intelligent and trustable. More and more useful functions are added in this system. in the following paragraph the contents of research will be introduced.

Safety

The safety is the most important part for a nursing-care robot. Firstly, we need to make sure that the robot do not runaway i.e. the cane system should be robust enough to tolerate the sensing error or misunderstand the human intention. For the user and the environment there also many safety issues that we need to over come. We divide the safety issue into three parts:

- ***Detection*:** As the preconditions for avoiding the danger, to detect and predict the risk are particularly important. The dangers including two sides, the inner and the external; the inner risk means the fall over risk of human subject and the tip-over risk of cane robot. As we investigated the falling accident is the most remarkable factors that leading the elderly to be injured or even dead. So the cane robot system mostly be improved around the user walling safety. In the **Chapter 4** we discuss some fall detection methods for human subject and the stability of cane robot. By

using the laser rangefinder which is fixed on the base of cane robot, the obstacles can be detected e.g. walls, steps or some moving object closing to the user.

- ***Caution*:** As soon as dangers be detected the cane robot should notify the user, so that he/she can make a optimal decision to avoidance the dangers. There are many ways to sending the risk caution to the user by using the auditory, visual or tactile sense.

- ***Avoidance*:** The user can actively avoid the danger based on the cautioned information or passively do it with the help of cane robot. In the **Chapter 5**, a fall prevention method is propose to help the user to keep balance, and a tip-over prevention strategy is investigated to guarantee the stability of cane robot.

Assistance

The cane robot does not only can aid the elderly walking, but also have numbers of helpful functions. For examples, in the **Chapter 3**, a optimized motion control method is proposed for easing muscular fatigue during user walking. By using a smartphone, the cane robot can also play an important role in the navigation. In our future works, the function of standing up and sitting down assistance will be realized.

Usability

For the elderly, it will takes much more time to learn how to use a high-tech machine. The complicated operations and multi-functions make the elderly confused. Therefore, in our previous study(see **Chapter 2**), a concept idea called "Intention Direction" was proposed to estimate the human walking intention. By using a force sensor as the input single source, the direction to which the user intended is estimated. The magnitude of the force is used to represent the intended walking speed.

1.4 Organization of Thesis

In **Chapter 1**, we discuss the research background about the aging population and falling birth rate. The motivation of this study is to development a downsized cane-type robot to aid the elderly in daily life. In order to achieve this goal, at the beginning of this project a prototype have been manufactured. An omni-wheel robot is used as the mobile base of cane robot. A concept called "Intention Direction" was proposed to estimate the human

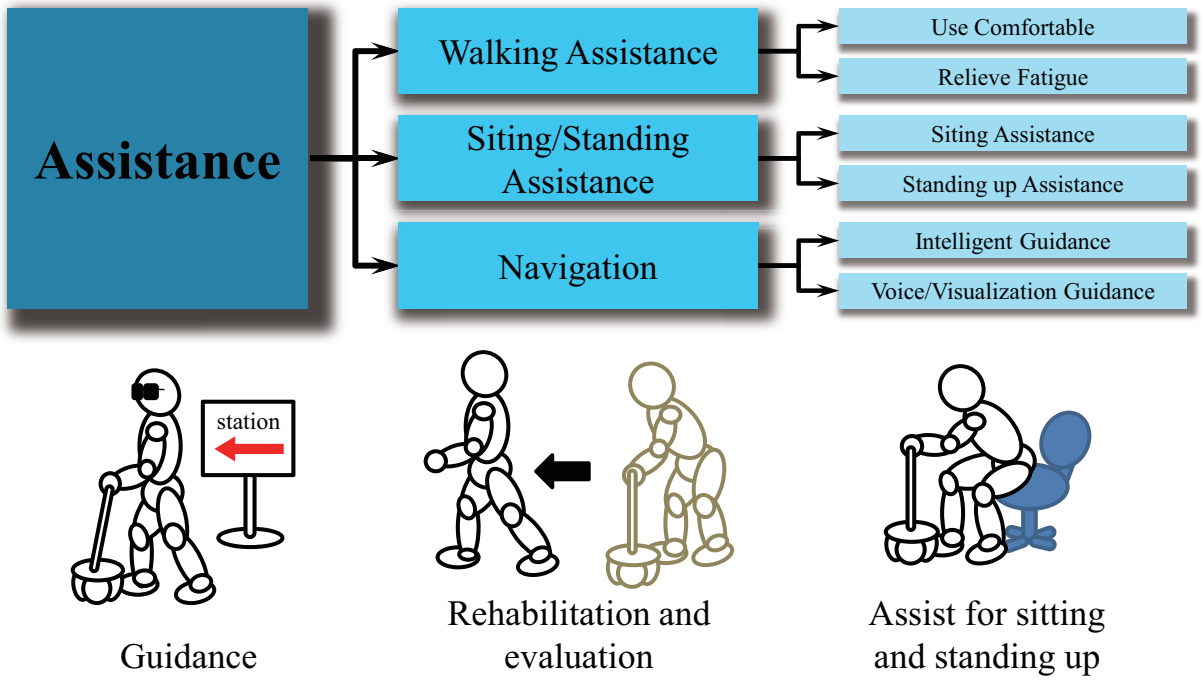

Figure 1.32: Research contents of intelligent cane robot - Assistance.

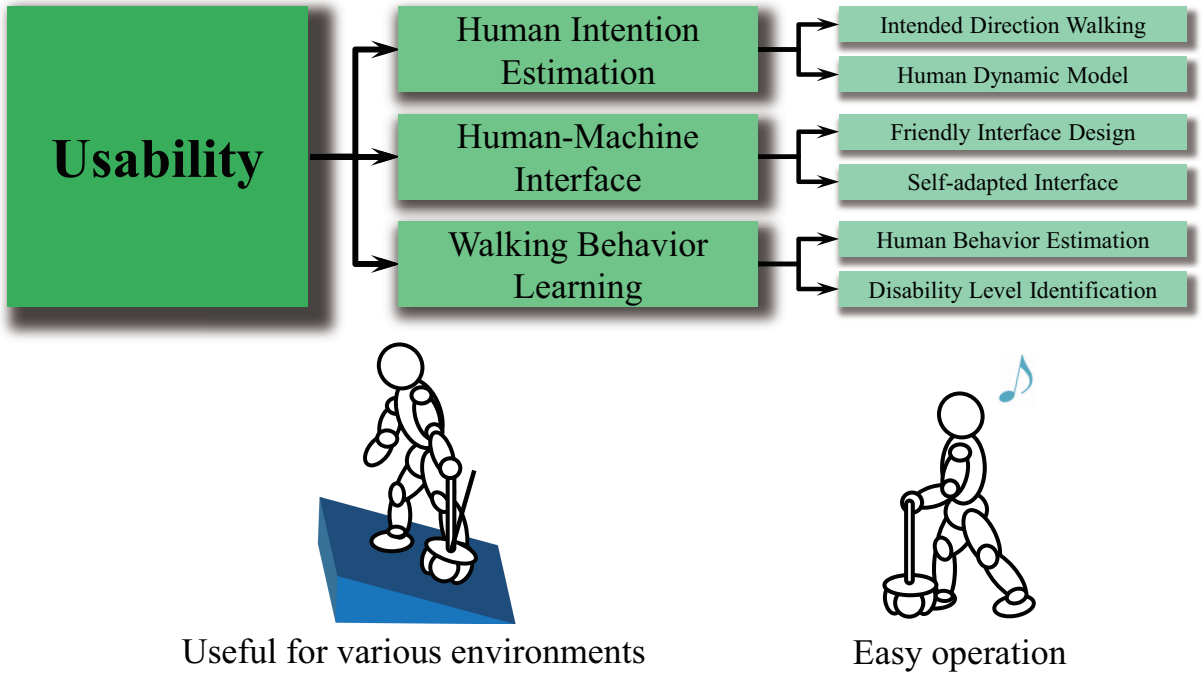

Figure 1.33: Research contents of intelligent cane robot - Usability.

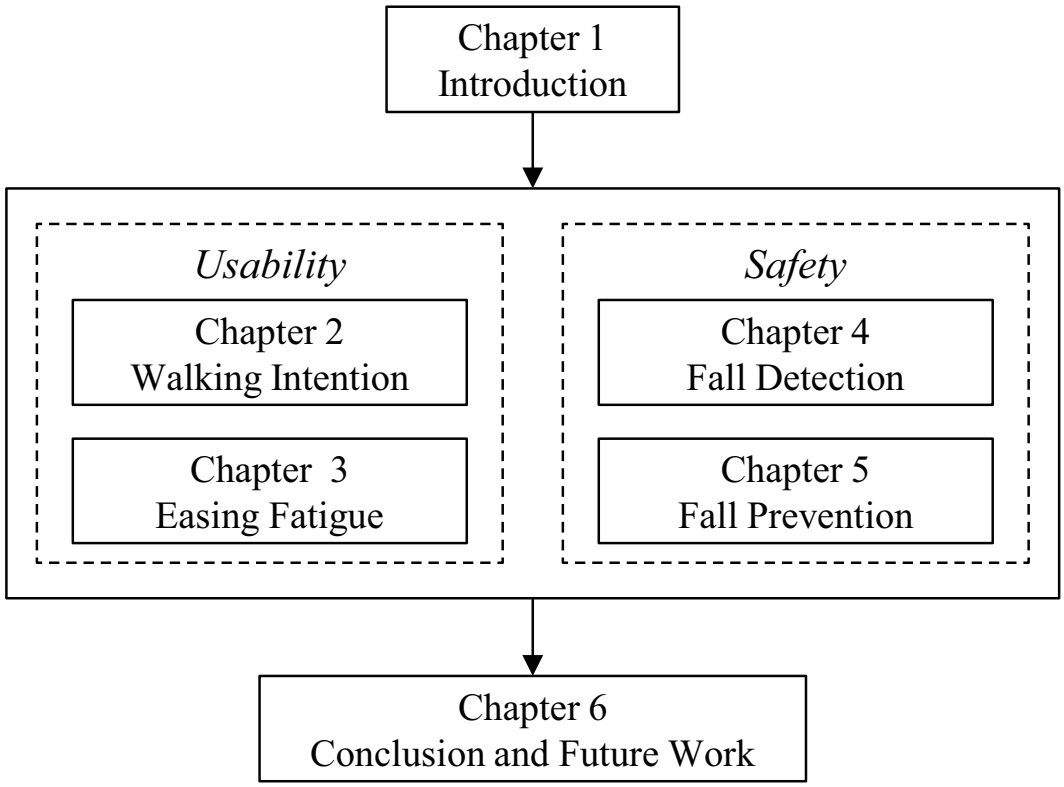

Figure 1.34: Structure of thesis.

walking intention. This quantized human intention is used to control the cane robot to move in the same velocity as human operator(see **Chapter 2**). A optimized motion control method is proposed for easing muscular fatigue during user walking in the **Chapter 3**. And a useful device - on-shoe load sensor is proposed to test the effectiveness of fatigue relieving. Because the safety is the most important issue in this study, in **Chapter 4** and **Chapter 5** we proposed the fall detection and prevention methods to guarantee the safety of both the human user and the cane robot.

Chapter 2

Human Walking Intention Estimation

The intelligent cane robot is designed for aiding the elderly and handicapped people walking. The robot consists of a stick, a group of sensor and an omni-directional basis driven by three Swedish wheels. Recognizing the user walking intention plays an important role in the motion control of our cane robot. To quantitatively describe the user's walking intention, a concept called "intentional direction (ITD)" is proposed. Both the state model and observation model of ITD are obtained by enumerating the possible walking modes and analyzing the relationship between the human-robot interaction force and the walking intention. From these two models, the users walking intention can be online inferred using Kalman filtering technique. Based on the estimated intention, a new admittance motion control scheme is proposed for the cane robot. Walking experiments aided by the cane robot on a flat ground and a slope are carried out to validate the proposed control approach. The experimental results show that the user feels more natural and comfortable when our intention based admittance control is applied.

The recognition of user walking intention plays an important role in the study of the walker-type rehabilitation robots. From the point of view of the control system of robot, the walking intention provides a real-time reference trajectory for the robot motion controller. Therefore, the more accurately the walking intention is inferred, the more satisfactory control performance of the robot may be obtained. Yamada et. al. proposed a manufacturing system controlled based on the human intention or desire . Kosuge, Hirata, et. al. proposed the dance partner robot which estimates the intention of human dancer . When we pay attention to the walker type walking support system, similar researches can be found in . In the study of motion intention recognizing approaches, the EMG-based methods are widely applied . However, the EMG signals are easily influenced by the location of electrodes, the thickness of fattiness, the body temperature and the perspiration. Meanwhile,

the information of the EMG signals is so large that a complicated preprocessing procedure is required before using them as the control input.

In this section, we improved our former intelligent cane system and studied its motion control problems in several situations based on estimating human walking intention. The human walking behavior is described by switching walking modes. To model the human walking intention, an important concept called 'intentional direction' (ITD) is proposed as well as its dynamic model during human walking. Without knowing the ITD accurately, it is not an easy task to design a motion controller of cane robot for an elderly or a handicapped user. Normally these people cannot walk along their ITD clearly and smoothly due to their weak or handicapped lower limbs. For instance, even an elderly intends to walk straightforwardly, he or she might finally walk along a zigzag trajectory because of stumbling. Therefore, the interactive forces measured by the cane robot consist of plentiful users unintentional walking information, which is part of the observation noise in the dynamic model of ITD. Comparing with a young healthy subject, apparently this observation noise of ITD is much bigger. Thus, it is necessary to pick up the ITD as accurately as possible from the noisy measurement. After that, we may design a robot motion controller based on ITD to aid the user walking in accordance with his actual walking intention. Some filtering technologies are used to online estimate the ITD, based on which a new force control scheme called intention based admittance control (IBAC) is proposed to provide a natural and intuitive interface for elderly users.

In this section, we first introduce a prototype system of omni-directional type cane robot shown in **Fig. 2.1**, which is developed to help the elderly walking and training their walking ability. The cane robot consists of an omni-directional mobile base, a metal stick and sensor groups including the force sensor, tilt angle sensors and the laser ranger finders (LRFs).

2.1 Omni-Directional Type Cane Robot

Fig. 2.2 shows the concept of the intelligent cane robot. As we stated in the introduction, the aim of our intelligent cane robot is to perform optimized actions to help the user walking or facilitate their recovery. These actions include 'walking assistance', 'fall prevention', 'rehabilitation training' and so on. To provide these optimized actions, one of the most important tasks should be accomplished by the robot is to correctly estimate the user walking intention online. From the point of view of the robot control system, the user walking intention provides a reference trajectory for the robot motion controller. Therefore,

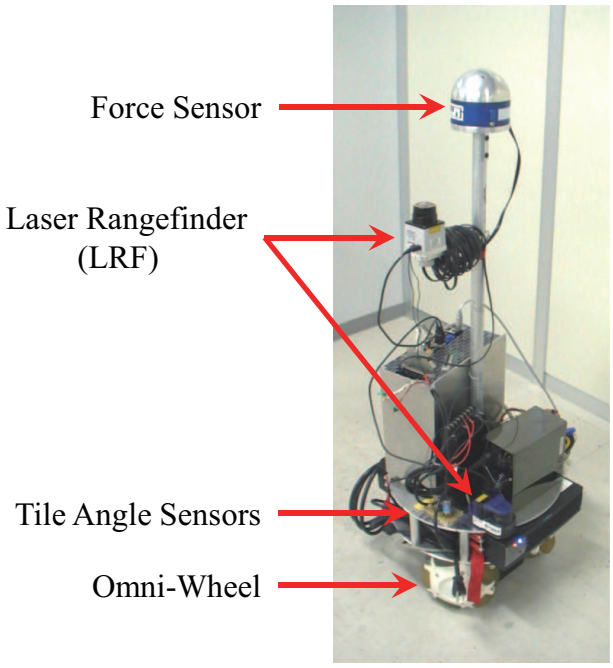

Figure 2.1: Omni-directional type cane robot prototype III.

in this paper we focus on the design of robot motion control strategy, in which the user's walking intention should be explicitly involved. This control strategy plays an important role in the design of a safe, reliable and compliant cane robot, which is the prerequisite of the rehabilitation training for the elderly and disabled.

The omni-directional mobile base comprises three commercially available omni-wheels and actuators, which are specially designed for the walker systems. Despite the small size, the load capacity of this mobile base is up to 50 kilograms. A six-axis force/torque sensor is used as the main control input interface. The force sensor plays an important role in the estimation of human walking intention, which is illustrated in the following sections. Two LRFs are used to measure the distances between the stick and the knees, and between the stick and the body, respectively. According to the online acquired distance information, fall-prevention function of the cane robot can be implemented as Hirata did in [53]. We use two tilt angle sensors to measure the slope angle when the cane robot is located on a slope. This angle is useful in the calculation of gravity compensation. The current position and posture of cane robot are inferred from the sensory data of encoders mounted in the omni-wheels.

To ensure the safety of cane robot, some measures are also taken. In the preprocessing of measured force signals, thresholds are used to get rid of outliers caused by impulsive

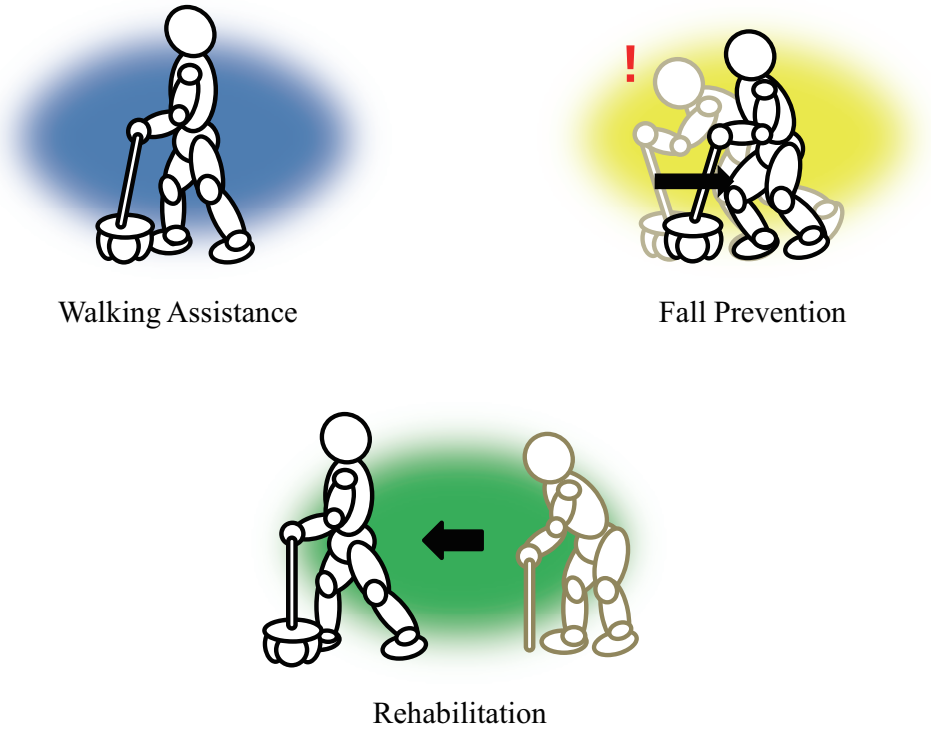

Figure 2.2: Concept of intelligent cane robot.

external disturbances. The output of motion controller is also restricted by some thresholds, which can avoid the sudden change of robot movement. On the other hand, the state of user is monitored by multiple sensors. If any emergency state is detected, the robot is braked to avoid possible injury to the user.

2.2 Modeling and Estimation of Human Walking Intention

2.2.1 Intentional Direction (ITD) and Its State Model

In order to facilitate the development of dynamic model and control strategy, the coordinate systems of cane robot is illustrated first.

As shown by **Fig. 2.3-(a)**, the coordinate system $O - x_0y_0z_0$ is the reference frame. The coordinate system $O - x_1y_1z_1$ rotates with the slope angel α around axis x_0. The slope plane is denoted by Π. The local coordinate system is fixed on the cane robot and rotates with the yaw angle ψ. $O - x_ry_rz_r$ is the local coordinate system fixed on the cane

robot**Fig. 2.3-(b)**.

To describe the human walking intention during using the cane robot, an important concept is introduced as follows.

Definition 1. The direction to which a person intends to move is referred to as the ITD.

As shown by **Fig. 2.4**, the ITD can be evaluated by the angle between the forward direction (along with axis y_r) and the ITD itself. The sight line is denoted by the broken line, which indicates the direction that the user is intentional to move. Obviously, the ITD is a time-dependent value and is denoted by $\rho(n)$ in the rest of the paper. Further, the quantity of this intention is characterized by the measured resultant force $F_p(n)$ along the ITD. Note that discrete time scale n is assumed for the requirement of filtering technology.

To formulate the walking intention quantitatively, it is required to obtain the dynamic model of ITD. The first thing we should do is to enumerate possible human walking modes. Although there are plentiful of possible modes during walking, only several of them are often used in the daily life. In this study, five simple walking modes are considered, which

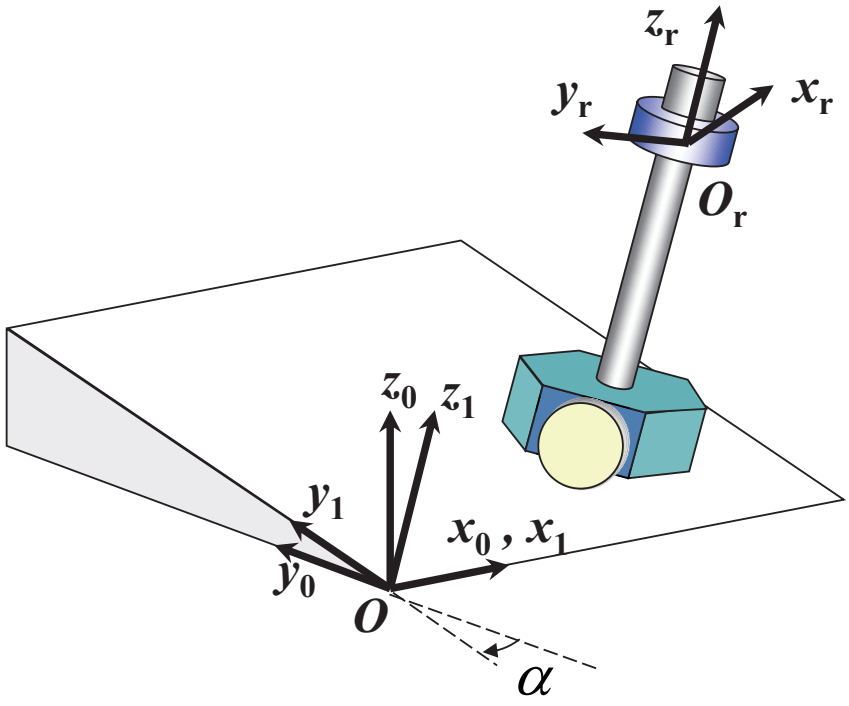

(a) Coordinate systems of cane robot on the slope.

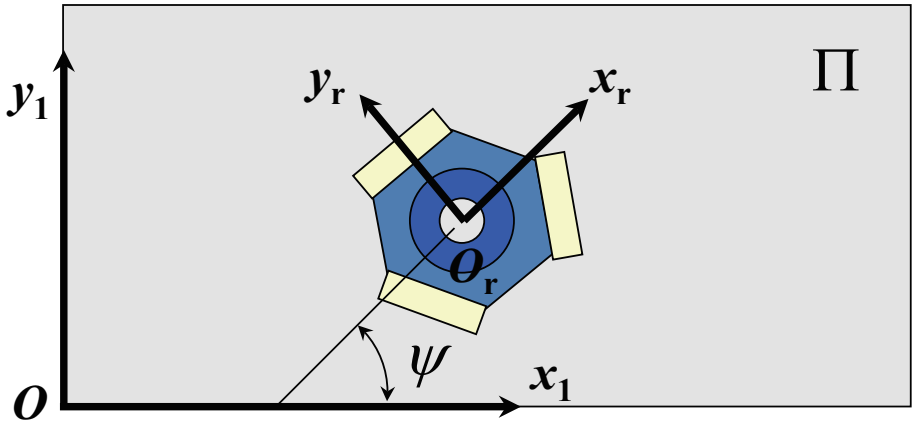

(b) Top view of the cane robot.

Figure 2.3: Coordinate system definition of the cane robot.

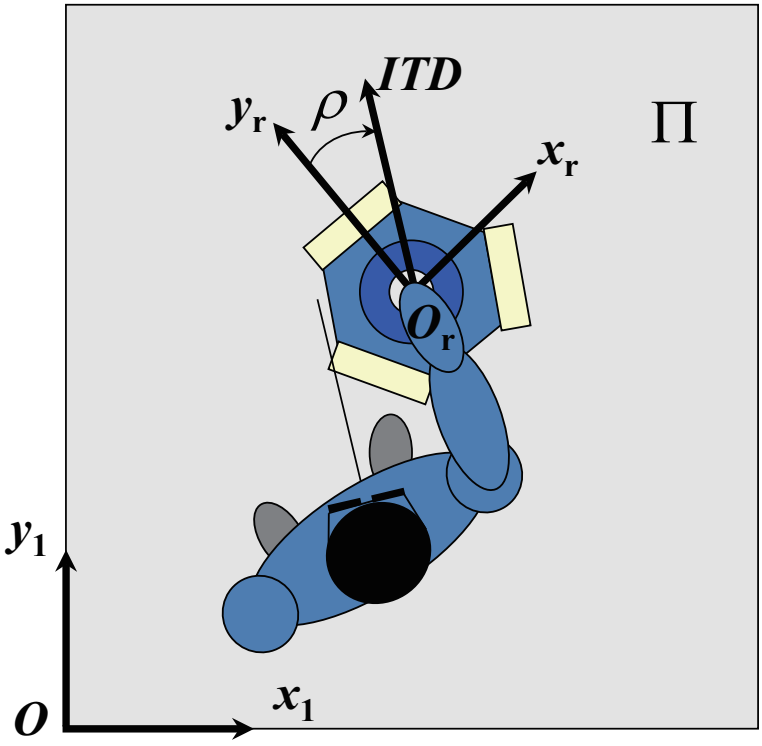

Figure 2.4: Quantitative representation of the intentional direction (ITD).

are listed in **TABLE 2.1**. We assume that there are three main types of walking modes including 'Stop' (mode I), 'Go straight' (mode II) and 'Turn around' (mode III) in daily

Table 2.1: Possible Walking Modes

Mode	Description
I	Stop
IIa	Go straight forward
IIb	Go straight in other directions
IIIa	Turn to the right
IIIb	Turn to the left

life. Further, mode II can be categorized into two sub-modes, 'go straight forward' (mode IIa) and 'go straight in other directions' (mode IIb). A typical case of human walking mode IIb is the fast lateral move to avoid a coming car. Mode III also can be further categorized into two sub-modes, 'Turn to the right' (mode IIIa) and 'Turn to the left' (mode IIIb). During walking, empirically we know that transitions may occur between any two walking modes. Therefore, all possible transitions among the five modes are illustrated by **Fig. 2.5**.

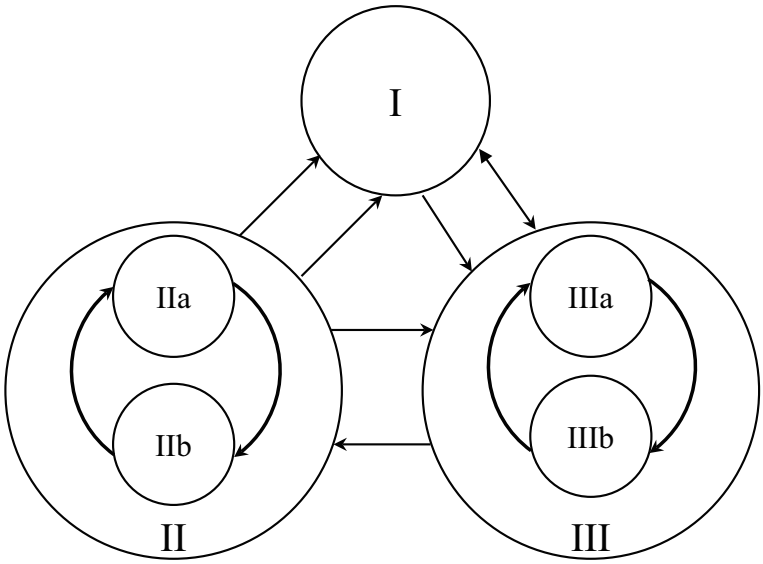

Figure 2.5: Transition diagram of possible move modes.

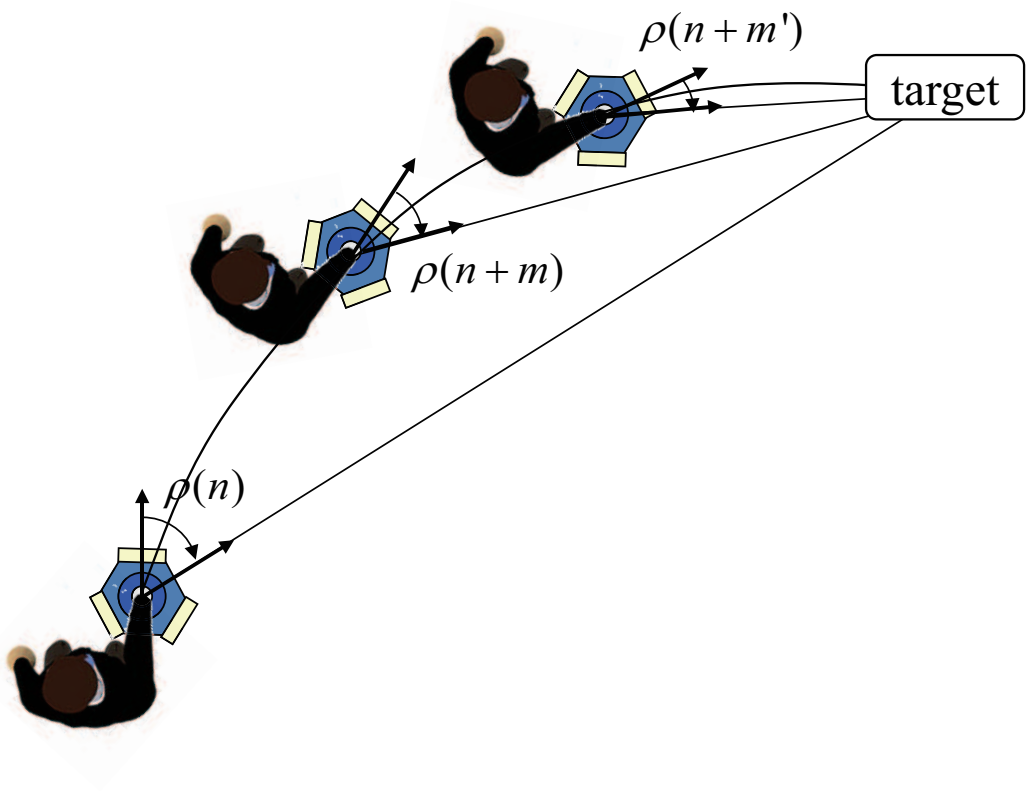

Figure 2.6: Typical turning around move mode.

Empirically, we have following assumptions on the walking intention in different walking modes.

- ***Assumption 1.*** In mode I, the ITD is supposed to be always zero.
- ***Assumption 2.*** In mode II, the ITD is supposed to be a constant.
- ***Assumption 3.*** In mode III, the ITD monotone converges to zero from an initial non-zero value.

Assumption 3 is proposed based on the natural behavior when a person turns around. As shown in **Fig. 2.6**, at the beginning of mode IIIa, normally there is a certain target one wants to move, which generates the initial ITD of the mode. During the process of turning around, the value of $\rho(n)$ decreases gradually and finally converges to zero, which causes a transition to mode I or II.

In terms of the enumerated walking modes and given assumptions, a hybrid state model of ITD is described by

$$\rho(n+1) = A_{\sigma(n)} \cdot \rho(n), \;\; \sigma(n) \in \{I, II, III\} \tag{2.1}$$

where $\sigma(n)$ denotes the different walking mode given by **TABLE 2.1**. The state transition matrices are given by

$$A_I = 0, A_{II} = 1, A_{III} = a(n) \tag{2.2}$$

where $a(n)$ satisfies

$$0 < a(n) < 1 \tag{2.3}$$

2.2.2 Observation Model of ITD Based on Human-Robot Interaction Force

Obviously, the ITD is indicated by the interaction force between the user and the cane robot. To compensate the gravity effect on the force sensor, first we analyze the static forces exerted on the upper part of stick. As shown by **Fig. 2.7**, P is used to denote the contact point between the force sensor and the upper part of stick. ${}^r\mathbf{F}$ and ${}^r\mathbf{n}$ are the force and torque exerted on the upper part of stick by the force sensor, respectively. ${}^r\mathbf{G}$ denotes the gravity force of the upper part of stick. ${}^r\mathbf{l}$ is the vector from point P to the center of gravity (COG) of the upper part of stick. In the rest of paper, we use a superscript on the left side of a vector to indicate the coordinate frame in which the coordinate value is represented.

To maintain the static equilibrium, the required force ${}^r\mathbf{F}^*$ and torque ${}^r\mathbf{n}^*$ are given by

$$\begin{aligned} {}^r\mathbf{F}^* + {}^r\mathbf{G} &= 0 \\ {}^r\mathbf{n}^* + {}^r\mathbf{l} \times {}^r\mathbf{G} &= 0. \end{aligned} \tag{2.4}$$

Let us assume

$${}^r\mathbf{F}^* = \begin{bmatrix} {f_x}^* \\ {f_y}^* \\ {f_z}^* \end{bmatrix}, {}^0\mathbf{G} = \begin{bmatrix} 0 \\ 0 \\ mg \end{bmatrix} \tag{2.5}$$

It follows from **Eq. (2.4)** and **Eq. (2.4)** that we have

$$\begin{bmatrix} {f_x}^* \\ {f_y}^* \\ {f_z}^* \end{bmatrix} = \begin{bmatrix} mg \cdot \sin\psi \sin\alpha \\ mg \cdot \cos\psi \sin\alpha \\ -mg \cdot \cos\alpha \end{bmatrix} \tag{2.6}$$

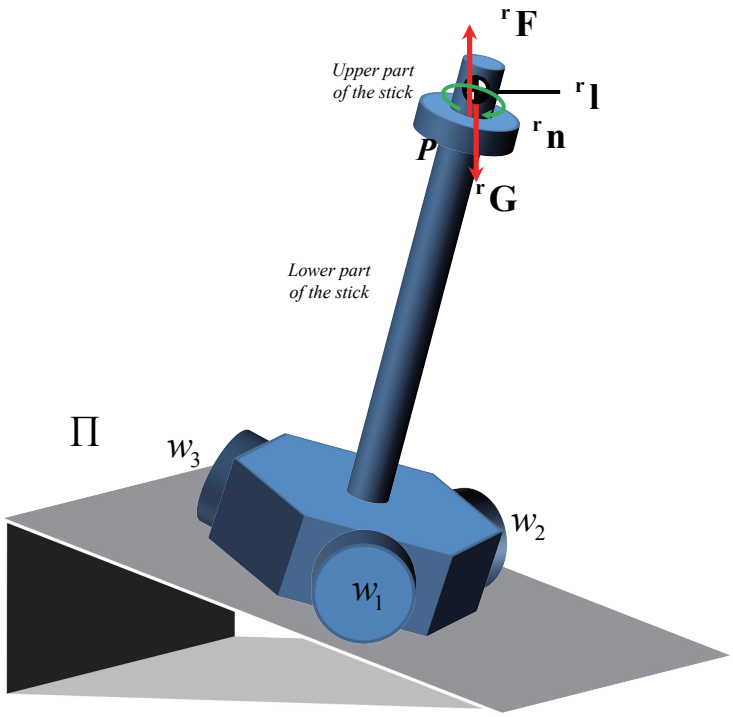

Figure 2.7: Static force analysis of the upper part of stick above the force sensor.

During the walking procedure supported by the cane robot, let us suppose the measured force and torque at time n satisfy

$$\begin{aligned} {}^{r}\mathbf{F}(n) &= \Big[f_x(n)\ f_y(n)\ f_z(n) \Big]^{\mathrm{T}}, \\ {}^{r}\mathbf{n}(n) &= \Big[n_x(n)\ n_y(n)\ n_z(n) \Big]^{\mathrm{T}} \end{aligned} \tag{2.7}$$

Then, the observation model of ITD can be described by

$$y(n) = \tan^{-1}\left(\frac{f_x(n) - {f_x}^*}{f_y(n) - {f_y}^*} \right) = \rho(n) + \omega(n) \tag{2.8}$$

where $\omega(n)$ is a combination of sensor noises and human gait habit. Note that the observation model is available for all the three modes listed in **TABLE 2.1**.

Everyone has particular gait habit when walking. For example, some people will unintentionally move laterally when they walk straight forward. For simplicity, we assume $\omega(n)$ is a white noise sequence with a direction-dependent covariance $Q(\rho)$ that differs from person to person. For the same person, experiments show that is almost the same

for different directions. This makes it possible to use traditional Kalman filter to estimate the ITD based on **Eq.** (2.1) and **Eq.** (2.8).

Rule set. (Rule-Based Method)

1. IF $\sigma(n-1) \neq$ I AND ${}^{r}F_x(n) \approx 0$ AND ${}^{r}F_y(n) \approx 0$ AND ${}^{r}n_z(n) \approx 0$, THEN $\sigma(n) =$ I.
2. IF $\sigma(n-1) \neq$ IIa AND ${}^{r}F_x(n) \approx 0$ AND $|{}^{r}F_y(n)| > 0$ AND ${}^{r}n_z(n) \approx 0$, THEN $\sigma(n) =$ IIa
3. IF $\sigma(n-1) \neq$ IIb AND $|{}^{r}F_x(n)| > 0$ AND $|{}^{r}F_y(n)| > 0$ AND ${}^{r}n_z(n) \approx 0$, THEN $\sigma(n) =$ IIb
4. IF $\sigma(n-1) \neq$ IIIa AND ${}^{r}n_z(n) > 0$, THEN $\sigma(n) =$ IIIa
5. IF $\sigma(n-1) \neq$ IIIb AND ${}^{r}n_z(n) < 0$, THEN $\sigma(n) =$ IIIb

In mode I and II, the dynamics of ITD is described by a linear state model. Therefore a conventional Kalman filter is suitable to be applied to online estimate the ITD.

In mode III, the state model of ITD can be rewritten as

$$\rho(n+1) = (a_0 + \Delta a(n)) \cdot \rho(n) \tag{2.9}$$

where a_0 is a constant and satisfies $0 < a_0 < 1$ is the model uncertainty. It is well known that normal Kalman filter will generally not guarantee satisfactory performance when uncertainty exists in the system model. Thus, we choose a robust Kalman filter to calculate the estimation of ITD in this case. In [**?**], Xie considered the uncertain dynamic

$$\begin{aligned} \mathbf{x}(n+1) &= [\mathbf{A} + \Delta\mathbf{A}(n)]\mathbf{x}(n) + \mathbf{w}(n) \\ \mathbf{y}(n) &= [\mathbf{C} + \Delta\mathbf{C}(n)]\mathbf{x}(n) + \mathbf{v}(n) \end{aligned} \tag{2.10}$$

with $x(n)$ denoting the state vector, $y(n)$ the measurement, $w(n)$ the driving disturbance with covariance matrix $W \geq 0$, $v(n)$ the measurement noise with covariance matrix $V \geq 0$ and matrices $\Delta A(n)$ and $\Delta C(n)$ representing the model uncertainty. If the uncertainties satisfy some matching conditions and the system is quadratically stable, then the estimator given by

$$\hat{\mathbf{x}}(n+1) = \mathbf{A}\hat{\mathbf{x}}(n) + \left(\bar{\mathbf{A}}\bar{\mathbf{Q}}\bar{\mathbf{C}}^{\mathrm{T}} + \mathbf{M}\right)\left(\bar{\mathbf{R}} + \bar{\mathbf{C}}\bar{\mathbf{Q}}\bar{\mathbf{C}}^{\mathrm{T}}\right)^{-1}\left(\mathbf{y}(n) - \bar{\mathbf{C}}\hat{\mathbf{x}}(n)\right) \tag{2.11}$$

provides a guaranteed steadyCstate estimation error as given by

$$E\left[\left(\mathbf{x}(n)-\hat{\mathbf{x}}(n)\right)^{\mathrm{T}}\left(\mathbf{x}(n)-\hat{\mathbf{x}}(n)\right)\right] \leq \operatorname{trace}(\bar{\mathbf{Q}}) \tag{2.12}$$

The detail of robust Kalman filter can be found in [?] and the estimator **Eq.** (2.11) can be efficiently solved through the Linear Matrix Inequalities (LMI) toolbox and the Discrete-time Algebraic Riccati Equations (DARE) function in MATLAB.

We conclude the above discussion by proposing the following online ITD estimation algorithm.

Algorithm 1. (Online ITD Estimation Algorithm)

Input: ${}^{r}\mathbf{F}(n-1)$, ${}^{r}\mathbf{n}(n-1)$, $y(n)$, $\hat{\rho}(n-1)$, $\sigma(n-1)$

1. Apply the rule-based method to determine $\sigma(n)$
2. IF $\sigma(n-1)=\sigma(n)$ THEN
3. SWITCH $\sigma(n)$
4. CASE I:Let $\hat{\rho}(n)=0$
5. CASE II:
6. Use the Kalman filter to infer $\hat{\rho}(n)$
7. IF $\sigma(n)=$ IIa THEN let $\hat{\rho}(n)=0$
8. CASE III:
9. Use the robust Kalman filter to infer $\hat{\rho}(n)$
10. ELSE
11. Let $\hat{\rho}(n)=y(n)$ to initialize the filter.
12. ENDIF

Output: $\hat{\rho}(n)$, $\sigma(n)$

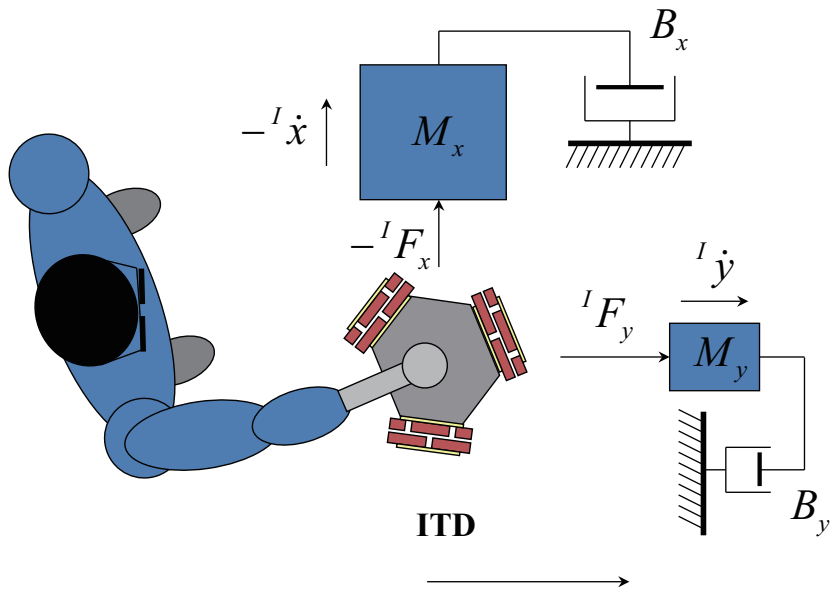

Figure 2.8: The principle of IBAC scheme.

2.3 Walking Intention Based Admittance Control

The cane robot motion controller uses an admittance control scheme based on the inferred human intention, which is called intention based admittance control (IBAC) scheme. The conventional admittance control uses an admittance model emulates a dynamic system and gives the user a feeling as if he is interacting with the system specified by the model. This model is defined as a transfer function with the users forces and toques, $F(s)$, as the input and the reference velocity of cane robot, $V(s)$, as the output. It is expressed as:

$$G(s) = \frac{V(s)}{F(s)} = \frac{1}{Ms + B} \tag{2.13}$$

where M and B are the mass and damping parameters respectively.

During walking, people feel comfortable if the cane is easily maneuvered in the ITD and hardly maneuvered in the direction perpendicular to the ITD. To meet the requirement, we propose the IBAC scheme in which two admittance models are used. One model is defined for the motion along the ITD, which has selected mass and damping parameters from the acceptable area presented in [**?**]. The other model is defined for the motion perpendicular to the ITD, which has much bigger mass and damping parameters. The general idea is shown by **Fig. 2.8**. The final three-DOF mass-damping model for our cane robot is defined as:

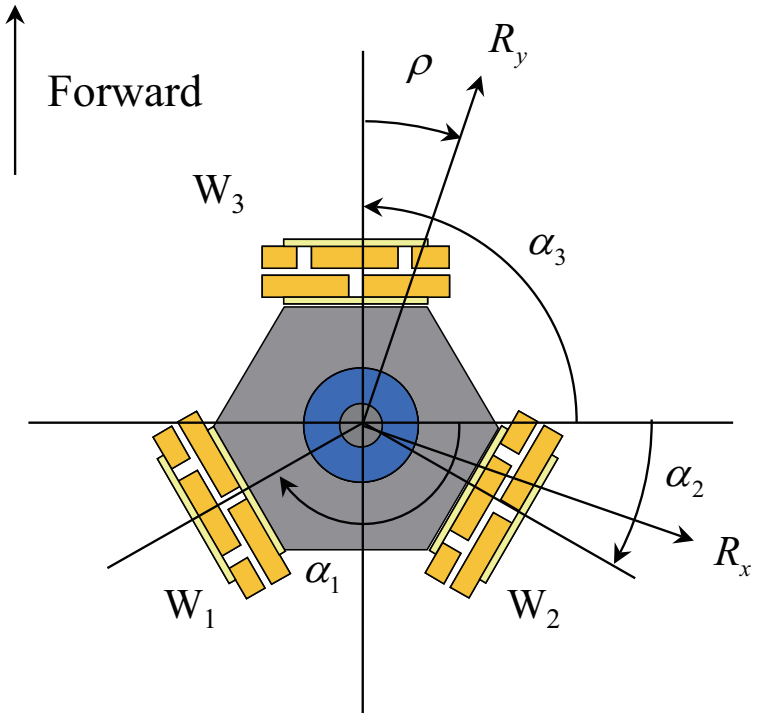

Figure 2.9: Coordinate frame I based on the ITD.

$$\mathbf{M^d} \cdot {}^I\ddot{\mathbf{q}} + \mathbf{B^d} \cdot {}^I\dot{\mathbf{q}} = {}^I\mathbf{F} \tag{2.14}$$

where state $\mathbf{q}$ and the measured force $\mathbf{F}$ are represented in the coordinate frame {I} **Fig. 2.9** based on the current walking intention, satisfying

$${}^I\mathbf{q} = \begin{bmatrix} {}^Ix \\ {}^Iy \\ \rho \end{bmatrix}, {}^I\mathbf{F} = \begin{bmatrix} {}^IF_x \\ {}^IF_y \\ n_z \end{bmatrix} \tag{2.15}$$

Matrices $\mathbf{M^d}$ and $\mathbf{B^d}$ are the desired mass and damping coefficients. These coefficients are described by

$$\mathbf{M^d} = \begin{bmatrix} {M_x}^d & 0 & 0 \\ 0 & {M_y}^d & 0 \\ 0 & 0 & {J_z}^d \end{bmatrix}, \mathbf{B^d} = \begin{bmatrix} {B_x}^d & 0 & 0 \\ 0 & {B_y}^d & 0 \\ 0 & 0 & {B_z}^d \end{bmatrix} \tag{2.16}$$

where ${M_x}^d >> {M_y}^d, {J_z}^d$and ${B_x}^d >> {B_y}^d, {B_z}^d$

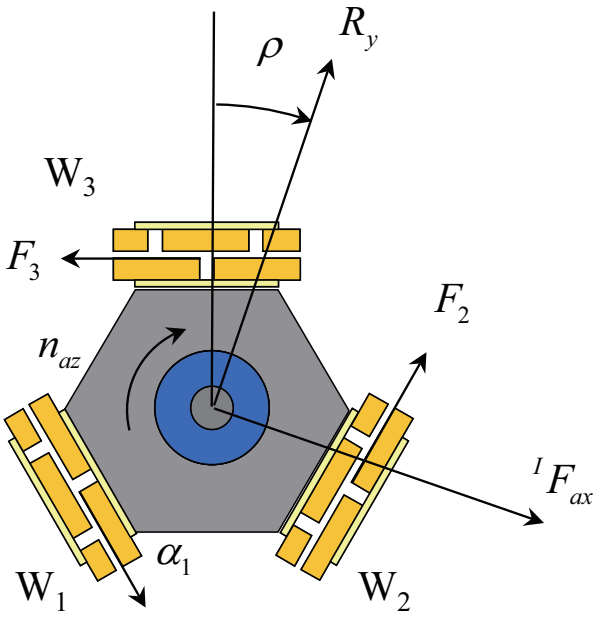

Figure 2.10: Resultant driven force.

In the motion control of cane robot, we assume that there is no slip between the wheels and the ground in active driving direction. The real dynamics of cane robot is then described by

$$\mathbf{M} \cdot {}^I\ddot{\mathbf{q}} = {}^I\mathbf{F} + {}^I\mathbf{M_G} + {}^I\mathbf{F_a} \tag{2.17}$$

where ${}^I\mathbf{M_G}$ is the gravity of the whole robot represented in frame {I}. ${}^I\mathbf{F_a} = \begin{bmatrix} {}^I F_{ax} & {}^I F_{ay} & n_{az} \end{bmatrix}$ is the resultant driven force caused by the frictions between wheels and the ground (**Fig. 2.10**). The driven force acts as the control input to the robot and is generated by regulating the three motors of omni-wheels. Matrix $\mathbf{M}$ contains the mass and moment coefficients, satisfying

$$\mathbf{M} = \begin{bmatrix} m & 0 & 0 \\ 0 & m & 0 \\ 0 & 0 & J \end{bmatrix} \tag{2.18}$$

where m and J are the real mass and moment of cane robot respectively.

By eliminating the acceleration from **Eq.** (2.14) and **Eq.** (2.17), the required resultant driven force is computed as follows:

$${}^I\mathbf{F_a} = -\mathbf{M}\left(\mathbf{M^d}\right)^{-1}\mathbf{B^d} \cdot {}^I\dot{\mathbf{q}} + \mathbf{M}\left(\mathbf{M^d}\right)^{-1} \cdot {}^I\mathbf{F} - {}^I\mathbf{F} - {}^I\mathbf{M_G} \tag{2.19}$$

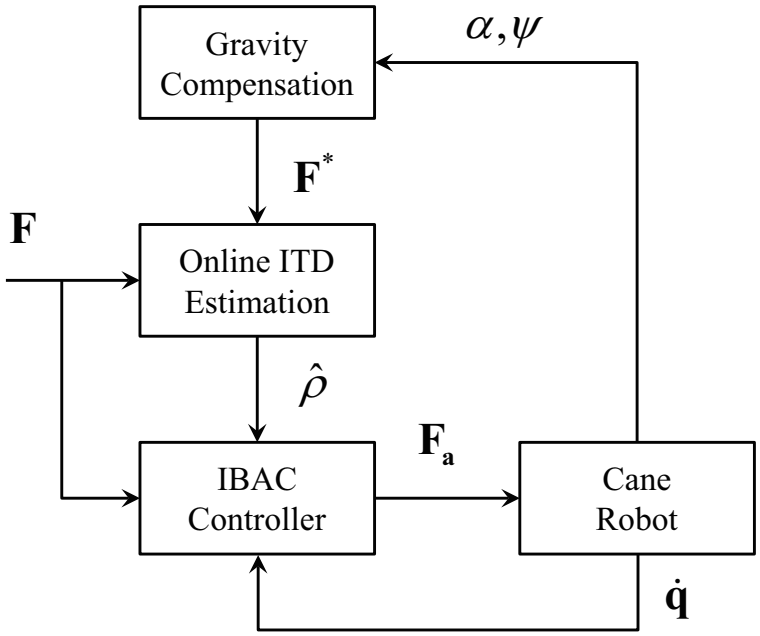

Figure 2.11: Control diagram of the whole system.

The control diagram of the whole cane robot system is shown by **Fig. 2.11**. At each control period, the interactive force $\mathbf{F}$ between the user and the cane robot is measured by the multi-axis force sensor. The current robot yaw angle ψ and slope angle α are measured by the tilt sensors and encoders. The velocity of robot $\dot{\mathbf{q}}$ is measured by the encoders. Then the ITD is online estimated by using ***Algorithm 1***. This estimation is fed into the IBAC controller model to calculate the driven force ${}^{I}\mathbf{F_a}$, which is finally allocated to the three wheels.

2.4 Experiments

To verify the effectiveness of our proposed walking intention estimation approach and the IBAC control strategy, several experiments were performed in different situations. First, we investigated the assumption that the covariance of observation noise of a same person is almost the same for different walking directions. Then, we conducted the experiments in three situations including:

1. a subject walks on the flat ground (**Fig. 2.12-(a)**)

2. a subject walks on a slope (**Fig. 2.12-(b)**)

(a) walking on the flat ground

(b) walking on the slope

(c) walking on the flat ground while wearing a brace

Figure 2.12: Three experiment situations.

3. a subject walks on the flat ground while wearing a brace (**Fig. 2.12-(c)**)

In all the situations, experimental results show good agreement with our expectation.

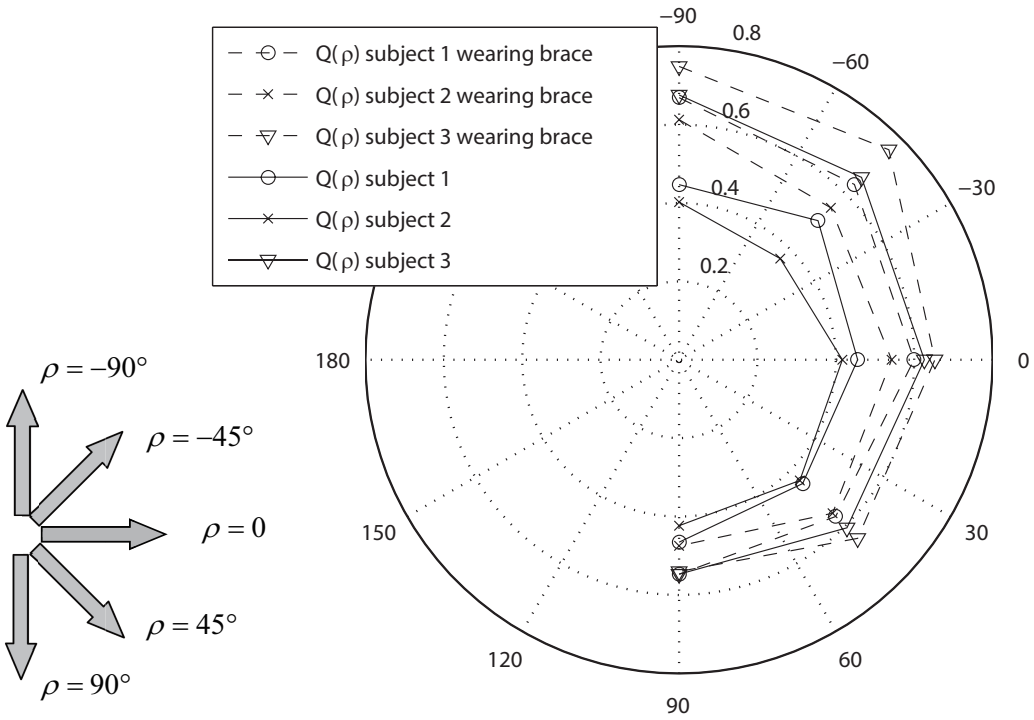

Figure 2.13: The covariance of noise when a person moves straight.

2.4.1 Investigating Observation Noise

Three university students (subject A, B and C) utilized the cane robot realizing mode II and III in these experiments. Same experiments were performed by them while wearing the brace to imitate a handicapped people. To verify the white noise assumption of the observation noise, firstly the subjects were requested to intentionally maneuver the robot moving straight along five fixed directions, which is shown by **Fig.** 2.13. From these experiments, we can investigate the observation noise characteristics of ITD by applying statistic techniques. For "moving-straight" experiments (mode II), the observation noise $\omega(n)$ can be easily obtained and analyzed from the observation model **Eq.** (2.8). For the obtained noise signal of each experiment, we tested both the normality and independence of residuals by applying Jarque Bera and Portmanteau test methods. It was found that more than 80% of the experiment results passed the statistical tests. Thus, a white noise assumption is thought to be acceptable in our study.

Further, the results of evaluated covariance **Q** of the white observation noise $\omega(n)$ are also depicted in **Fig. 2.13**. For each subject, the direction-dependent **Q** of this subject can be thought as a random variable. Coefficients of variation (cv) of these random variables were calculated and found to be less than 10%. Therefore, it is reasonable to assume that values of **Q** are almost the same in different directions for the same person, as pointed out in subsection **B** of **section 2.3**. Another interesting phenomenon that should be pointed out is that the covariance **Q** of the subject wearing a brace is higher than that of the subject performing a normal walking. This proves the fact that the observation noise of a handicapped peoples walking is usually bigger than that of a normal people.

2.4.2 Experiment on Flat Ground

In the experiments for illustrating the validity of the IBAC control strategy, subject A utilized the cane robot to implement two series of walking modes. The inferred ITDs and their observations based on force signals are shown in **Fig. 2.14**-(a) and **Fig. 2.15**-(a). Trajectories of estimated mode are also shown in these figures, where we use integers from 1 to 5 to denote the five walking modes sequentially (see the value of mode trajectory depicted by the dot-dash line). Note that even if there are some fault recognitions of mode transition, the performance of rule-based mode transition function is sufficiently satisfactory in the practice. In the experiment results, the main fault recognitions of mode transitions are mistaking mode IIa for mode IIb. This will not affect the system performance much because mode IIa is actually a special case of mode IIb. The advantage of fast detection of mode IIa is to quickly get an accurate ITD estimation ($\hat{\rho}(n) = 0$), which can be used to guide the motion control very clearly. However, even mode IIa is mistaken for mode IIb, the ITD which is estimated by Kalman filter is nearly equal to zero and smooth enough to obtain a satisfactory intention-based motion control.

As mentioned above, Kalman filter and robust Kalman filter are used in mode II and III respectively. Coefficient a in model **Eq.** (**2.3**) satisfies $a(n) = a_0 + \Delta a(n)$ with $a_0 = 0.93$, $|\Delta a(n)| < 0.3$. Comparing with the observation $y(k)$ from the noisy force signals, the online estimated ITD $\rho_e(n)$ reflects the human intention smoothly and distinctly, which provides explicit guidance to the IBAC controller. In particular, when the subject moves straight forward, which is the walking mode in most of the time, the inferred ITD is exactly the forward direction. This reduces meaningless lateral movements of the cane robot to a great extent. In addition, typical force responses are shown in **Fig. 2.15**-(b) and **Fig. 2.15**-(b) of the walking experiments.

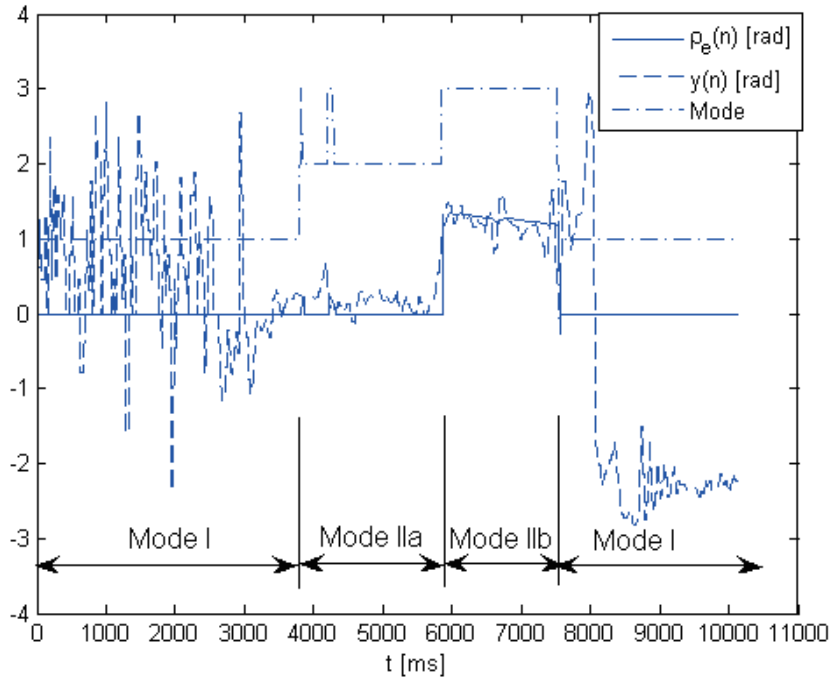

(a) Observed and inferred ITD vs Time (ms).

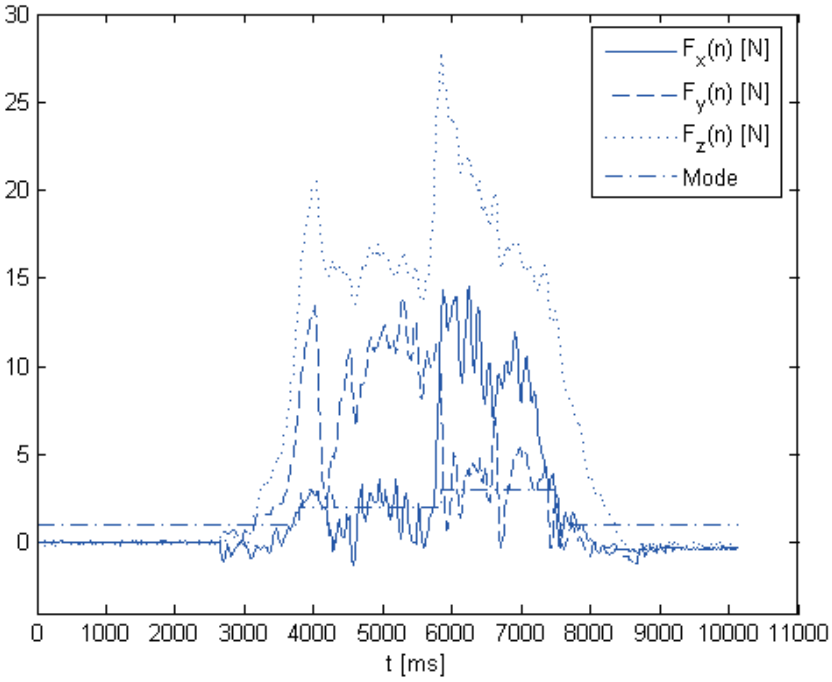

(b) Force signals vs Time (ms).

Figure 2.14: Experiment 1 on the flat ground (I→IIa→IIb→I).

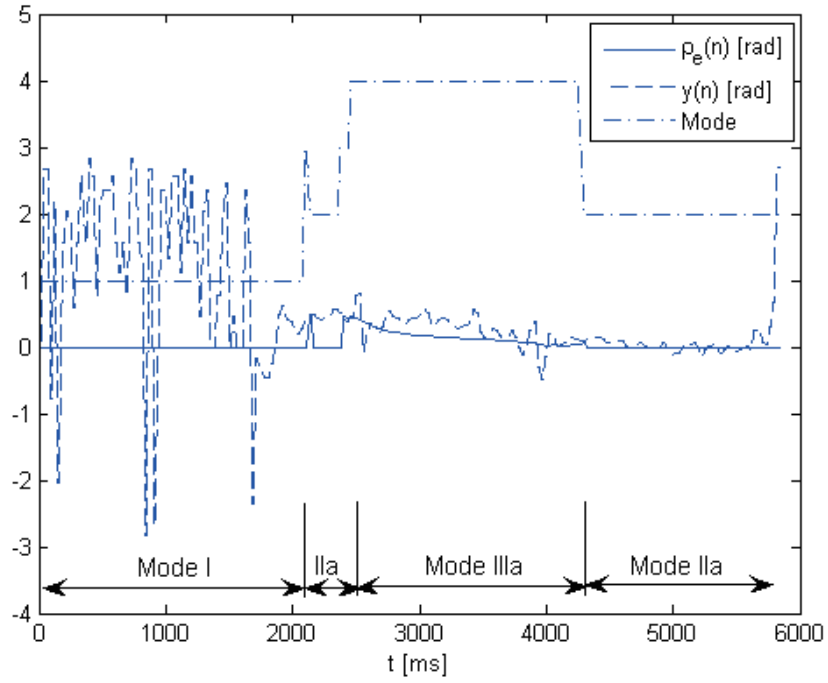

(a) Observed and inferred ITD vs Time (ms).

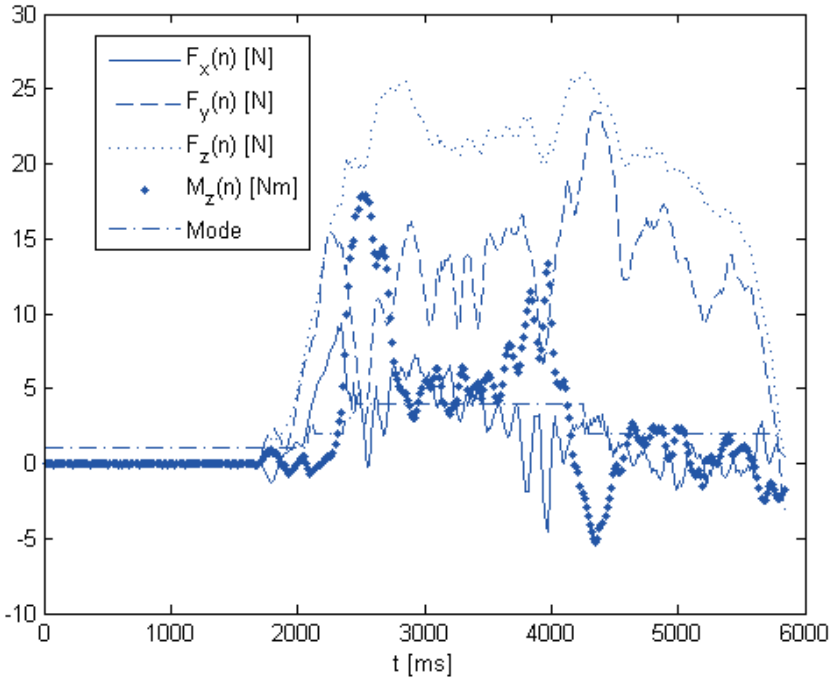

(b) Force signals vs Time (ms).

Figure 2.15: Experiment 2 on the flat ground (I→IIa→IIb→I).

2.4.3 Experiment on Slope

To further verify the proposed intention based motion control strategy, some experiments were also performed on a slope with an angle of 5 degree. Subject A was asked to implement two series of walking modes with the aid of the cane robot. One experiment is to climb the slope while turning to the right. The other experiment is to climb the slope straightforward and suddenly laterally move to the right (to pretend to avoid a coming obstacle). The experiment results are shown by **Fig. 2.16**.

Fig. 2.16-(a) shows the experimental data of the user performing the first experiment. At the beginning and the end of the experiment, the recognized mode is "go straight". This is because the turning torque (M_z) is very small in these cases. Obviously these fault recognitions will not affect the control performance much because any turning action is started and ended by a short "go straight" mode.

The result of the second experiment is depicted in **Fig. 2.16**-(b). In this experiment, all the modes are recognized correctly. When the user went forward, the ITD was estimated as 0. When the user turned to the right, the estimated ITD is nearly equal to $\pi/2$.

Fig. 2.16-(c) shows the velocity of the robot during the user performing the second experiment. F_ρ, v_ρ are the measured force and velocity which are along the ITD. F_v, v_v are the measured force and velocity which are along the directionperpendicular to the ITD. Note that F_ρ and F_v are effective forces in which the gravity effect has been eliminated. The robot velocity is 0 when F_ρ and F_v are zeroes, which demonstrates that the gravity compensation is effective. Velocity v_v is approximately 0 during the whole experiment, and it does not depend on the force F_v. Velocity v_ρ depends on the force F_ρ. These facts prove the effectiveness of our IBAC strategy in the experiments on the slope.

2.4.4 Experiment on Subject Imitating the Handicapped

A very troublesome procedure is required to recruit handicapped or old subjects to test our cane robot. Therefore, a university student wore a brace to imitate a handicapped subject in this experiment (**Fig. 2.12**-(c), the red brace was bound on the left leg). The brace restricted the motion of the left knee of subject.

First, the subject was asked to implement a walking mode series on the flat ground without wearing the brace. The experimental result is shown in **Fig. 2.17**-(a). Then the subject conducted the same experiment wearing the brace and the experimental result is shown in **Fig. 2.17**-(b). Compared with the normal case shown by **Fig. 2.17**-(a), there is no significant difference about the inferred ITD except a lager observation noise. By

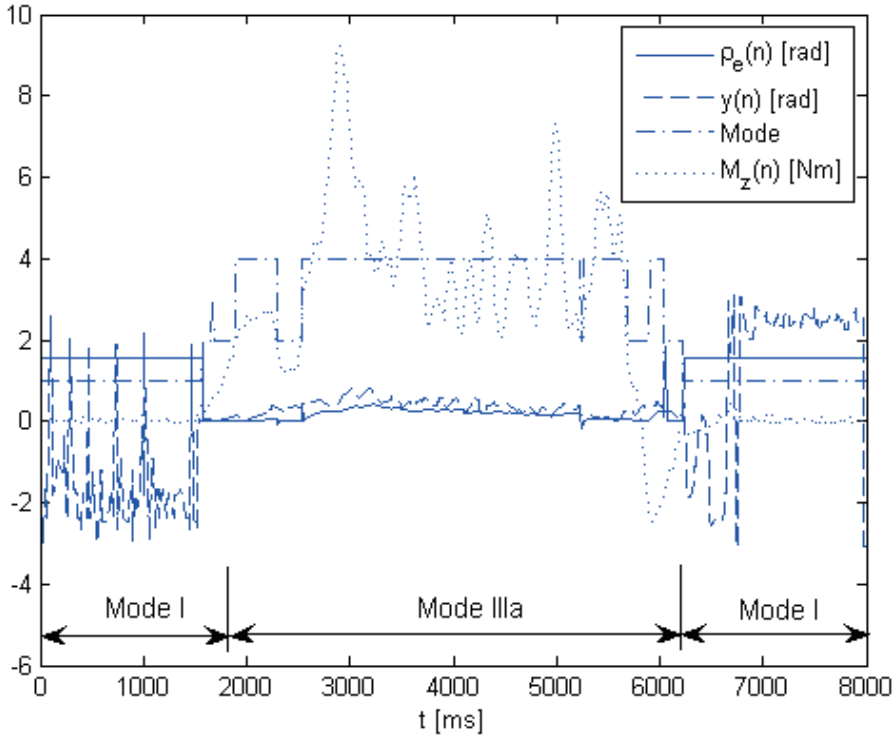

(a) Experiment 1 on the slope (I→IIIa→I).

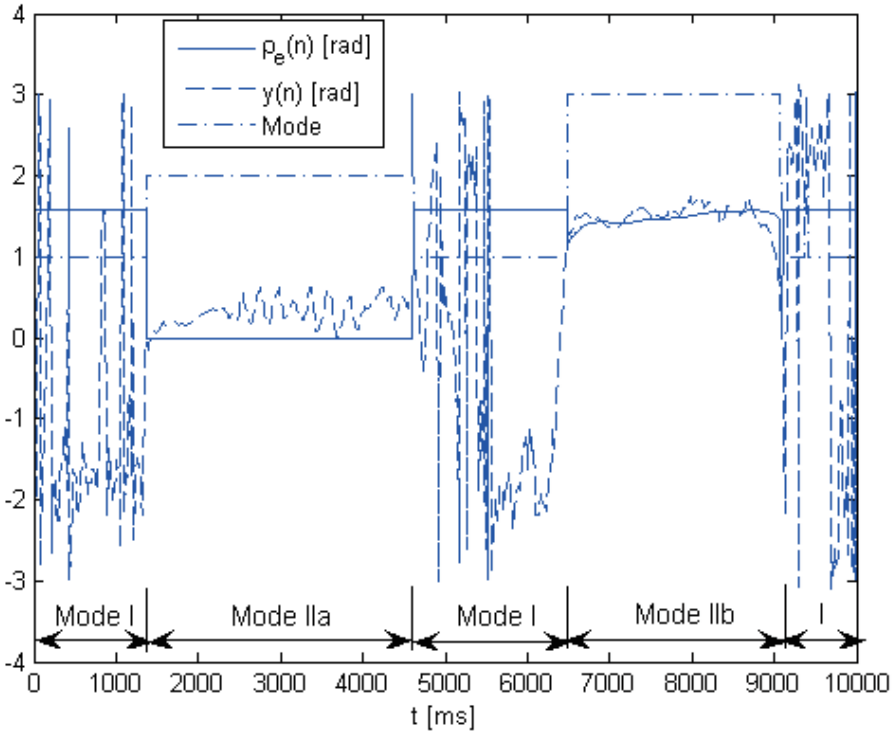

(b) Experiment 2 on the slope (I→IIa→I→IIb→I).

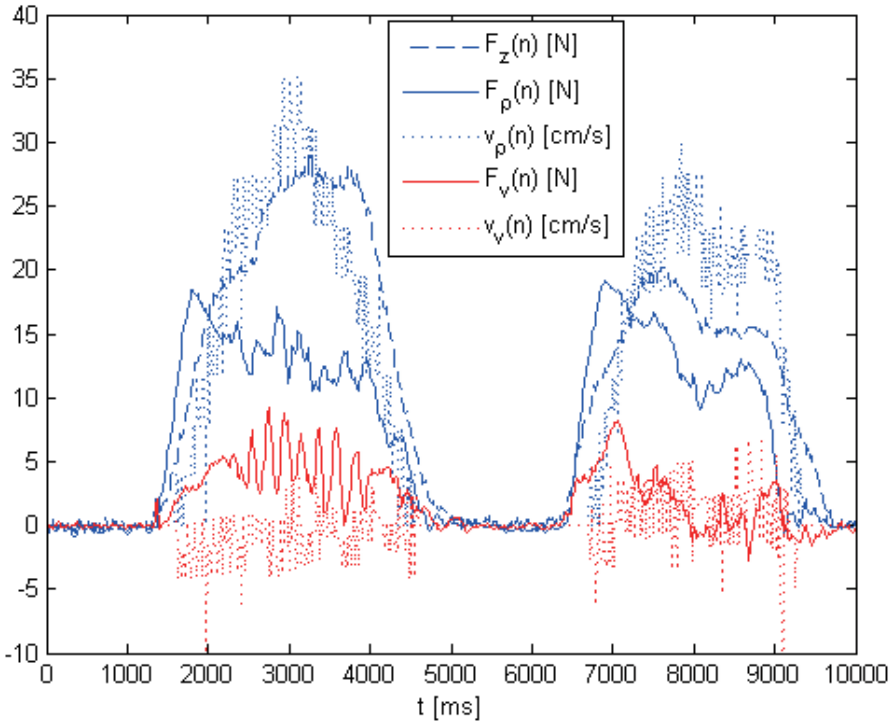

(c) Force and velocity vs time of experiment 2.

Figure 2.16: Experiments on slope.

investigating the feeling of the subject, we know that the movement of cane robot was coincident with the users walking intention very well. This proves that the IBAC control strategy is also effective in this case.

2.4.5 Experimental Comparison Study

As illustrated in **section 2.4.1**, observation noise of the ITD always exists while the cane robot is operated by either a normal user or an imitated disabled user. If a conventional force control approach is applied, the cane robot will move unexpectedly due to the effect of noise. This unexpected motion makes the user feel uncomfortable and deteriorates the maneuverability of robot. To safely assist the elderly or disabled walking, the proposed IBAC approach overcomes the disadvantage of conventional force control to a great extent. The validity of IBAC approach is further illustrated by the following experimental comparison study.

In this experiment, a subject was asked to perform two series of walking modes depicted by **Fig. 2.18**. A conventional admittance control (CAC) strategy which is often used in

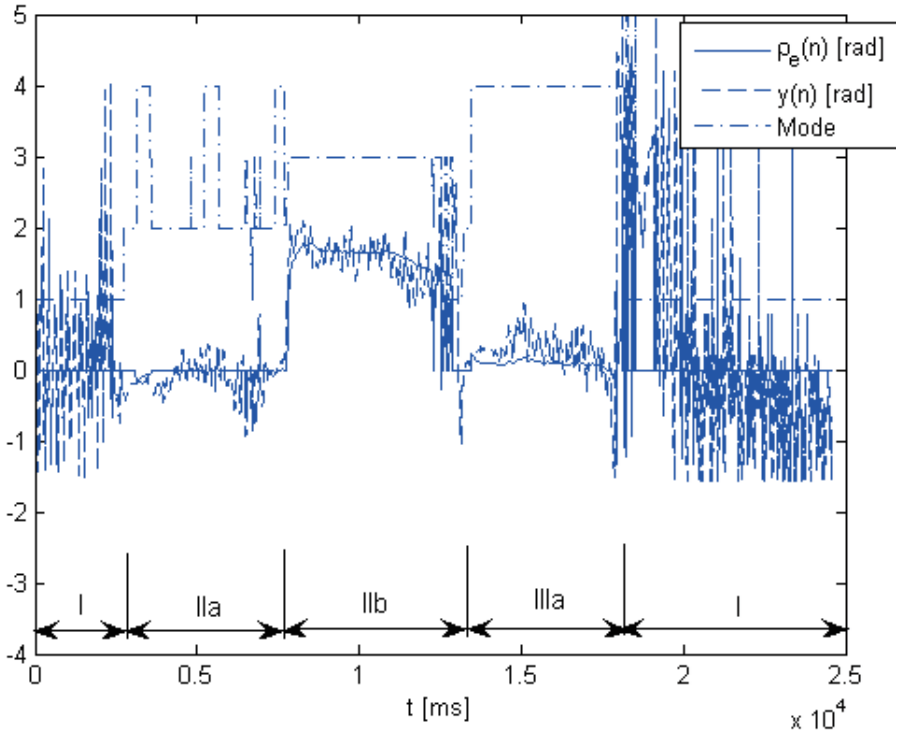

(a) Normal walking without wearing the brace

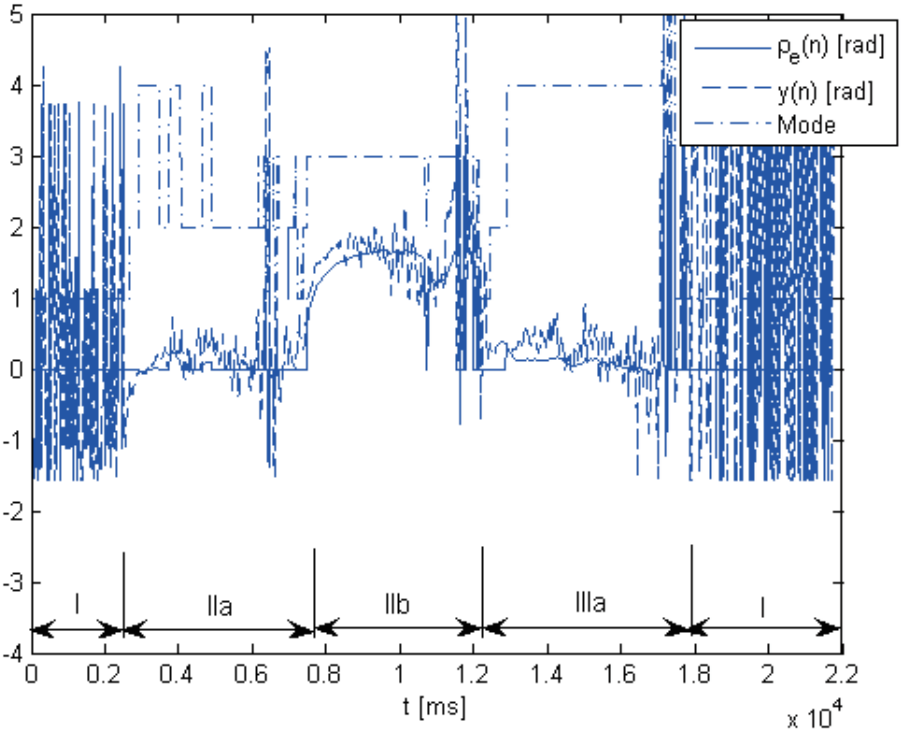

(b) Walking while wearing a brace
to imitate a handicapped

Figure 2.17: Experiments when imitating a handicapped.

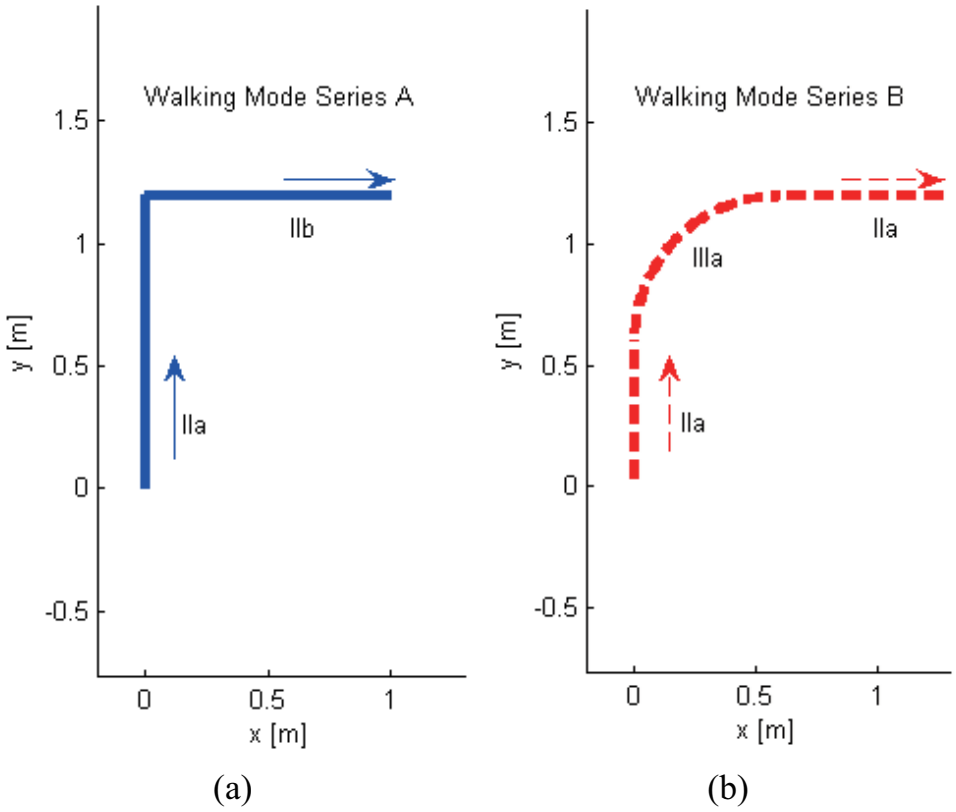

Figure 2.18: Two walking mode series used in the comparison study.

HRI [?] was tested first and the motion trajectories of cane robot were recorded. The same experiments were conducted on the cane robot controlled by the IBAC strategy.

To quantitatively evaluate the coincidence between the motion of cane robot and the user's walking intention, we assume a metric which is given by

$$D(cane, ITD) = \frac{1}{N}\sum_{i=1}^{N}\sqrt{\left(x_c(i) - x_{fit}(i)\right)^2 + \left(y_c(i) - y_{fit}(i)\right)^2} \tag{2.20}$$

where N is the data number of a motion trajectory of cane robot. $(x_c(i), y_c(i))$ is the i-th point in the motion trajectory. $(x_{fit}(i), y_{fit}(i))$ is the i-th point of the best-fit line through the point set of the motion trajectory. Note that the best-fit line should be obtained according to the given walking mode series, which reflect the users walking intention. For instance, the best-fit line of walking experiment A (see **Fig.** 2.18-a) consists of two straight lines representing the walking mode IIa and IIb respectively. The best-fit line of walking experiment B (see **Fig.** 2.18-b) is composed of two straight lines (representing mode IIa at the beginning and end of the walking mode series) and an arc (representing mode IIIa).

Table 2.2: Comparison of *D(CANE,ITD)* using different control strategies

		Experiments Using CAC Strategy		Experiments Using IBAC Strategy	
		Experiment number	Average value of *D(CANE,ITD)*	Experiment number	Average value of *D(CANE,ITD)*
On Flat Ground	A	50	0.0129	50	0.006
	B	50	0.0117	50	0.006
With Brace	A	50	0.0108	50	0.0081
	B	50	0.0103	50	0.0076
On Slope	A	50	0.0085	50	0.0034
	B	50	0.0083	50	0.0031

Fig. 2.19 shows two comparison results of walking experiments on flat ground using the IBAC strategy and the conventional admittance control strategy. The difference between the robot motion trajectory in the case of using the IBAC strategy and its best-fit line is much smaller than that in the case of using normal admittance control. This fact was further proven by calculating the average values of $D(cane, ITD)$ after conducting a number of comparison experiments in different cases illustrated in the above subsections (see Table II). As a conclusion, smaller values of $D(cane, ITD)$ are obtained when the IBAC strategy is applied to our cane robot. That is, there are less unexpected motions of the cane robot if the IBAC strategy is employed. This is very important in the sense of making the user feel safe and comfortable while operating the cane robot.

2.5 Summary

In this section, a new omni-directional type cane robot is developed for the elderly and handicapped. Motion control of this robot is studied based on online estimating human walking intention. The main contribution of this study is to present dynamic models and online inference algorithm for the human walking intention, which is significant to lead the user walking in a natural and comfortable way. An intention based admittance control (IBAC) scheme is also proposed and used to drive cane robot. Experiments were performed

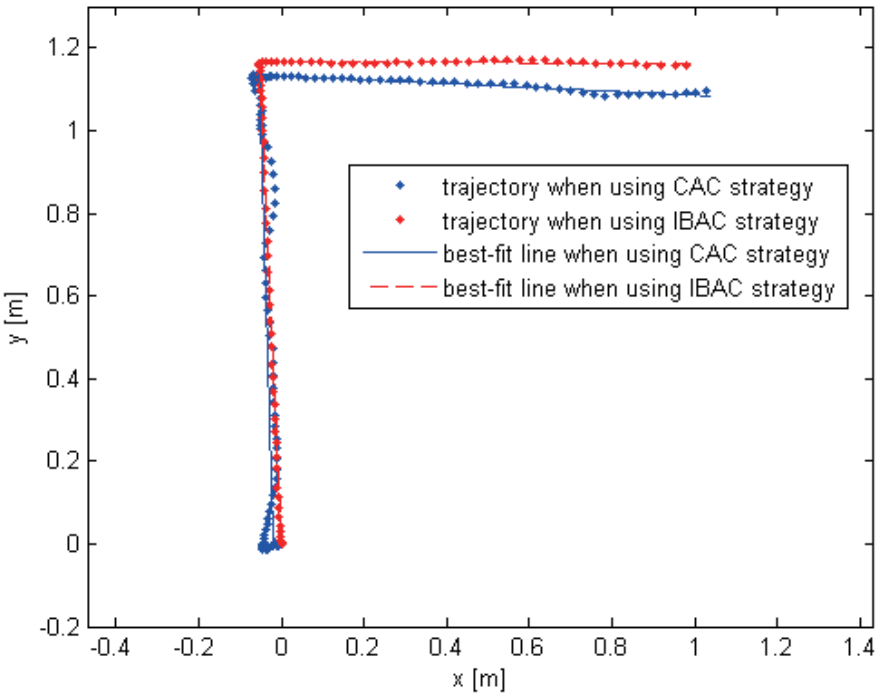

(a) A comparison of experiment results for walking mode series A

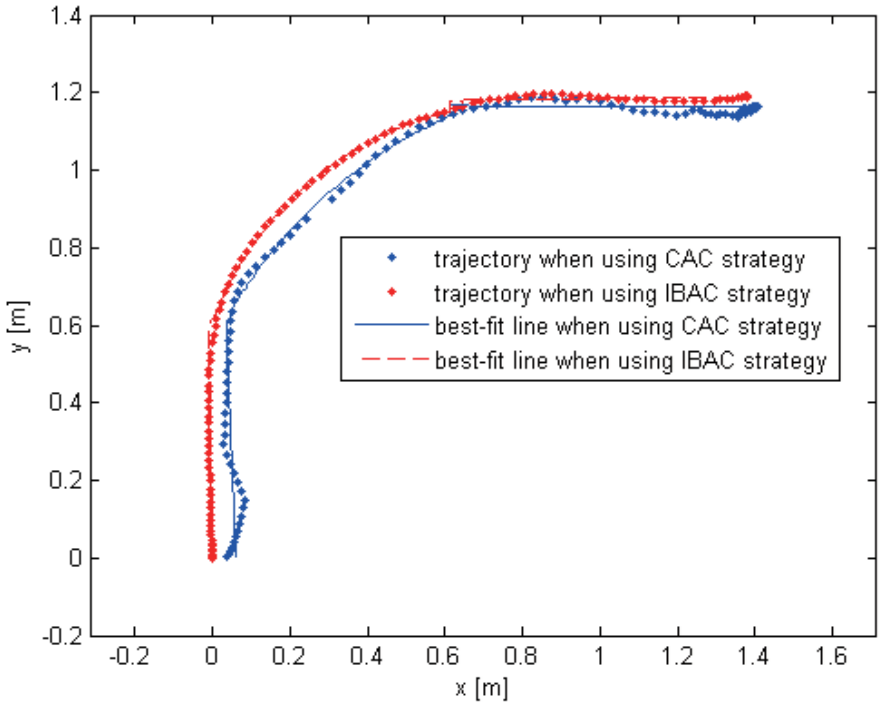

(b) A comparison of experiment results for walking mode series B

Figure 2.19: Comparisons of experiment results using the IBAC strategy and the CAC strategy.

on the flat ground and slope. The effectiveness of proposed algorithm is confirmed through experiments. It should be pointed out that the interface between the human and the robot is the multi-axis force sensor, which is expensive and fragile. To lower the cost and improve the system reliability, in the future we would like to construct a low-cost sensing system comprising cheaper force sensors (e.g. force sensing resistors) and range finding sensors for the cane robot. By utilizing some sensor fusion approaches, the state of user can then be reliably recognized and provided to the motion controller.

Chapter 3

Optimized Motion Control for Easing Muscular Fatigue

3.1 Introduction

In previous **Chapter** 2 the intentional direction (ITD) concept is proposed to estimate the user walking intention by analyzing signals from a six-axis force/torque sensor. An admittance control method controls the motion of the cane robot. In some cases, however the elderly can not walk uniformly because one leg suffers from muscular weakness. [?,?,?] When the affected leg is in the support phase, the cane robot should stop to absorb more strain than the affected leg. When the healthy leg is in the support phase, the cane robot should move forward according to ITD. In contrast to ITD, the motion of the cane robot should be controlled considering the walking pattern characteristics of the elderly to ensure safety and effectiveness. In this paper, an optimized motion control of the cane robot is proposed that is based on the characteristics gait pattern (CGP). An on-shoe load sensor was used to evaluate the reduction in muscular fatigue for the user's affected leg.

This chapter discusses the "ability to support" which denotes a system's ability to reduce the load applied to the elderly and ease muscular fatigue. An on-shoe device is proposed to detect the foot load. The on-shoe load sensor is used to measure the reduction in load on the user's affected leg. In order to produce a high-efficiency and ergonomic cane for elderly dynamic motion planning is proposed to control the movement of the cane robot in order to help the elderly walk. The effectiveness of the proposed method was verified through experiments.

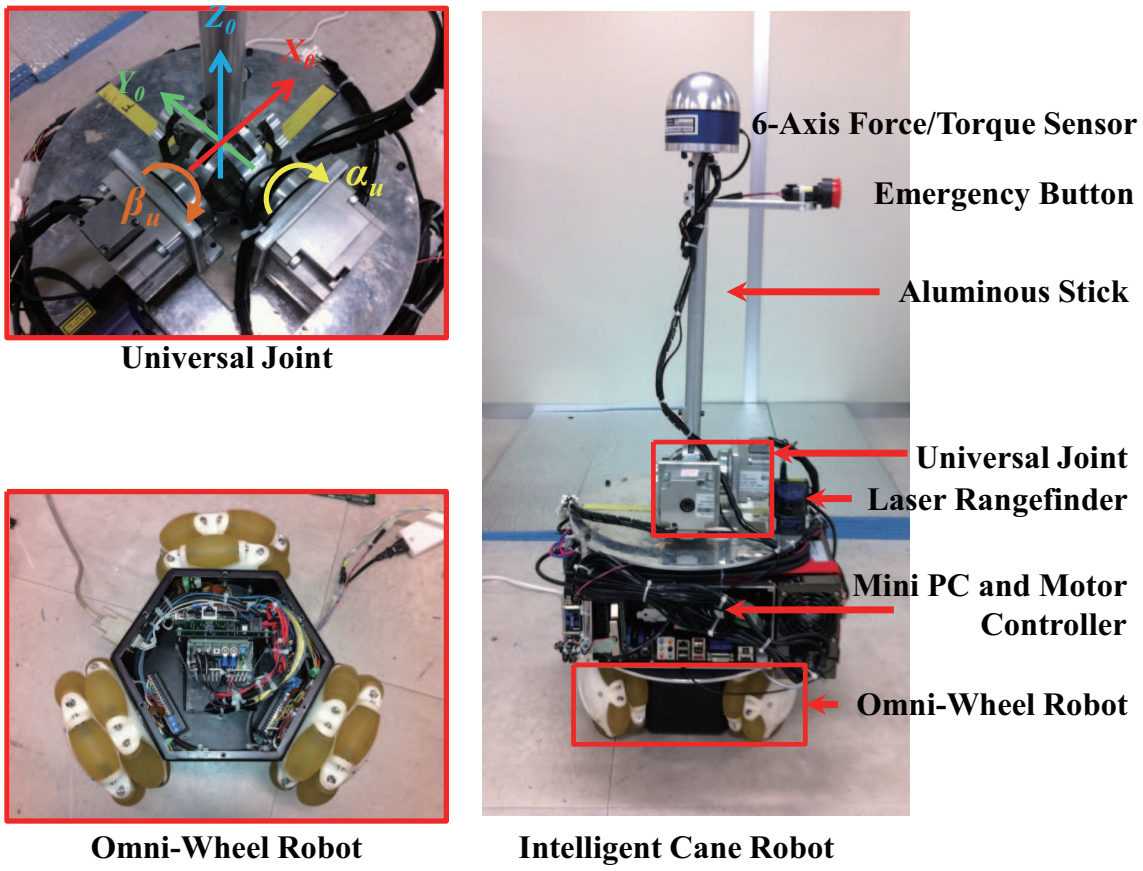

Figure 3.1: Intelligent cane robot prototype IV.

3.2 System Configuration

3.2.1 Cane Robot with Sensor Group

The prototype IV of intelligent cane robot shows in **Fig.** 3.1 and is intended to aid the elderly in walking and train their walking function. The cane robot consists of an omnidirectional mobile base, aluminous stick, and sensor system comprising a six-axis commercial force/torque sensor and laser rangefinder (LRF). A mechatronics device called universal joint is links the base of the cane robot and the aluminous stick to control the posture of the stick.

The omnidirectional mobile base comprises three commercially available omni-wheels and actuators, which were specially designed for the walker system. Despite the small size, the mobile base has a load capacity of up to 50kg.

The six-axis force/torque sensor is the main control input interface. The force sensor

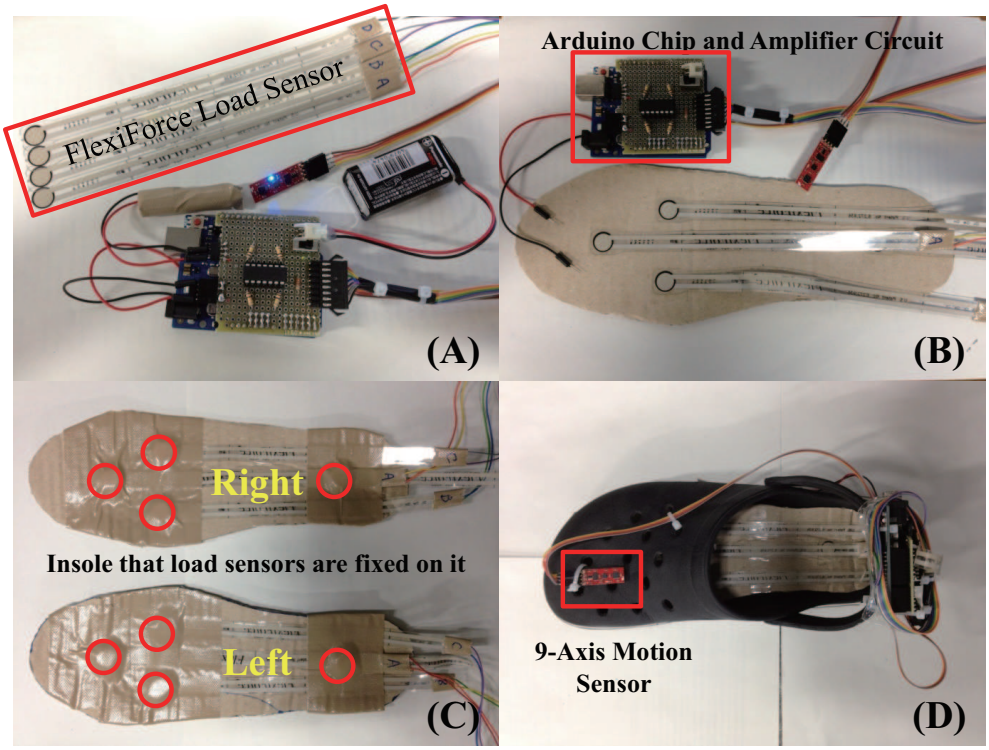

Figure 3.2: On-shoe load sensor with motion sensor

estimates the user's walking intention and probability of falling over. In a previous paper. The concept (ITD) was proposed to estimate the user's walking intention.

The intelligent cane robot was designed to be small in size and light in weight with multiple functions. It can achieve high maneuverability but at the cost of losing robust stability. Therefore, an important research topic is preventing the cane robot from falling over by a forceful thrust. In a previous paper, a mechatronics universal joint was proposed to significantly enhance the stability of the cane robot. A constrained nonlinear programming algorithm was applied to optimize the posture stability of the cane robot [].

3.2.2 On-shoe Load Sensor

A motion control method for an intelligent cane robot is proposed to reduce fatigue of the user's affected leg. In order to measure the load on the foot, a wearable load sensor system is proposed to obtain the dynamic reaction force at contact of the foot with the ground. This system integrates three parts: four *FlexiForce* load sensors, an Arduino electronics prototyping platform and a nine-axis sensor (**Fig. 3.2**). The sensor stick has nine-degrees of freedom and includes an accelerometer, gyroscope, and magnetometer.

Table 3.1: Experimental result of on-shoe load sensor

Input Load	Observed Load			Covariation
	Sensor #1	Sensor #2	Sensor #3	
20	4.1	3.8	4.3	0.26667
40	12.2	13.1	13.6	0.76667
60	26.1	25.1	26.8	0.9
80	38.9	37.1	36.8	1.3
100	45.3	42.1	47.2	2.76667

The *FlexiForce* sensors are applied by using a force-to-voltage circuit. The pressure on the sensing area causes a change in the resistance of the sensing element in inverse proportion to the force applied. The FlexiForce sensors are constructed of two layers of substrate. This substrate is composed of polyester film. On each layer, a conductive material is applied, followed by a layer of pressure-sensitive ink. The silver circle on top of the pressure-sensitive ink defines the "active sensing area". Silver extends from the sensing area to the connectors at the other end of the sensor, forming the conductive leads.

This circuit uses a non-inversion operational amplifier arrangement to produce an analog output based on the sensor resistance and fixed reference resistance. The *Arduino* platform is used as an analog-to-digital converter that changes this voltage to a digital output. When a load is applied to the sensing area of *FlexiForce*, the resistance value decreases. R_c is the original resistance of *FlexiForce* without load applied, F is the load applied to the sensing area, and C is the constant value that was previously set by calibration. V_{in} is the input voltage, V_{out} is the output voltage.

$$F = \frac{C}{R_c}(\frac{V_{out}}{V_{\text{int}}} - 1) \tag{3.1}$$

Even the *FlexiForce* sensor is not accurate enough, and quite a bit of noise is generated. This can be resolved by calibrating and applying a proper noise filter; the Kalman filter is used to reduce the noise. The performance of *FlexiForce* is shown in **TABLE 3.1**. Constant force($20N$, $40N$, $60N$, $80N$ and $100N$) apply on these three sensors(see **Fig. 3.3**) and the output voltage is measured by the *Arduino* platform. The observed load is calculated by using the **Eq. 3.1**. We can find the applied load is linearity relation with the observed load, so the accuracy is satisfy to the experiment.(see **Fig. 3.4**)

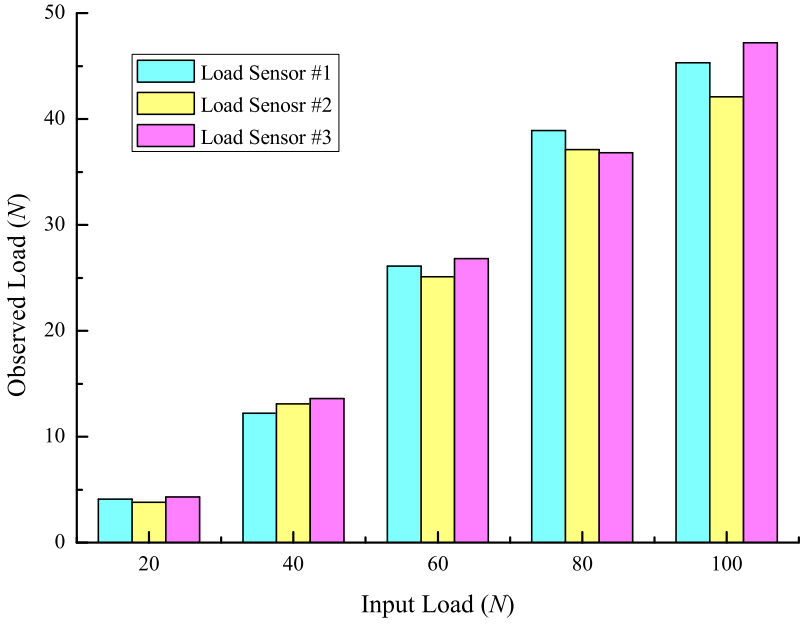

Figure 3.3: Experimental results of *FlexiForce* sensor

3.3 Motion Control Based on Walking Pattern Characteristics of Elderly

Canes are the lightest walking aid and transfer weight to the wrist or forearm. They are generally used to recovery from light injuries or to improve balance. Canes are helpful if a person has a small problem with balance or instability, some weakness in the leg or trunk, an injury, or pain. Particularly for the elderly, a single-point cane may allow them to continue living independently.

The intelligent cane was proposed to assist the elderly or handicapped people in walking. However, walking support comfort is hard to calculate or define. An important evaluation criterion for a walking assistance device is how effectively it absorbs the load on the affected leg. Generally, a person with one affected leg uses a cane in order to reduce the load applied to the affected leg.

In this section, a motion control algorithm for a cane robot based on the characteristics gait pattern (CGP) is proposed to reduce the load applied to one affected leg when the user is walking with the intelligent cane robot.

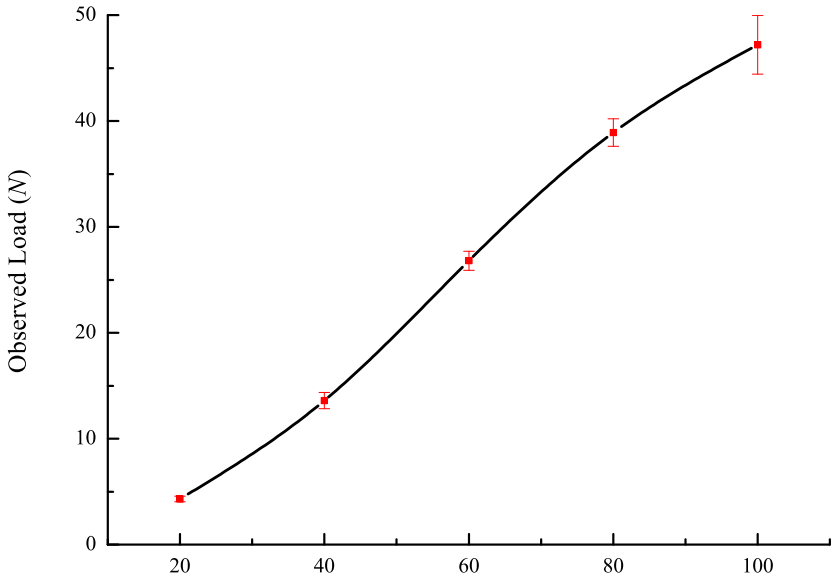

Figure 3.4: Performance of *FlexiForce* sensor

3.3.1 How to use a cane

The proper length for a cane is designed by having the person stand up straight with shoes on and arms at the sides. The top of the cane should reach the crease on the under-side of your wrist. If the cane fits properly, the elbow is flexed 15-20 when the user holds the cane while standing(**Fig. 3.5-(a)**).

Even though it sounds counterintuitive, the right way to hold a cane is using the hand that is on the same side as the good leg e.g., if the left leg is hurt, the cane should be held in the right hand and vice versa(**Fig. 3.5-(b)**).

The user should lean forward slightly and put the cane about ft ahead. The user begins the step as if going to use the injured foot or leg but shifts the weight to the cane instead of the injured foot. The user's body swings forward between the cane and affected leg. The step is finished normally with the non-injured leg. When the non-injured leg is on the ground, the user moves the cane ahead in preparation for the next step. The user focuses on where he or she is walking, not on the feet.

When humans walk, the hands swing with the striding feet at the same time. When the person strides with the left foot, the right hand should swing and vice versa. Holding

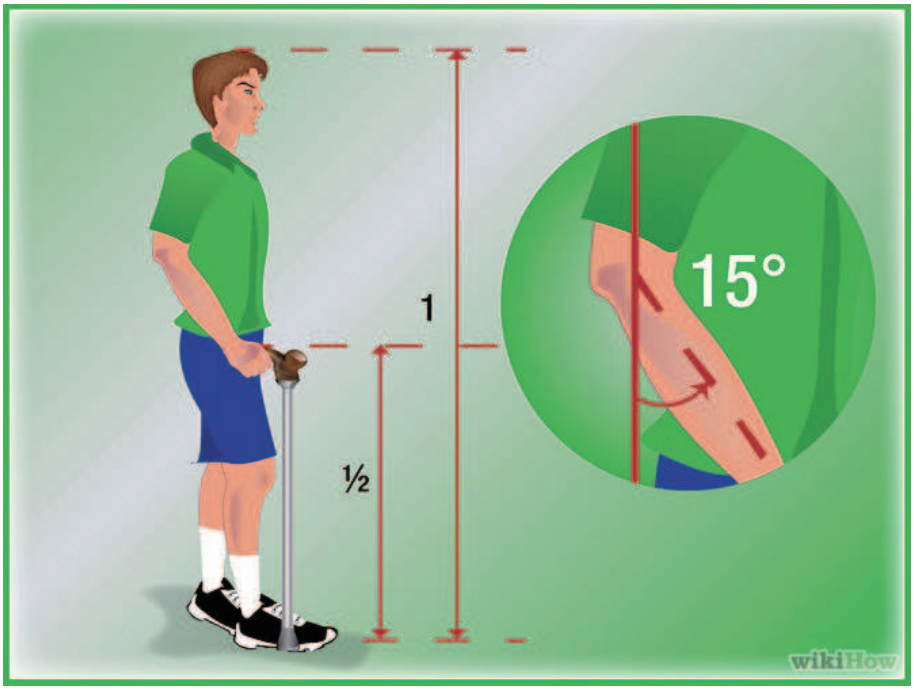

(a) How to chose the suitable length.

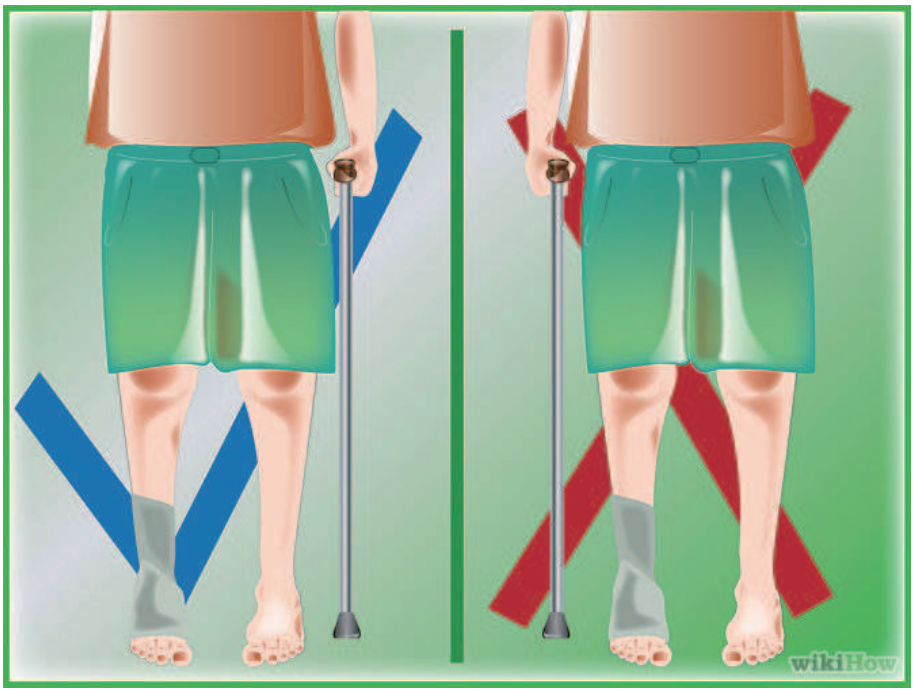

(b) How to hold a cane.

Figure 3.5: How to select and hold a cane.

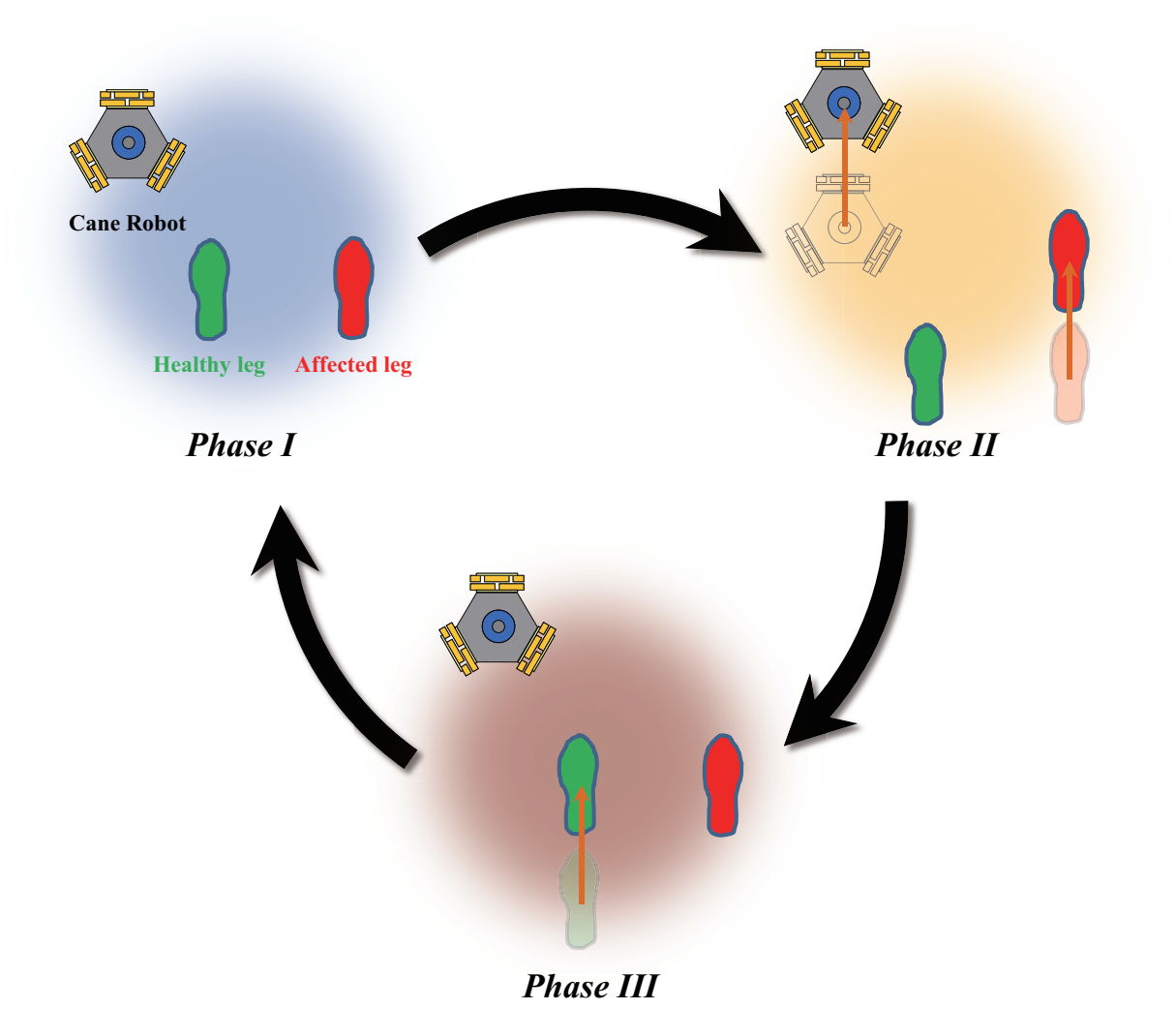

Figure 3.6: How to walk with a cane

a cane in the hand opposite the side with the injury replicates this natural arm movement and gives an opportunity for the hand to absorb some of the weight while walking(**Fig. 3.6**).

3.3.2 Proposed algorithm for controlling intelligent cane

As noted above, the proposed method differs from ITD in the affected support phase. In this phase, the user needs the cane robot to stop, so that it can absorb part of the load instead of the affected leg. However, But, if ITD is used to control the cane robot, the cane robot moves forward, which can cause the user to fall.

A series of walking movement with an ordinary cane is divided into three phases as

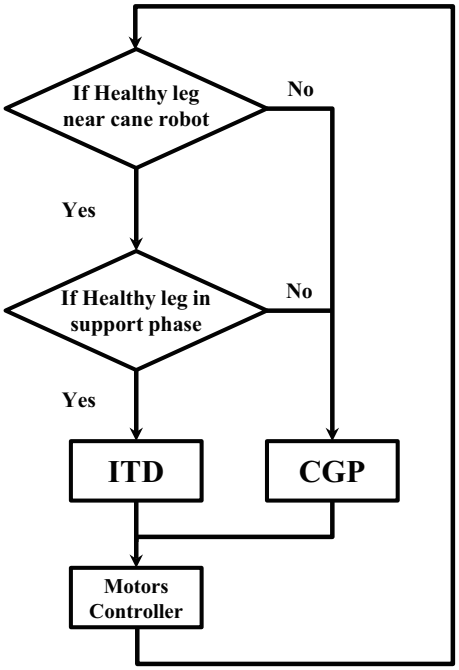

Figure 3.7: Proposed flowchart to reduce load applied to affected leg

shown in **Fig. 3.6**. In the ***phase I***, the two legs line up, and the cane is positioned ahead of user. In the second phase, the cane moves forward by a distance equivalent to one step. In the third phase, the weak leg moves forward just one step length. In the fourth phase, the normal leg moves forward just one step, and then both legs are lined up. This series of walking movement is repeated. The most important phase is the fourth phase, where part of the body weight can be absorbed by the cane instead of the affected leg. The user may move the cane forward (***phase II***) and move the affected leg forward (i.e., ***phase III***) at the same time. In this case, the user can walk faster, but the stability is slightly reduced. The elderly who do not need much support can walk this way.

After the cane moves forward in the second phase, the cane should stop according to the proposed CGP method. If the cane moves forward continuously, the user falls over. Therefore, when the distance between the normal leg and cane robot is large, the cane robot should stop in order to absorb part of the load for the affected leg. The flowchart **Fig. 3.7** shows the flowchart for controlling the cane robot using ITD and CGP.

Table 3.2: Comparative experiment results for ITD and CGP

	Case 1	Case 2
Maximum Load(N)	67.6	59.9
Average of Peak Load(N)	59.1	52.9
Average Velocity(cm/s)	16.2	10.5
Average Load(N)	40.6	28.4

3.3.3 Experiment Conditions

Experiments were performed on a flat floor in a room. The user of the cane robot attached a fixture to his left leg under the assumption that the left leg was weak. The experiments were performed for two cases. In case 1, the user walked forward with the cane robot using the ITD only. In case 2, the user walked forward using the proposed algorithm.

3.3.4 Experiment Result

Fig. 3.8 shows snapshots of the experiment with case 2. **Fig. 3.9** shows the relationship between the dynamic reaction force obtained by the on-shoe sensors and the robot velocity. The velocity of the cane robot was measured by the motor encoder. In case 1, the cane robot moved without considering the user gait. In case 2, the cane robot stopped when the user needed support. **Fig. 3.10** shows the load applied to the affected leg in each of the two cases. **TABLE 3.2** shows comparative data to evaluate the results. With the proposed method, the maximum load applied to the weak leg was reduced by 11.4%. In addition, the proposed method reduce the average peak load by 10.5%. This means that the cane robot can reduce the peak load with the proposed method.

Next, the average velocities of the cane robot for the two cases were compared. The proposed method decreased the average velocity by 35.2%. This means that the walking pace was decreased. When the proposed method was used, the cane robot stopped when the user needed support; this decreased the walking pace. Owing to the decreased walking pace, the remaining load on the weak leg was reduced. **Fig. 3.10** shows that case 2 had a lower remaining load on the weak leg than case 1.

Finally, the average loads of the two cases were compared. The proposed method reduced the average load by 30%. In conclusion, the proposed method reduces the load applied to the affected leg. Thus, the proposed control algorithm is more effective than

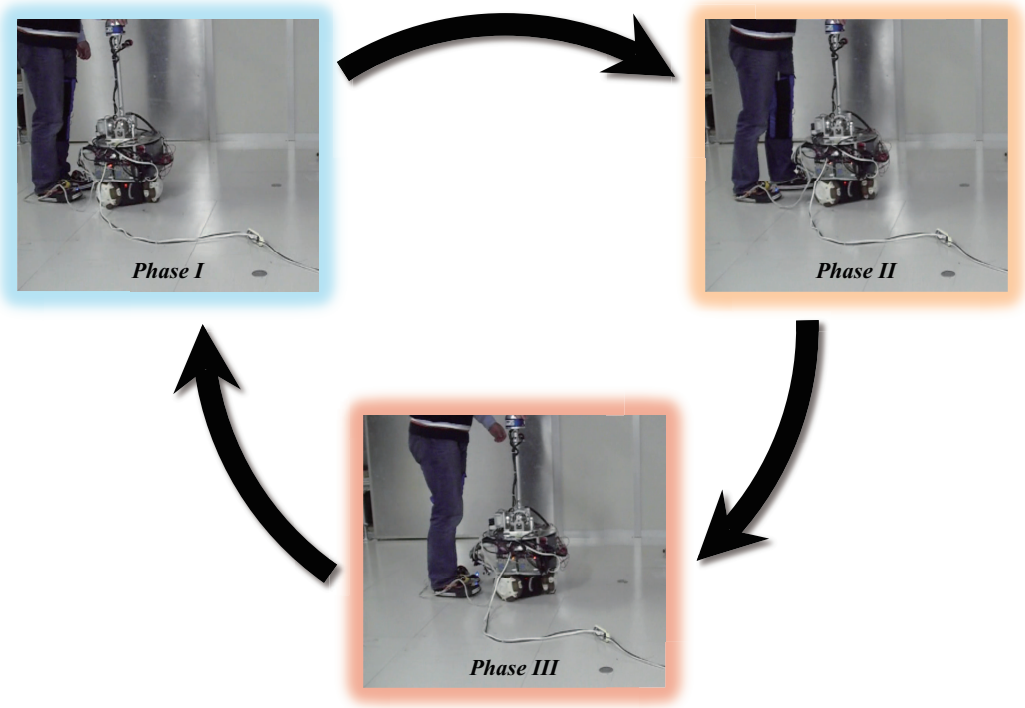

Figure 3.8: Experiment of case 2

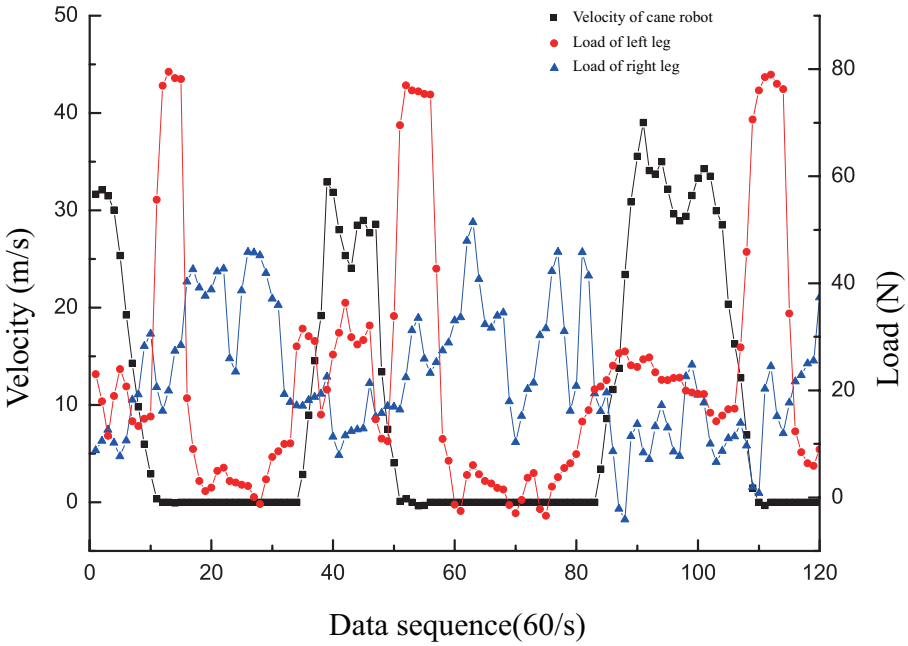

Figure 3.9: Velocity of cane robot

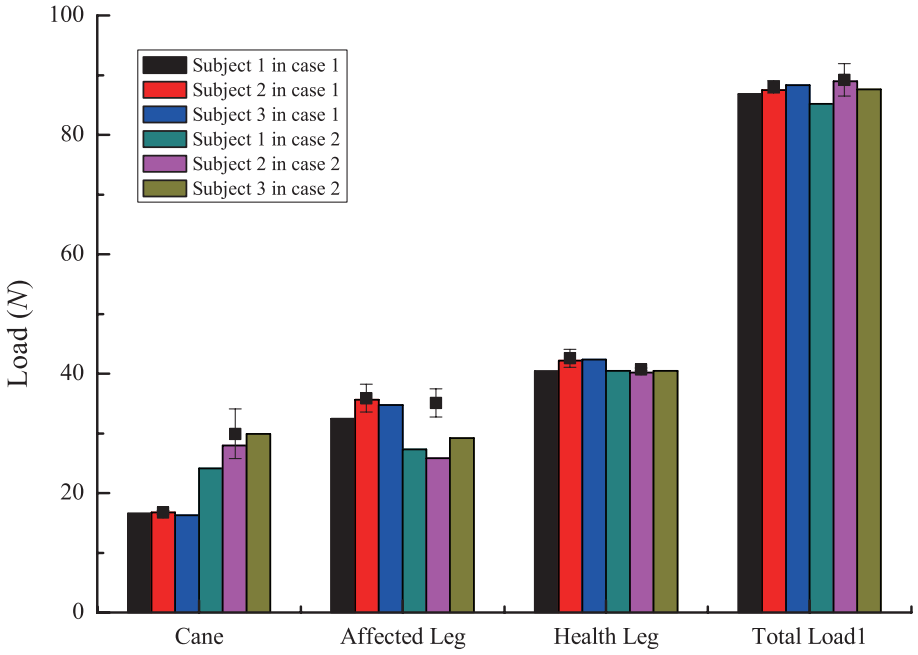

Figure 3.10: Load on user's leg and cane

the control algorithm using only ITD.

3.4 Summary

In this study, a new algorithm was proposed that considers the user's gait pattern characteristics. An on-shoe load sensor was designed to evaluate the reduction in muscular fatigue for the affected leg. By making the cane robot function similarly to the proper function of an ordinary cane, the load applied to the affected leg is reduced. On the other hand, the walking pace is reduced. Owing to the decreased walking pace, the remaining load on the affected leg is reduced. The effectiveness of the proposed walking support algorithms was confirmed experimentally.

Chapter 4

Fall Detection

4.1 Introduction

Many countries have entered the aging society very rapidly. Elders suffer from physical and cognitive degradation, such as poor eyesight, lack of muscle strength and so on. In addition, the growing elderly population causes the shortage of people for nursing care. Hence it is significant to design intelligent robots assisting the elders in daily life. Walker-type support systems are important ones among them because the ability of walk is one of the most fundamental functions for humans.

So far, many researchers have developed various intelligent walkers comprising active or passive wheels and supporting frame. Kotani et al. proposed the Hitomi system to help the blind in outdoor environment . Fujie et al. developed a power-assisted walker for physical support during walking . The Care-O-bot and Nursebot are developed as personal service robots for elderly and disables . Yu et al. proposed the Personal Aid for Mobility and Monitoring (PAMM) system to provide mobility assistance and user health status monitoring. Hirata et al proposed a new intelligent walker based on passive robotics to assist the elderly, handicapped people and the blind.

There are still many deficiencies in the present walker systems. First, many walkers are designed for the indoor environment. Second, most of them are big in size and/or heavy in weight. An indoor robot is often restricted within limited places. Big size makes it impossible to be used in narrow space and heavy weight restricts the maneuverability. Many elders and patients are not so weak that they have to be nursed carefully. Nevertheless, sufficient support, like a cane or stick, is necessary to help them take a walk outside, which enables them to realize high-quality lives or accelerate the rehabilitation. In these cases, an intelligent cane system may be more useful than walkers due to its flexibility

and handiness. In , a SmartCane system is also proposed, which has relative smaller size and nonholonomic constraint in kinematics. The nonholonomic constraint is useful for moving along a path stably, but reduces the maneuverability of the system. In the living environment including the narrow space, the cane system is expected to be movable in omni-directions. Thus, omni-directional mobile platform is needed in the robot design. This kind of platform has been considered in some applications. Whereas, their designs are special and not commercially available. Particularly, they are proposed for walker systems but cane systems, which are much smaller in size. Recently, commercial omni-wheels are applied in the area of walker systems. The problem that slender rollers of omni-wheels have limited load capacities is partly solved by the modern technology. In addition, small omni-directional platform can be constructed by this kind of wheels.

In our previous study, an intelligent cane system was designed based on a commercially available three-wheeled omni-directional platform. A hierarchical control scheme was proposed with estimation algorithm for human intentional moving direction. Because falling down of the user is the most serious problem for using the walker or cane system, we investigate the fall detection function of these systems in this study. Hirata utilized the distance between the user and RT Walker as a feature to distinguish between the walking state and the emergency state. This distance was measured by a laser range finder (LRF) mounted on the RT Walker. Whereas, this distance is not a significant feature for all possible falling cases, especially for a lateral falling-down. This will be further analyzed in the following. Vishwakarma proposed a fall model and an adaptive background subtraction method to detect human fall from video clips. But background subtraction method is only applicable when there is an immovable background in the processed videos. Some other fall detection methods including wearable sensor based systems, acoustic based systems and video based systems can be found in.

4.2 Fall Detection based on Sensor Fusion (*Prototype II*)

In this section, we introduce a new human fall detection method based on fusing sensory information from a vision system and a laser ranger finder (LRF). This method plays an important role in the fall-prevention for the cane robot. The human fall model is represented in a 2D space, where the distance between the head and the average leg position is a significant feature to detect the fall. The possibility distribution of this distance is estimated by using Dubois possibility theory. Fall detection is implemented by using a

simple rule based on the possibility distribution.

4.2.1 System Configuration of Cane Robot (*Prototype II*)

Mechanism of Cane Robot

The prototype system of omni-directional type cane robot shows in **Fig. 4.1**, it consists of an omni-directional mobile base, a metal stick and sensor groups including the force sensor, the CCD camera and the LRF.

The omni-directional mobile base comprises three commercially available omni-wheels and actuators, which are specially designed for walker systems. Despite the small size, the load capacity of this mobile base is up to 50 kilograms.

The CCD camera is used to monitor the head position of the user which is fixed on the top of stick. The LRF measures the distance between the cane robot and user's legs, which plays an important role in the function of fall-prevention.

A six-axis force/torque sensor attached to the stick is used as the main control input interface.

Control Architecture

There are many possible walking modes during the usage of the cane robot. Hirata et al considered three modes including 'normal walking', 'stop' and 'emergency' in their studies . we divided these rough modes further. Normally, different control scheme is required for different walking mode. Considering the high-level discrete walking modes and low-level motion control scheme based on continuous sensor signals, hybrid system theory is selected as the mathematical tool for the modeling and control design. A hierarchical control architecture is proposed, which is depicted by **Fig. 4.2**.

In the high-level supervising module, current walking mode is estimated from sensor signals. The inferred human behavior is taken as the input of the low-level motion controller module. In our previous study, a novel motion control scheme was investigated based on online resolved human intentional direction. In this study, we pay more attention to the emergency situation during human walking. A simple two-state finite state machine (FSM) model is implemented in the supervisor.

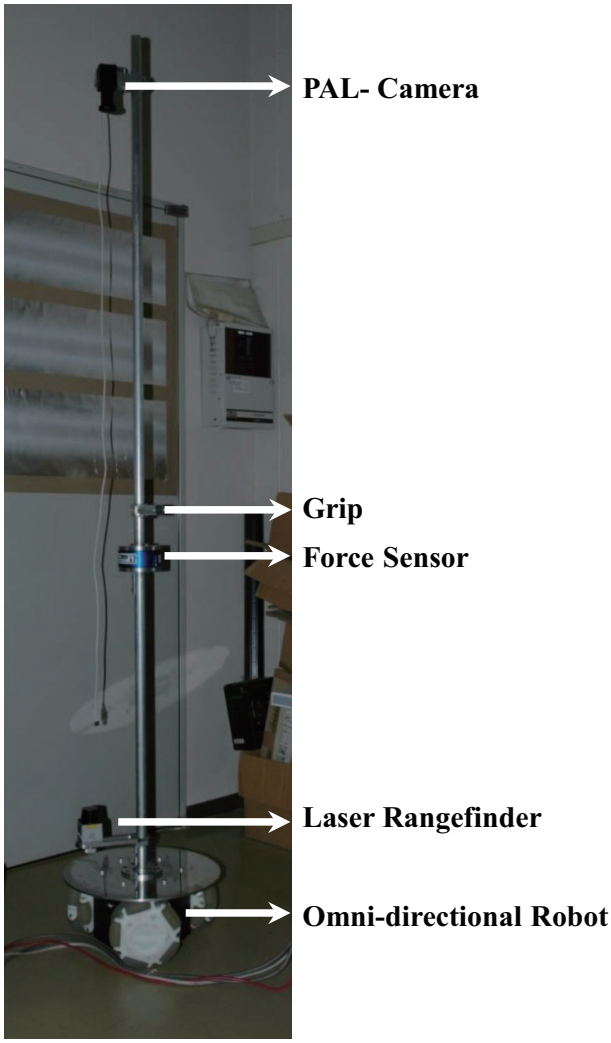

Figure 4.1: Prototype of the omni-directional type cane robot.

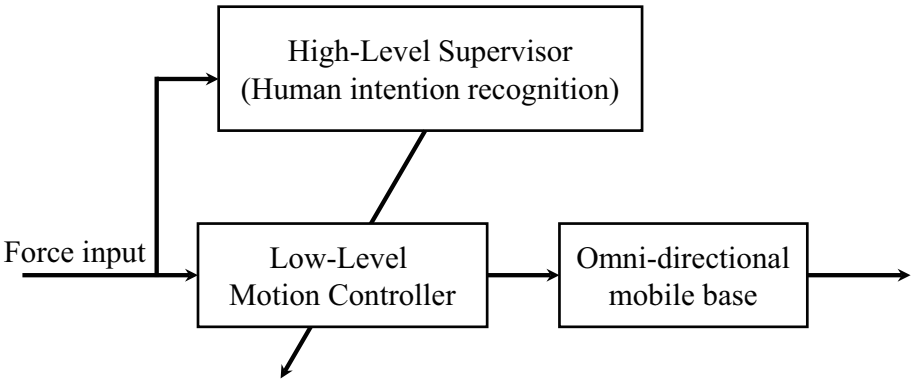

Figure 4.2: The control diagram of the intelligent cane system.

4.2.2 Data acquisition algorithms

Head Tracking using Image Processing

In our experiment the user wear a hat marked with a red pat. The CCD-camera sets on the top of the cane take a top view of user and gets the head position using color-tracking. We used the OpenCV function to achieve color-tracking processing. Before the color-tracking processing, we should prepare a template in the same color as the object which we want to track. Then convert the RGB type template image to HSV type, and do the back-projection processing which essentially produces a color probability distribution histogram image for the color template image. By using the information of the color distribution histogram the object can be tracked.

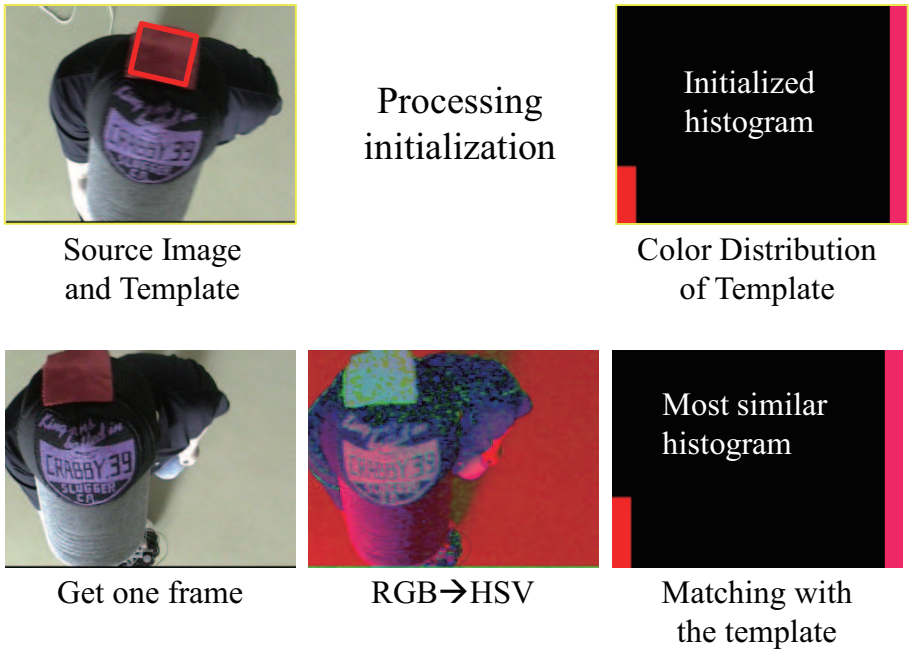

Figure 4.3: Tracking head position using CCD camera.

First, the input RGB color image is converted to an equivalent representation in the HSV color space. This step is independent of subsequent processing, and can be performed in parallel on successive input frames. Second, the HSV data is used in conjunction with a color histogram in a process called back-projection, which essentially produces a color probability image from the input color image. The back projection image encodes for each pixel, its probability of belonging to the color probability distribution represented by the histogram. The histogram itself must be initialized by sampling a representative area of one

frame. This is what we done before the beginning of the processing. The back-projection operation is independent of subsequent processing. The only persistent data used is the color histogram.

Finally, the CAMSHIFT algorithm is applied. It given an initial search window and a back-projection image, the function returns the bounding box of the most probable detection area in the image, and a size and orientation estimate of the distribution. The bounding box is used to infer the initial search window in the next input back-projection image. The back projection image is obviously volatile data. The initial search window data (input) is related to the detected area (output) in the previous frame. In an asynchronous approach, this information can be encoded as the last known detection result (bounding box), which is persistent information updated after the processing of each new frame, thus forming a feed-back loop.

Head Tracking using Image Processing

LRF is used to detect the each distance between users legs and cane robot. The LRF can scan a plane from 0 to 270 degree, but it takes more time than only scan the area which the user stand in. **Fig.** 4.4-(A) is all the possible data points indicating the legs, the points were classified into two groups using online K-mean algorithm. Each group denotes the left or right leg respectively(see **Fig.** 4.4-(B)).

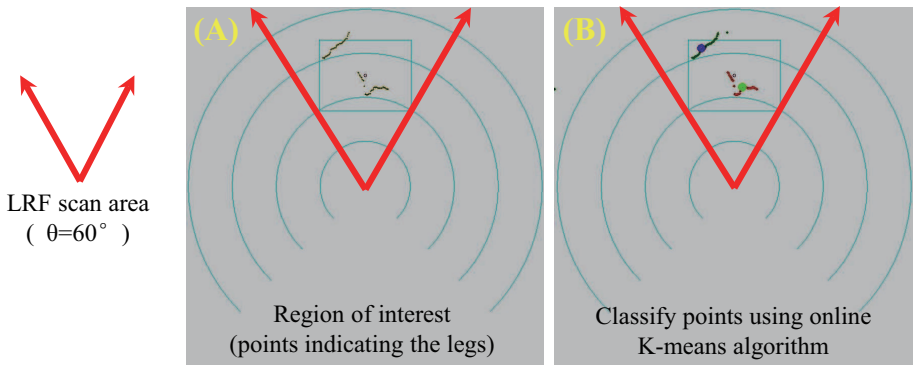

Figure 4.4: Tracking leg's positions using LRF.

4.2.3 Fall Model and Fall Detection

Fusion Method and Fall Model

In , Hirata used the distance between the user and RT Walker as a feature to detect if the user is falling down or not. Whereas, the falling state correctly cannot be reflected only by the position of the legs in many cases. Therefore, in our study the walking user is monitored simultaneously by a camera and a LRF as shown by **Fig. 4.5**.

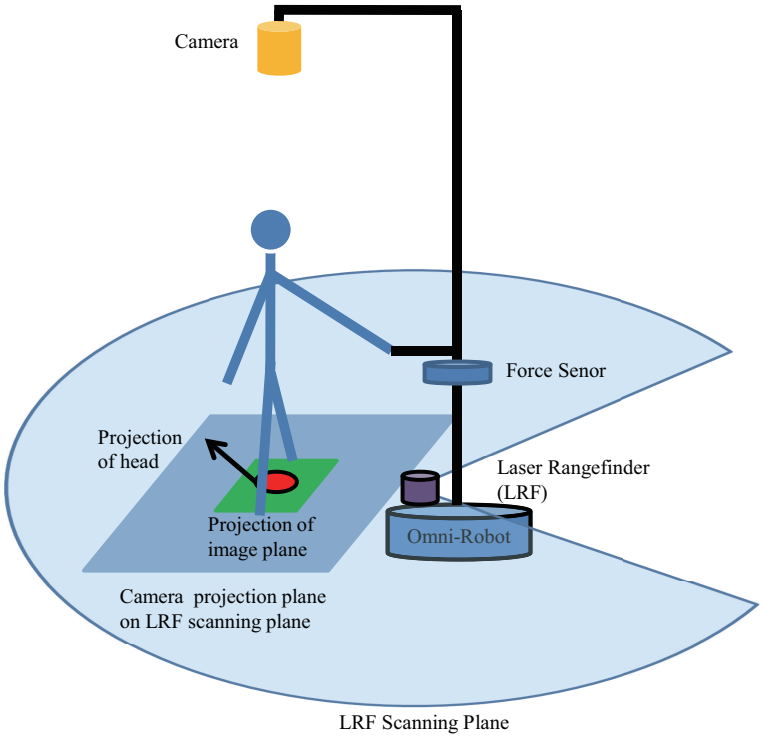

Figure 4.5: Walking state is monitored simultaneously by camera and LRF.

As shown in **Fig. 4.6**, possible falling states include 'forward falling', 'backward falling' and 'sideward falling'. Here state 'sideward falling' consists of all falling cases except forward and backward falling. Through appropriate coordinate transformation, the walking state can then be represented in a 2D space, which is depicted in **Fig. 4.7**. Two kinds of circles are used to indicate the positions of the user's head and legs.

The sensory information acquisition scheme is described in **Fig. 4.8**. The user wears a hat marked with a red pat during operating the cane robot (see **Fig. 4.8**-(a)). The head position is monitored by the CCD camera using color tracking algorithm. **Fig. 4.8**-(b) shows the data of one scan using the LRF. All the possible data points indicating the legs

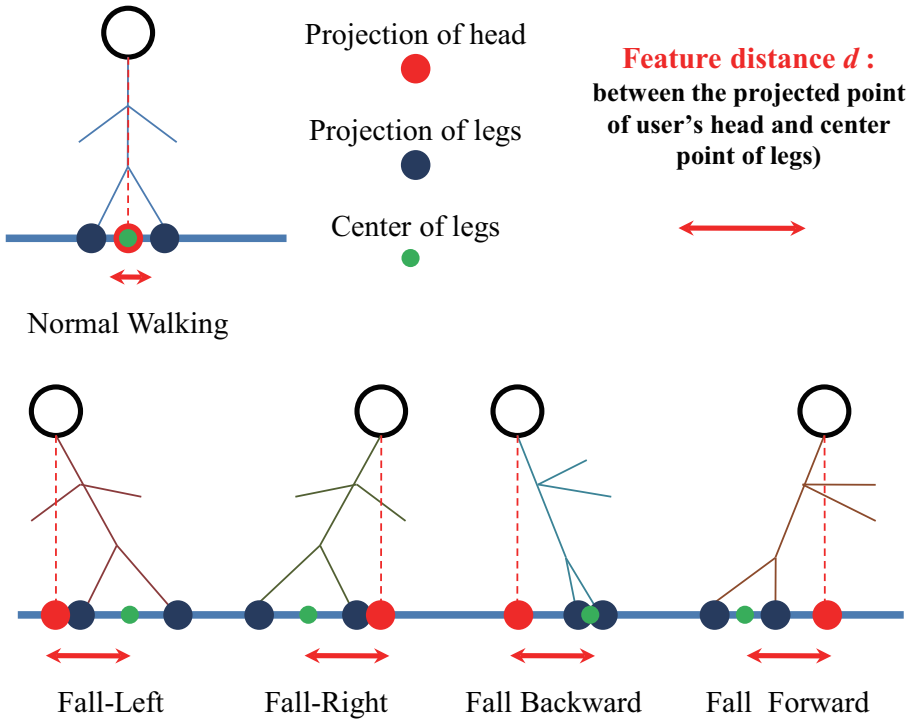

Figure 4.6: Normal walking and possible falling states.

are classified into two groups using online K-mean algorithm. Each group denotes the left or right leg respectively.

To obtain a data fusion from the two sensors, we integrate the two kinds of data into the image coordinate, as depicted in **Fig. 4.5**. The heights of the CCD camera and the user are denoted by C_h and U_h, respectively. A rectangular area of the LRF scan plane indicates the projected part to the image coordinate. L_1 and L_2 are used to denote the length and the width of this area. The size of the image coordinate is 640*480 pixels.

Obviously, the most important feature indicating the user's falling state is the distance d between the head and the center of two legs. While the user is walking normally, the value of d should fluctuate around a small constant. This constant and the fluctuation differ from different people. When the user is falling down, the distance d will increase suddenly in a certain direction.

We investigate the distribution of the distance d during the normal walking state. In , similar distribution was regarded as normal distribution and estimated to infer the users walking state. In this study, we use Dubois possibility theory to describe the distribution of the distance d during the normal walking state. The procedure starts by constructing the data histograms for the distance d during normal walking state. The number of bins h

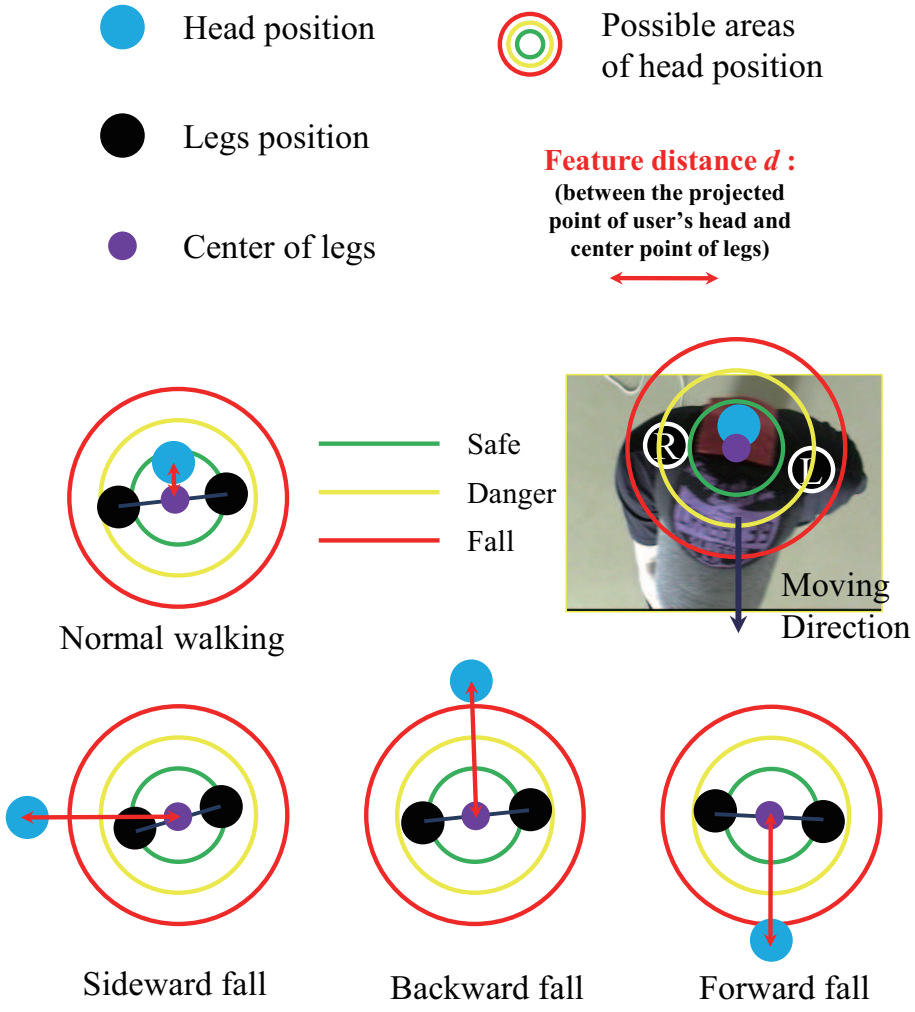

Figure 4.7: Walking states represented in 2D top view.

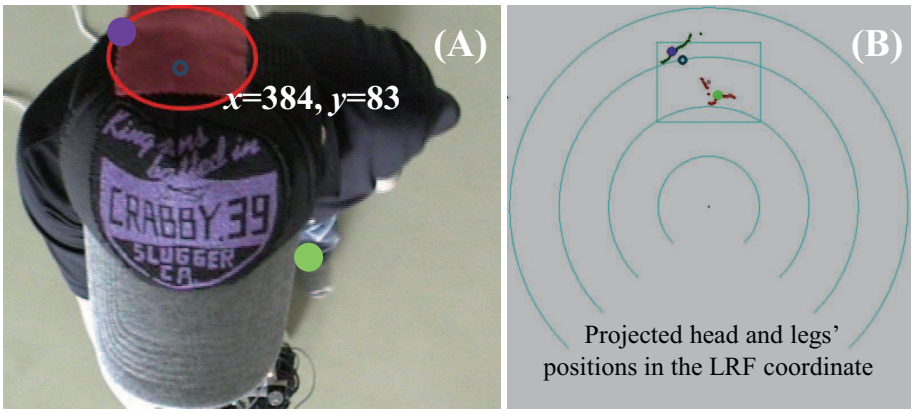

Figure 4.8: Tracking head and legs position.

for a histogram is experimentally determined. Each bin is represented by the center of the interval denoted by yj. The height of each bar is the number of learning points, located in this bin.

The probability distribution $\{p(y_j) : \ j = 1, 2, \cdots, h\}$ is calculated by dividing the height of each bin by the total number of learning points belonging to the same class. The possibility distribution $\{\pi(y_j) : \ j = 1, 2, \cdots, h\}$ is deduced from the probability distribution by the bijective transformation of Dubois and Prade defined by

$$\pi(y_k) = \sum_{j=1}^{h} \min\left[p(y_k), p(y_j)\right] \tag{4.1}$$

The membership functions $\mu(\cdot)$ that characterize the fuzzy set 'normal walking', is finally calculated from the corresponding possibility distributions by linear interpolation. Typical membership functions are given in section 4.

4.2.4 Fall Detection

The fall detection is implemented by a very simple rule, which is illustrated as follows: (assuming the human walking behavior is monitored at discrete times, t denotes the current time)

IF $\mu(d(t)) < c$ *and* $\mu(d(t-1)) < c$ *then a fall is detected*

Constant c is a small positive number which indicates a very low possibility of normal walking state.

4.2.5 Experiments

In this section, we experimented with the cane robot to illustrate the effectiveness of the proposed methods. First, the possibility distribution of 'normal walking' state is investigated. Then the validity of fall detection method is verified by experiments.

4.2.6 Experiments of Normal Walking

Two university students utilize the cane robot realizing normal walking in these experiments. The first student walked naturally during operating the cane robot, while the other one pretended to be a stooped old person walking with the help of the cane robot. The original fused position data are shown in **Fig. 4.9**. The solid and broken lines denote the x and y axial coordinate value respectively. The positions of head are plotted using red lines

and the leg positions are plotted using other colors.The feature distances of both cases are computed and depicted by **Fig. 4.10**. Choosing the number of bins as 7, the membership functions are obtained and plotted in **Fig. 4.11**. The distance d is normalized into the interval [0, 200].

As shown in **Fig. 4.10**, the average value of d of subject B is much bigger than that of subject A. This is because subject B who pretended an old person was bending forward during walking.

4.2.7 Experiment of Fall Detection

In this experiment, subject A pretended to fall down during walking. The fall detection rule described in **Section 4.2.4** was applied in the experiment. Constant c was chosen as 0.2. The fall was detected promptly as shown in **Fig. 4.12**-(left). The original video clips from just before to just after the detection time instant are also shown in **Fig. 4.12**-(right).

4.2.8 Summary

A new cane robot is designed to help the elderly walk. To prevent the user from falling down, a new fall detection scheme is proposed in this study. This scheme is based on the sensor fusion of different sensor resources. Fall model is created by using the simultaneous monitored information of the heads and the legs positions. The effectiveness is confirmed through experiments.

4.3 Fall Detection based on the ZMP Stability Theory

As a nursing-care robot, the safety is a most important concern; before the elderly fall over, the cane robot should detect the sign of the falling and control the robot to assist the elderly to prevent it. Therefore a fall detection concept is proposed to estimate the risk of the falling based on the theory of zero moment point (ZMP) stability. An on-shoe sensor is used to measure the foot-ground reaction force and calculate the ZMP. The safety walking status is defined in the case of the ZMP is in the boundary of the support polygon. While the ZMP moving out of that boundary, the user will fall over.

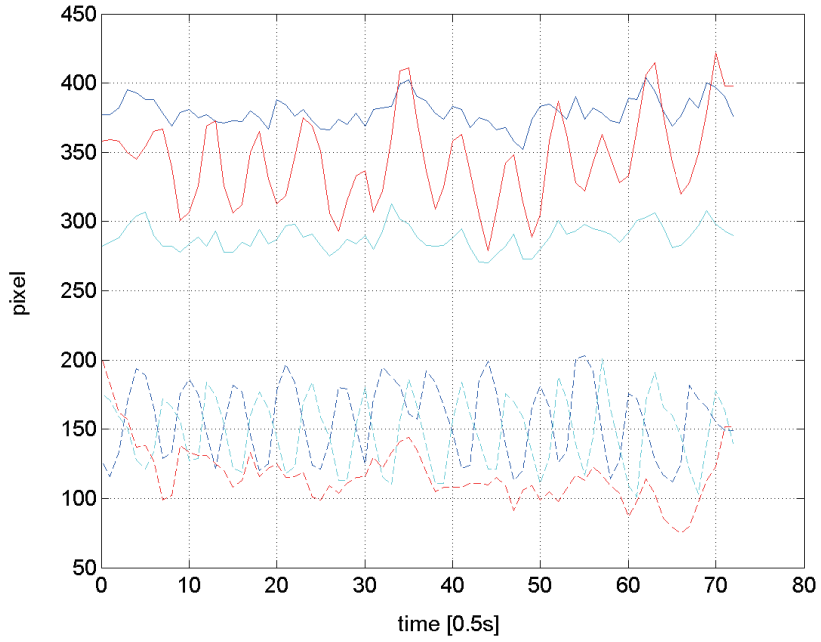

(a) The original legs and head position data of subject A

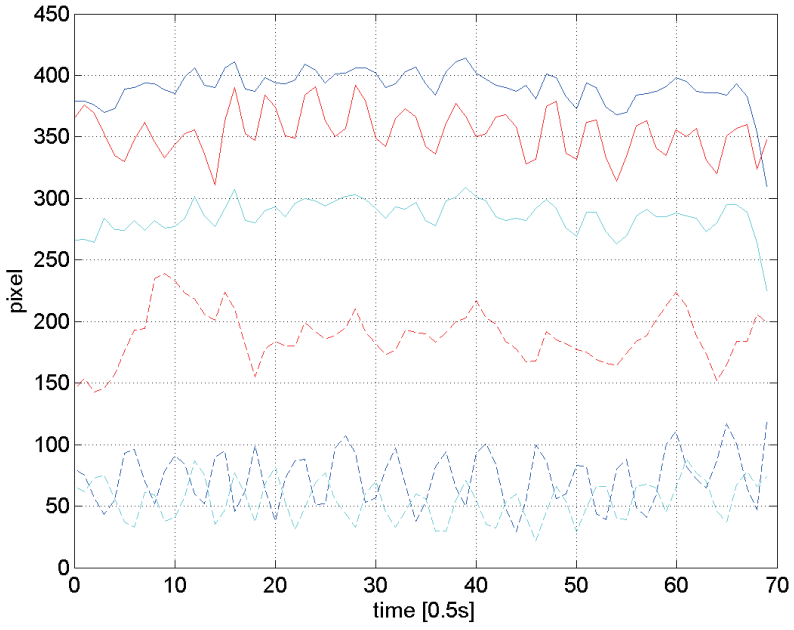

(b) The original legs and head position data of subject B

Figure 4.9: The original fused position data.

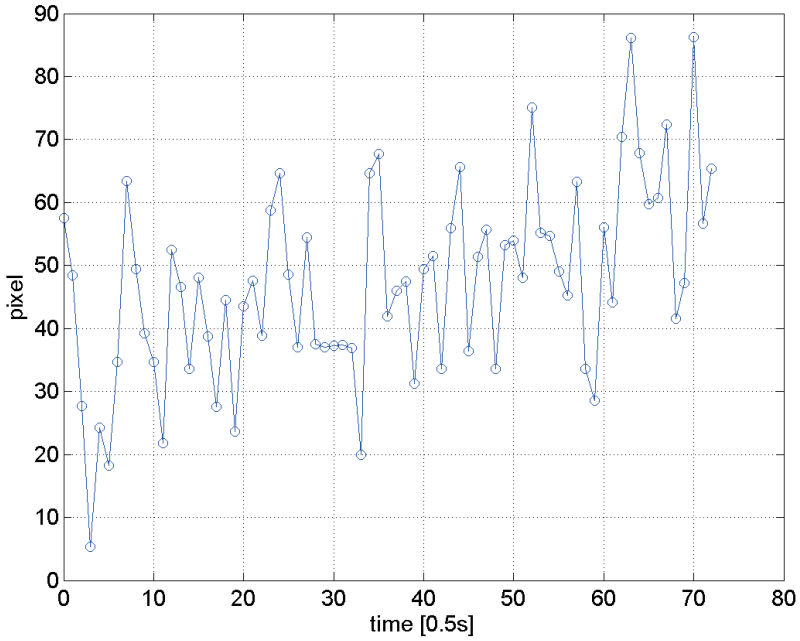

(a) The distance *d* of subject A

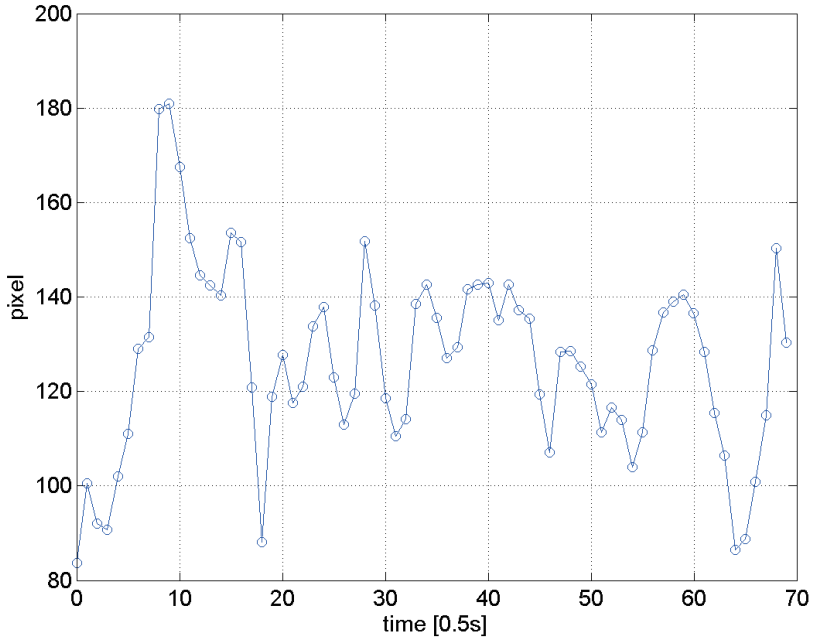

(b) The distance *d* of subject B

Figure 4.10: The computed feature distance d of both subjects.

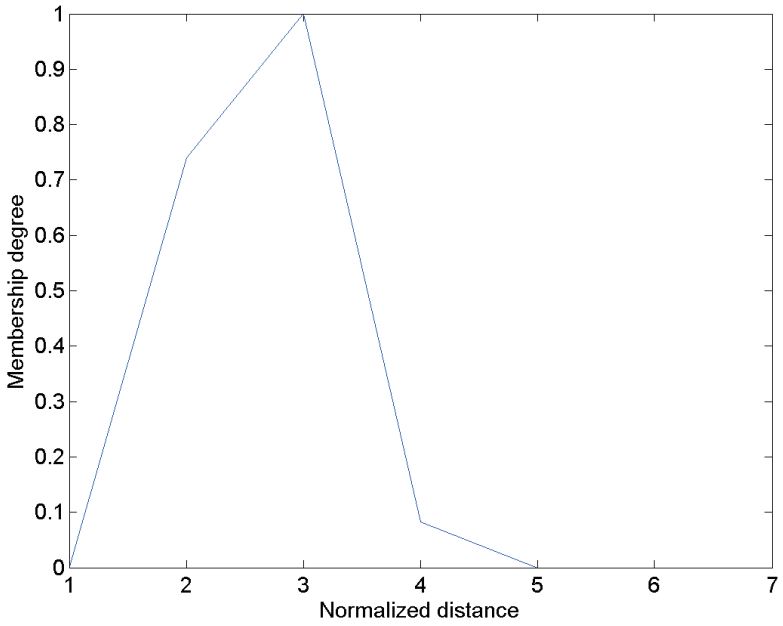

(a) The possibility distribution of distance *d* of subject A

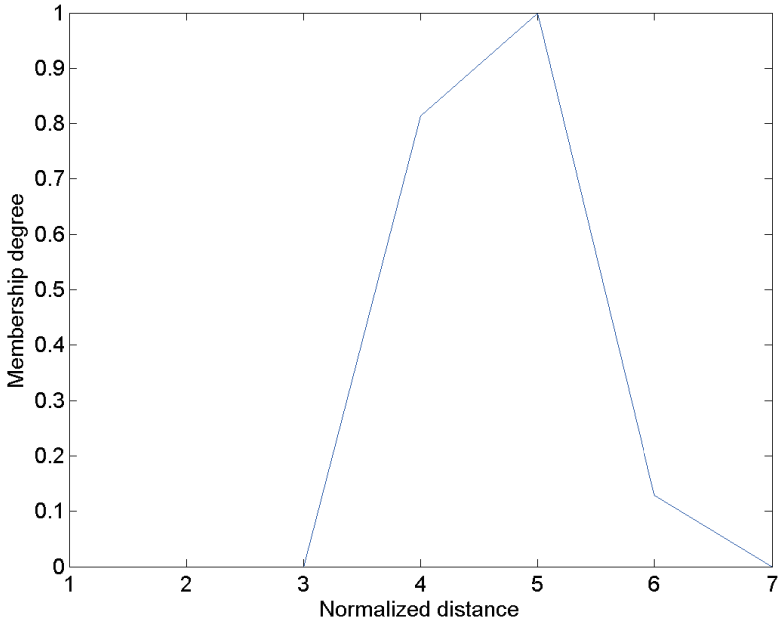

(b) The possibility distribution of distance *d* of subject B

Figure 4.11: The possibility distributions of feature distance d of both subjects.

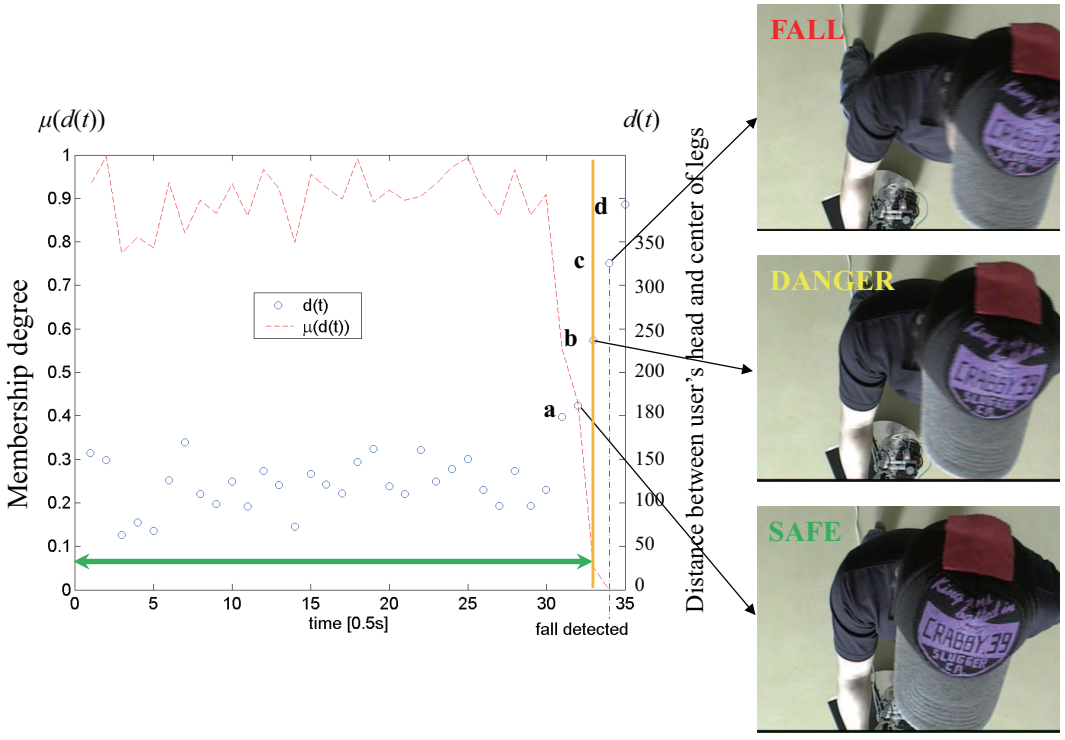

Figure 4.12: Experimental result of fall detection.

4.3.1 Intelligent Cane Robot System

The Cane Robot with Sensor Group

An intelligent cane robot as shown in **Fig. 4.13** was proposed for aiding the elderly walking and training their walking function. The cane robot consists of an omni-directional mobile base, an aluminous stick, and sensor system including a six-axis commercial force/torque sensor, and a laser rangefinder (LRF). A mechatronics device called universal joint, which is linked with the base of cane robot and an aluminous stick was designed to control the posture of stick.

The omni-directional mobile base comprises three commercially available omni-wheels and actuators, which are specially designed for the walker systems. Despite the small size, the load capacity of this mobile base is up to 80 kg.

The six-axis force/torque sensor is used as the main control input interface. The force sensor plays an important role in estimating human walking intention and falling over. In our previous work a concept called "intentional direction (ITD)" was proposed for estimating the user's walking intention .

The LRF is fixed on the omni-robot base for locating the relative position of the cane

robot and user's foot. A triangular area formed by three points including the position of robot and user's feet is defined as the support polygon. The support polygon plays an important role to determine the ZMP stability. If the ZMP moving out of this triangle area, the user will fall over.

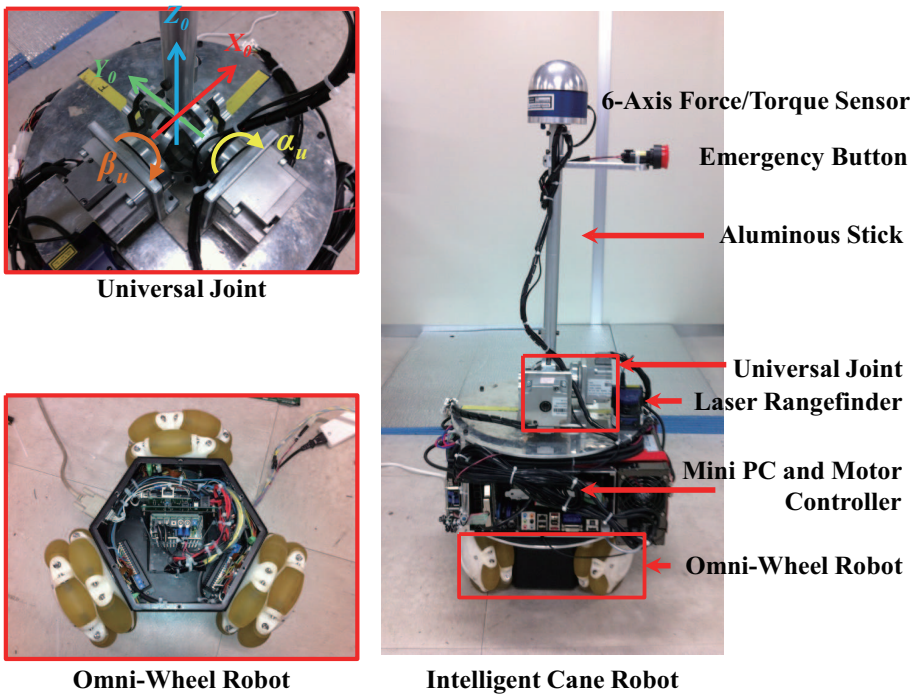

Figure 4.13: Intelligent cane robot prototype IV.

On-shoe Load Sensor

In this paper, a novel method was proposed to detect the risk of falling in the elderly based on ZMP estimation. For estimating the real ZMP, we should find the foot-ground reaction force. Therefore, a wearable load sensor system was proposed to obtain dynamics from the ground reaction force. This system includes four parts which is shown in **Fig.** 4.14-(A);

The nine-degree of freedom sensor stick includes an accelerometer, a gyroscope, and a magnetometer(see **Fig.** 4.14-(D)). The pressure on the sensing area of *FlexiForce* causes a change in the resistance of the sensing element in inverse proportion to the force applied. Even the *FlexiForce* sensor is not accurate enough, and also there is quite noise generated. By calibrating and applying a proper noise filter, where the Kalman-filter is used to reduce the noise, we can obtain the foot-ground reaction force satisfactorily to calculate the ZMP.

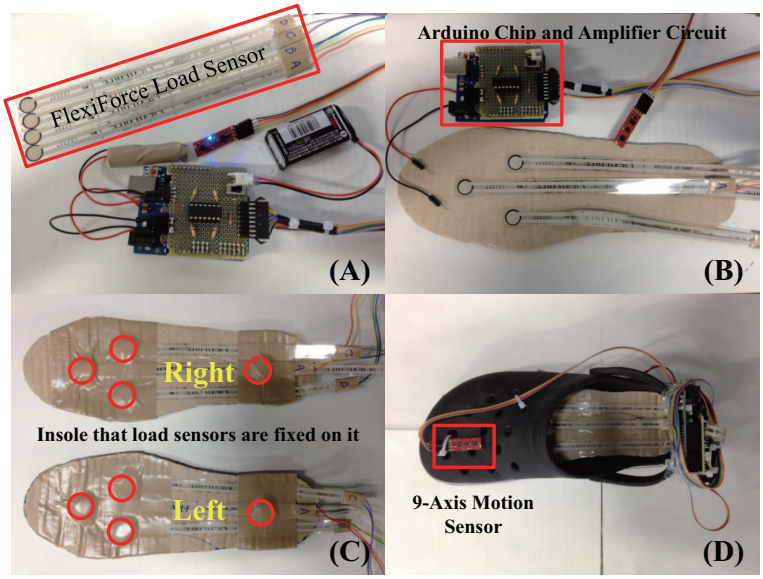

Figure 4.14: On-shoe load sensor system.

Human-in-the-loop control system

In this section, we introduce a shared control strategy for the human-machine control system to guarantee the stability, where the user is considered as the control object and the movement of user is regarded as the disturbance to the system stability. In the human-in-the-loop control system, two modes are prepared for the cases of normal and abnormal walking. "Mode switch" detects the walking status based on ZMP stability theory. The human-cane system block diagram is shown in **Fig. 4.15**.

4.3.2 Definitions of stability and instability statuses of human-cane system

The ZMP is a very important concept of the motion planning for biped robots, and also can be applied in the area of tripedal or multiped robot. There are two walking modes of legged robot from a stability viewpoint; one is statically stable walking and the other is dynamically stable walking. For dynamically stable walking robot, the ZMP can be computed using the **Eq. (4.2), (4.3)**. The stability can be achieved by controlling the position of ZMP of the robot to be inside the support polygon.

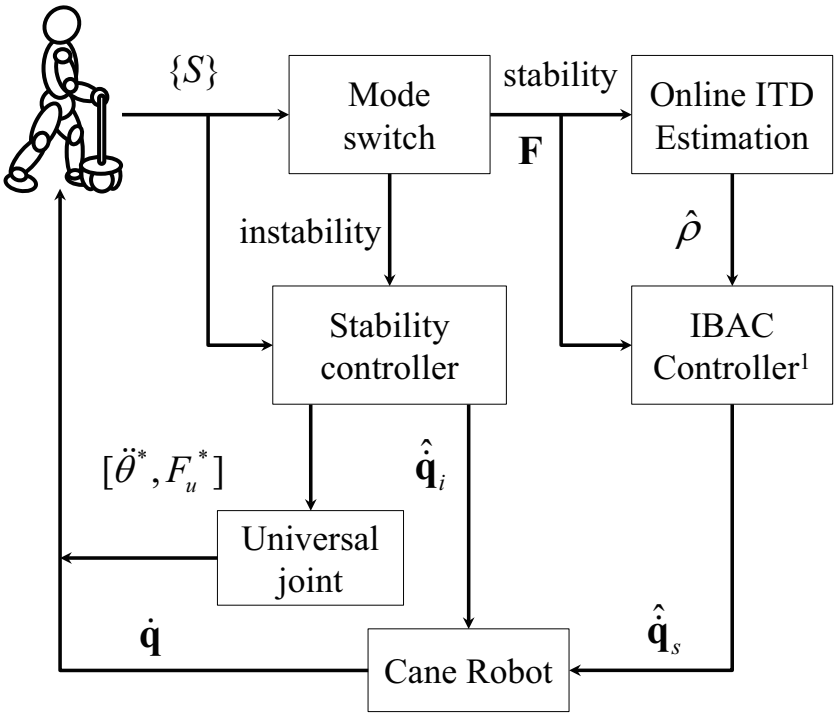

Figure 4.15: The human-in-the-loop system block diagram.

$$x_{zmp} = \frac{\sum_{i=1}^{n} m_i x_i \left(\ddot{z}_i + g\right) - \sum_{i=1}^{n} m_i \ddot{x}_i z_i - \sum_{i=1}^{n} I_{iy} \ddot{\theta}_{iy}}{\sum_{i=1}^{n} m_i \left(\ddot{z}_i + g\right)} \tag{4.2}$$

$$y_{zmp} = \frac{\sum_{i=1}^{n} m_i y_i \left(\ddot{z}_i + g\right) - \sum_{i=1}^{n} m_i \ddot{y}_i z_i - \sum_{i=1}^{n} I_{ix} \ddot{\theta}_{ix}}{\sum_{i=1}^{n} m_i \left(\ddot{z}_i + g\right)} \tag{4.3}$$

Where m_i is the mass of link, (I_{ix}, I_{iy}) are the inertial compo-nents, $(\theta_{ix}, \theta_{iy})$ are the acceleration of link (as shown in **Fig. 4.16**).

Unfortunately, these equations can just be used to compute the ZMP for a robot system, not for a human. Since the human is an uncontrollable factor in our human-cane system, we cannot control the movement and rotation of each part of human body. Furthermore, the position of each link (x_i, y_i, z_i) cannot be obtained by the existing sensors of the cane robot system. Therefore, we cannot control or even estimate the ZMP by using **Eq. (4.2), (4.3)**.

Therefore, the statically stable walking model is used instead of dynamics model. The static model can remain statically stable if and only if its center of gravity (COG) projects

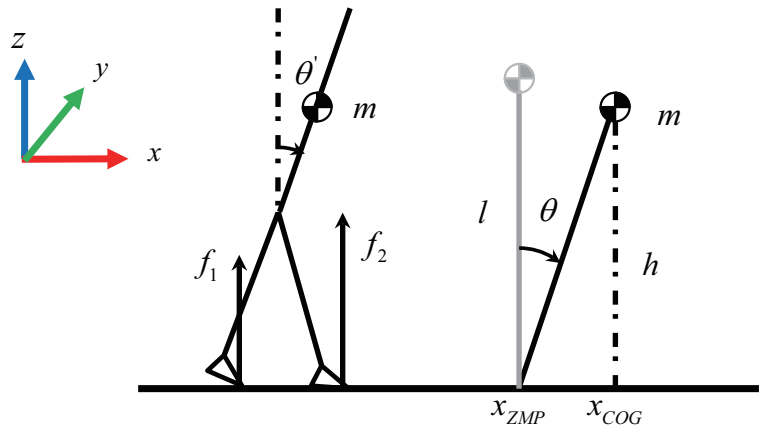

Figure 4.16: The simplified link model of human walking.

vertically inside the support polygon. By using this principle, we can detect the falling risk. The COG can be computed based on distributed forces as follows;

$$x_{cog} = \frac{\sum_{i=1}^{n} x_i f_i}{\sum_{i=1}^{n} f_i}, y_{cog} = \frac{\sum_{i=1}^{n} y_i f_i}{\sum_{i=1}^{n} f_i} \tag{4.4}$$

Where the (x_i, y_i) (n=1, 2, 3) denote the position of ground reaction force (the LRF is origin of the coordinate system), the denotes the magnitude of ground reaction force measured by on-shoe load sensor and six-axis force sensor.

4.3.3 Sensor configuration

To use the statically mode model (4.4), a wearable load sensor system was proposed to obtain the dynamical ground reaction force. This system includes four parts which is shown in **Fig.** 4.14-(A);

As shown in **Fig.** 4.17, the ground reaction forces f_1, f_2 and f_3 are measured by the six-axis force sensor and on-shoe load sensors respectively. The three contact points are denoted by P_1, P_2 and P_3. The coordinate value of point P_1, is easily obtained due to it is just the position of cane robot. By using a laser ranger finder, the coordinate values of point P_2 and P_3 can be approximately calculated (see the two yellow scanned segments on the legs in **Fig.** 4.17).

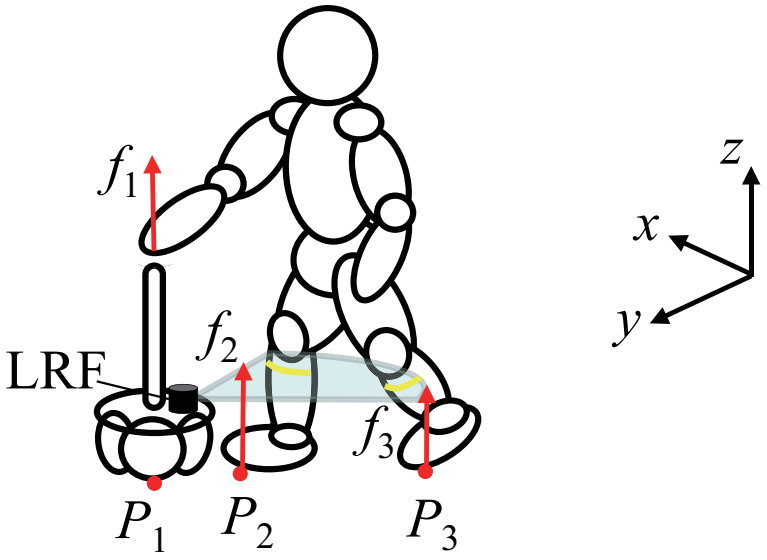

Figure 4.17: Sensory data required in ZMP calculation.

4.3.4 Falling detection method based on Fuzzy theory

As shown in **Fig.** ??-(a), possible falling states include 'forward falling', 'backward falling' and 'sideward falling'. Here state 'sideward falling' consists of all falling cases except forward and backward falling. In **Fig.** ??-(b), the positions of point P_1, P_2, P_3 and ZMP are depicted for all possible falling cases.

Obviously, an important feature indicating the user's falling state is the relative position between the ZMP and point P_0, which is the center of support triangle with vertices P_1, P_2 and P_3 (see **Fig.** 4.20). This relative position can be described by a two-dimensional vector $(\Delta x, \Delta y)^T$. While the user is walking normally, the ZMP should fluctuate around P_0 in a small area. This area differs from different people. When the user is falling down, the distance between ZMP and P_0 will increase suddenly. And the falling direction can also be easily obtained by observing vector $(\Delta x, \Delta y)^T$.

The distribution of feature during normal walking is analyzed similar to . Dubois possibility theory is applied to describe the distribution of vector $\overrightarrow{P_0P_zmp} = [\Delta x, \Delta y]^T$ P0PZMP = [x, y]T during the normal walking state .

The procedure starts by constructing the data histograms for Δx and Δy during normal walking state. The number of bins h for a histogram is experimentally determined. Each bin is represented by the center of the interval denoted by y_j . The height of each bar is the number of learning points, located in this bin.

The probability distribution $\left\{ p\left(y_i\right) : j = 1, 2, \cdots, h \right\}$ is calculated by dividing the

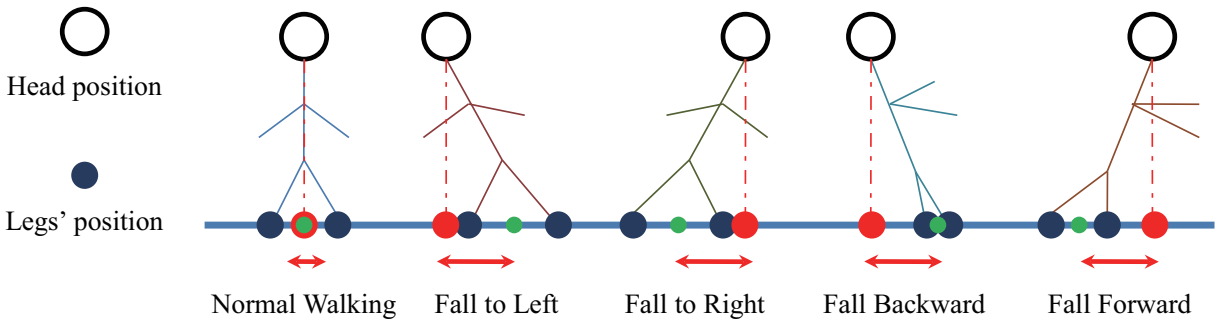

Figure 4.18: (a) Normal walking and possible falling states.

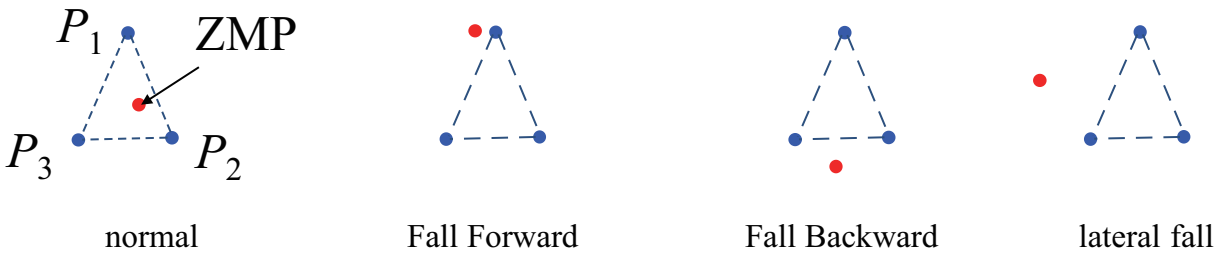

Figure 4.19: (b) Point positions of different falling cases.

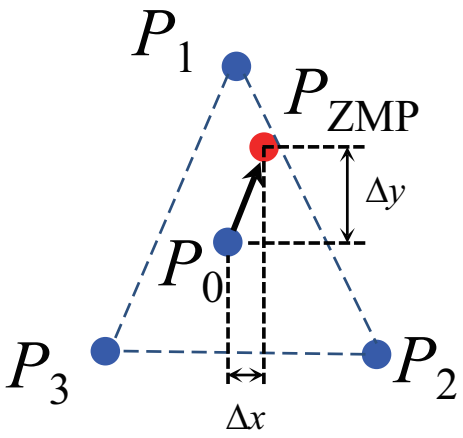

Figure 4.20: The feature $(\Delta x, \Delta y)^T$ of fall detection.

height of each bin by the total number of learning points belonging to the same class. The possibility distribution $\left\{ \pi\left(y_i\right) : j = 1, 2, \cdots, h \right\}$ is deduced from the probability distribution by the bijective transformation of Dubois and Prade defined by

$$\pi\left(y_k\right) = \sum_{j=1}^{h} \min\left[p\left(y_k\right), p\left(y_j\right)\right] \tag{4.5}$$

The membership functions $\mu(\cdot)$ that characterize the fuzzy set "normal walking", is finally calculated from the corresponding possibility distributions by linear interpolation.

The fall detection is implemented by a very simple algorithm, which is illustrated as follows: (assuming the human walking behavior is monitored at discrete times, n denotes the current time)

IF $\mu\left(\Delta x\left(n\right),\Delta y\left(n\right)\right) < c$ *and* $\mu\left(\Delta x\left(n-1\right),\Delta y\left(n-1\right)\right) < c$

Then a fall is detected.

Constant c is a small positive number which indicates a very low possibility of "normal walking" state.

4.3.5 Experiment study

We experimented with the cane robot to illustrate the effectiveness of the proposed methods. First, the possibility distribution of normal walking state is investigated. Then the validity of fall detection method is verified by experiments.

Experiments of "normal walking"

A university students were requested to operate the cane robot to conduct "normal walking" experiments. From the experimental data, the possibility distributions of "normal walking" were obtained as well as the membership degree function. The original trajectories and corresponding data histograms of $\Delta x(n)$ and $\Delta y(n)$ are shown in **Fig. 4.21** (I) and (IV). The constant h is assumed to be 10. The probability distribution p(nk), possibility distribution $\pi(n_k)$ are depicted in **Fig. 4.21** (II), (III), (V) and (VI). The obtained membership function $\mu(\Delta x(n), \Delta)$, $\Delta y(n))$ is given in Fig. 18

Experiments of "falling detection"

In this experiment, the subject pretended to fall down during walking. The fall detection rule described in **Section 4.3.4** was applied in the experiment. Constant c was chosen as 0.02. The fall was detected promptly as shown by Fig. 19.

A new omni-directional type intelligent cane robot is developed for the elderly and handicapped. Motion control and fall detection of this robot are studied based on online estimating human walking intention and the position of ZMP. The main contribution of this study lies in:

1. presenting dynamic models and online inference algorithm for the human walking intention, which is significant to lead the user walking in a natural and comfortable

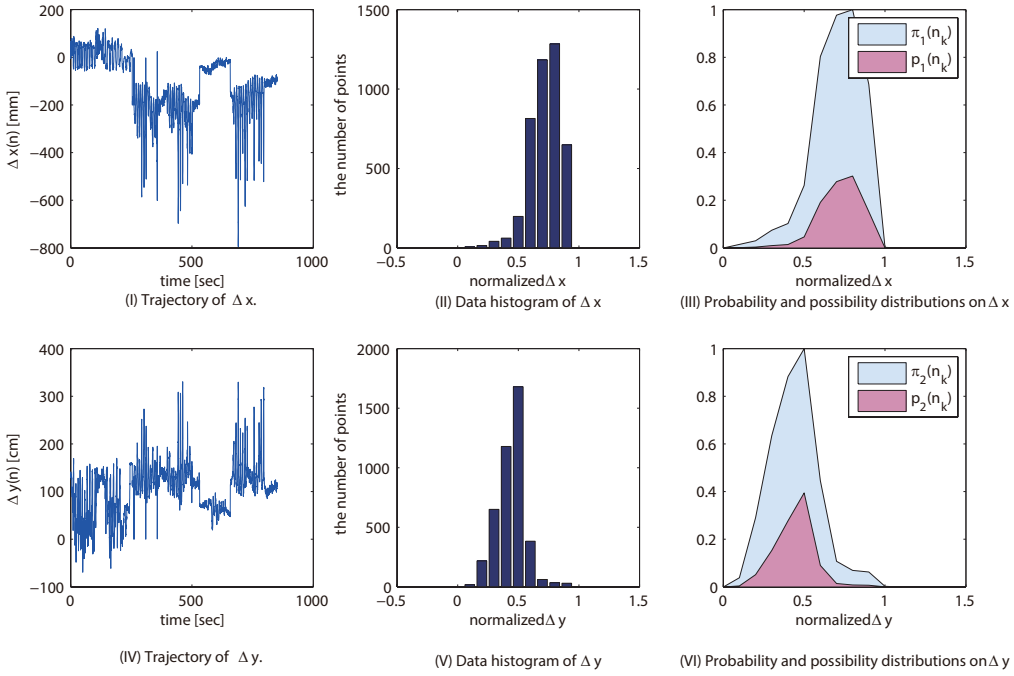

Figure 4.21: Trajectories, data histograms, probability and possibility distributions of "normal walking".

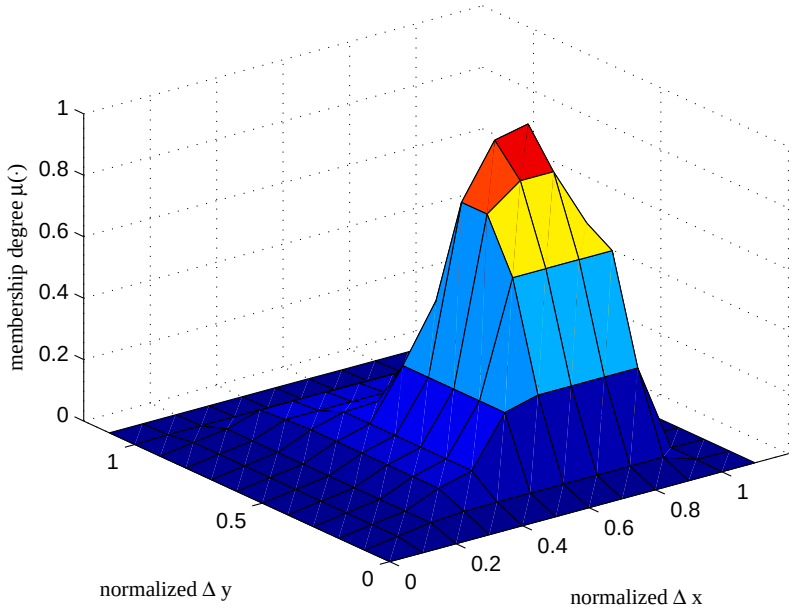

Figure 4.22: The membership degree function of "normal walking".

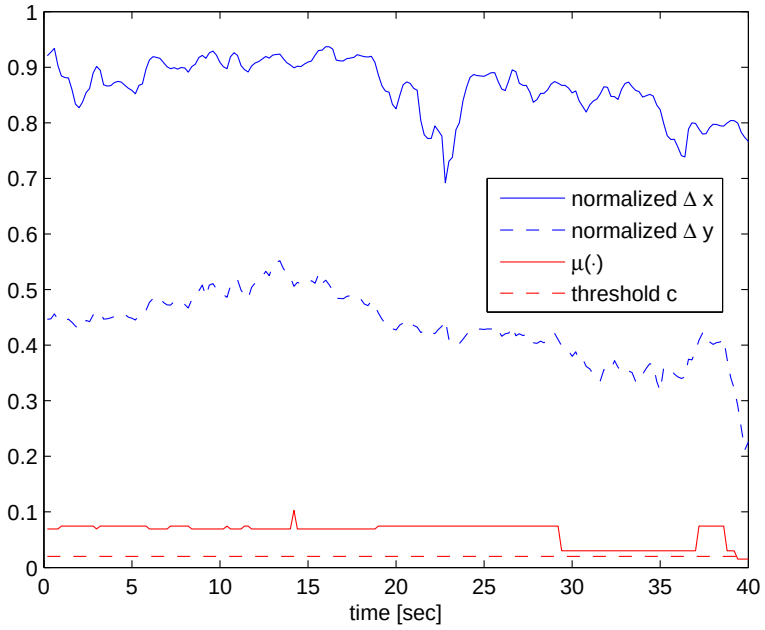

Figure 4.23: Fall detection experiment.

way.

2. proposing practical ZMP based fall detection method during operating the cane robot. An intention based admittance control (IBAC) scheme is also proposed and used to drive cane robot. Experiments were performed on the flat ground to verify the effectiveness of proposed algorithms.

4.4 Summary

A new omni-directional type intelligent cane robot is developed for the elderly and handicapped. Motion control and fall detection of this robot are studied based on online estimating human walking intention and the position of ZMP. The main contribution of this study lies in: 1) presenting dynamic models and online inference algorithm for the human walking intention, which is significant to lead the user walking in a natural and comfortable way. 2) proposing practical ZMP based fall detection method during operating the cane robot. An intention based admittance control (IBAC) scheme is also proposed and used to drive cane robot. Experiments were performed on the flat ground to verify the effectiveness of proposed algorithms.

Chapter 5

Fall Prevention

5.1 Introduction

In this section we proposes a novel human fall detection and prevention method for a walking aid. A three-wheeled omni-directional cane robot was developed previously for aiding the elderly walking. The relative position between the legs of user and the Center of Gravity (COG) of user play an important role in the fall detection when using the cane robot. The COG of user can be estimated from the angle of an inverted pendulum which represents human model. The angle of the inverted pendulum is computed by the support leg position, the hip position, and the force that the human pushes the cane. The fall direction and relative position between the human and the robot play an important role in the fall prevention.

5.2 Fall Prevention for the Elderly (*Prototype III*)

The aim of the intelligent cane is to perform optimized action for the user. These actions include guide, prevent fall, rehabilitation and so on. Optimized actions depend on the user intention. Therefore, the robot estimates the users intention from the sensory information. This estimated intention is used to determine the optimized action for the user.

5.2.1 Mechanism of cane robot

A prototype system of omni-directional type cane robot shows in **Fig.** 5.1, which is developed to help the elderly walking. The cane robot consists of an omni-directional mobile base, a metal stick and sensor groups including the force sensor and the LRFs.

The omni-directional mobile base comprises three commercially available omni-wheels and actuators, which are specially designed for the walker systems. Despite the small size, the load capacity of this mobile base is up to 50 kilograms. The LRF measures the distances between the stick and the knees, and between the stick and the body, which plays an important role in the function of fall prevention. A six-axis force/torque sensor is used as the main control input interface. Encorders that are loaded on the omni-wheel vehicle measured the position of the robot.

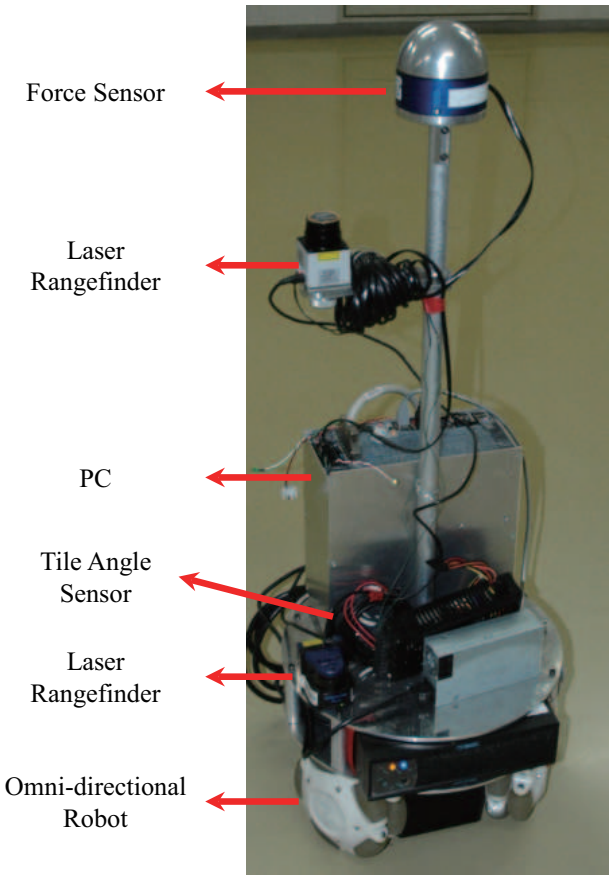

Figure 5.1: Omni-directional type cane robot.(*Prototype III*)

The kinematics of a robot using orthogonal universal wheels separated by 120° have been described previously

Introducing $\xi = \begin{bmatrix} {}^{I}x & {}^{I}y & \rho \end{bmatrix}^{\mathrm{T}}$ and $\varphi = \begin{bmatrix} \varphi_1 & \varphi_2 & \varphi_3 \end{bmatrix}^{\mathrm{T}}$ to denote the posture in coordinate I and the angles of three wheels, the kinematics of our omni-directional platform can be described by

$$\dot{\varphi} = \mathbf{R}(\rho) \cdot \dot{\xi} \tag{5.1}$$

where the rotation matrix $\mathbf{R}$ satisfies

$$\mathbf{R}(\rho) = \frac{1}{R} \cdot \begin{bmatrix} \sin(\rho - \alpha_1) & -\cos(\rho - \alpha_1) & L \\ \sin(\rho - \alpha_2) & -\cos(\rho - \alpha_2) & L \\ \sin(\rho - \alpha_3) & -\cos(\rho - \alpha_3) & L \end{bmatrix} \tag{5.2}$$

As shown in **Fig. 5.2**, R is the radius of each wheel and L is the effective distance between the center of force sensor and the rim of a wheel

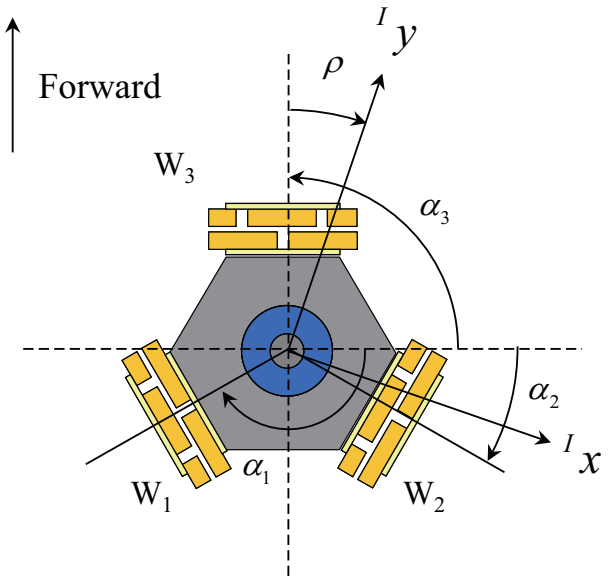

Figure 5.2: Coordinate frame I based on the ITD.

In **Fig. 5.3**, the velocity vector of the vehicle, $\dot{\xi} = \begin{bmatrix} {}^I\dot{x} & {}^I\dot{y} & \dot{\rho} \end{bmatrix}^{\mathrm{T}}$, is calculated by the following equation.

$$\begin{bmatrix} {}^I\dot{x} \\ {}^I\dot{y} \\ \dot{\varphi} \end{bmatrix} = J \begin{bmatrix} R\varphi_1 \\ R\varphi_2 \\ R\varphi_3 \end{bmatrix} \tag{5.3}$$

where

$$J = \begin{bmatrix} -2\cos\rho & \cos\rho + \sqrt{3}\sin\rho & \cos\rho - \sqrt{3}\sin\rho \\ -2\cos\rho & \sin\rho - \sqrt{3}\cos\rho & \sin\rho + \sqrt{3}\cos\rho \\ 1/L & 1/L & 1/L \end{bmatrix} \tag{5.4}$$

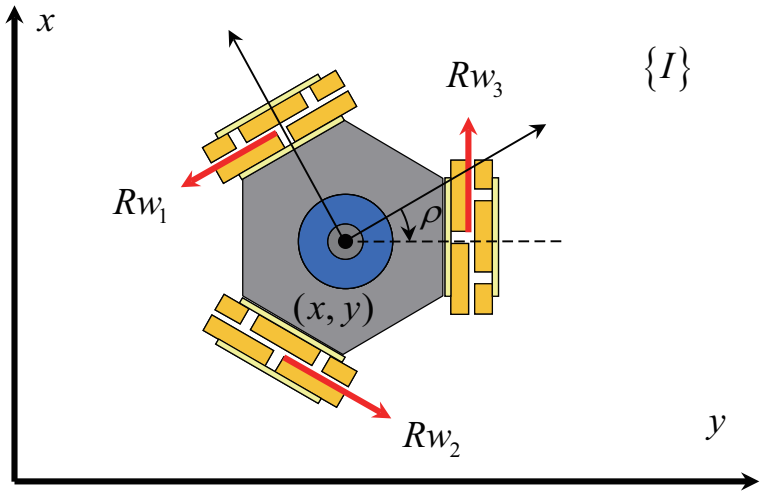

Figure 5.3: Kinematics of Omni-wheel robot.

5.2.2 Control Architecture

There are many possible move modes during the usage of the cane robot. Hirata et al considered three modes including 'normal walking', 'stop' and 'emergency' in their studies. Actually, we can divide these rough modes further. For instance, the mode 'normal walking' consists of 'go straight forward', 'turn left' , 'turn right' 'emergency' and so on. Normally, different control scheme is required for different move mode. Considering the high-level discrete move modes and low-level motion control scheme based on continuous sensor signals, hybrid system theory is selected as the mathematical tool for the modeling and control design. A hierarchical control architecture is also proposed, which is depicted by **Fig.** 5.4.

In the high-level supervising module, current move mode is estimated from sensor signals, which is used to choose appropriate filter to infer the human intention. The inferred human intention is taken as the input of the IBAC controller in the low-level motion controller module, which is proposed in our previous study [**?**]. All the methods are further illustrated in the following sections.

5.2.3 Walking model of human operator

Definition of orientation for walking model

The absolute coordinate system (X,Y,Z) is a right hand coordinate system in which the Z axis means the height, and the original point is set to the initial position of the robot.The

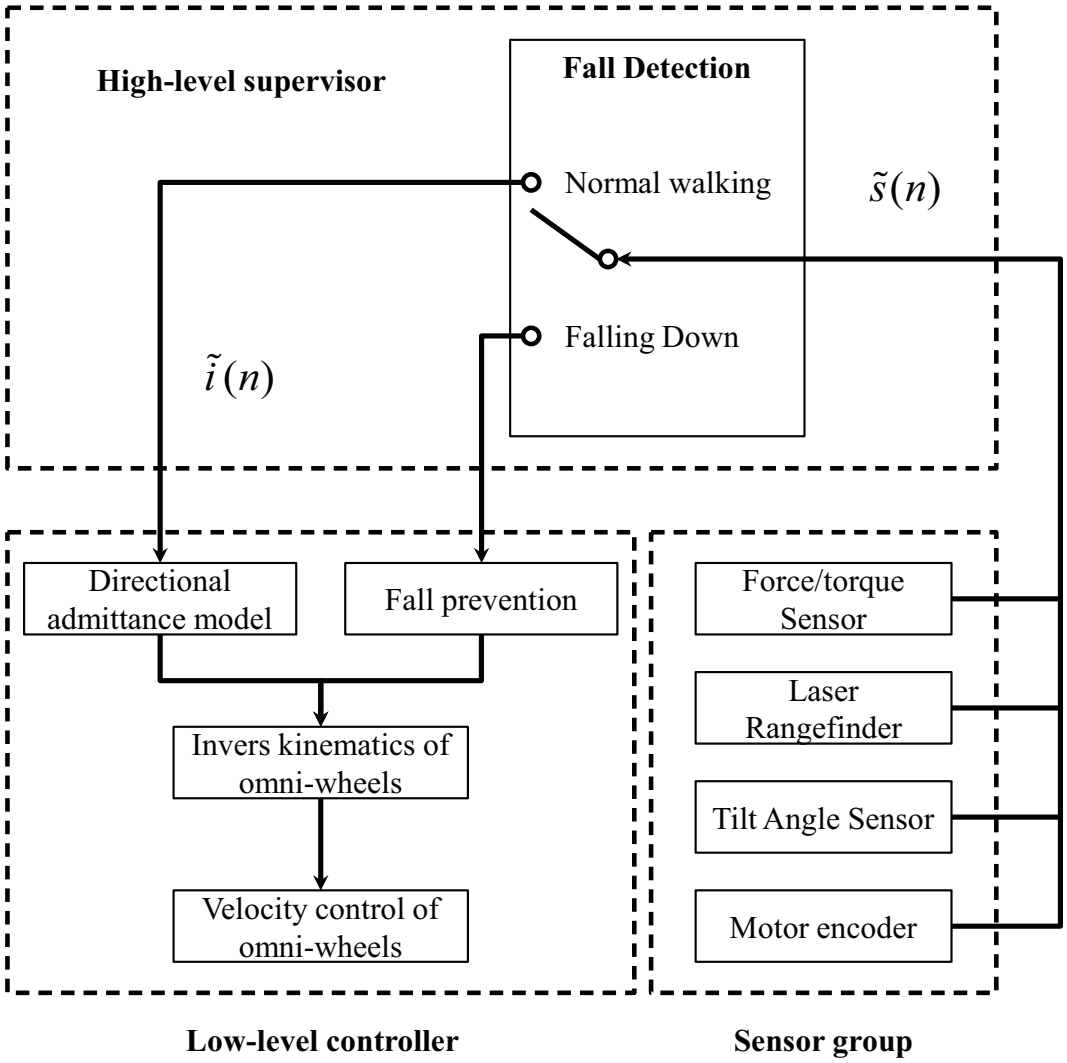

Figure 5.4: The hierarchial control structure.

support coordinate system (x, y, z) is a relative coordinate system in which the original point is set to the support point. (See **Fig. 5.5**)

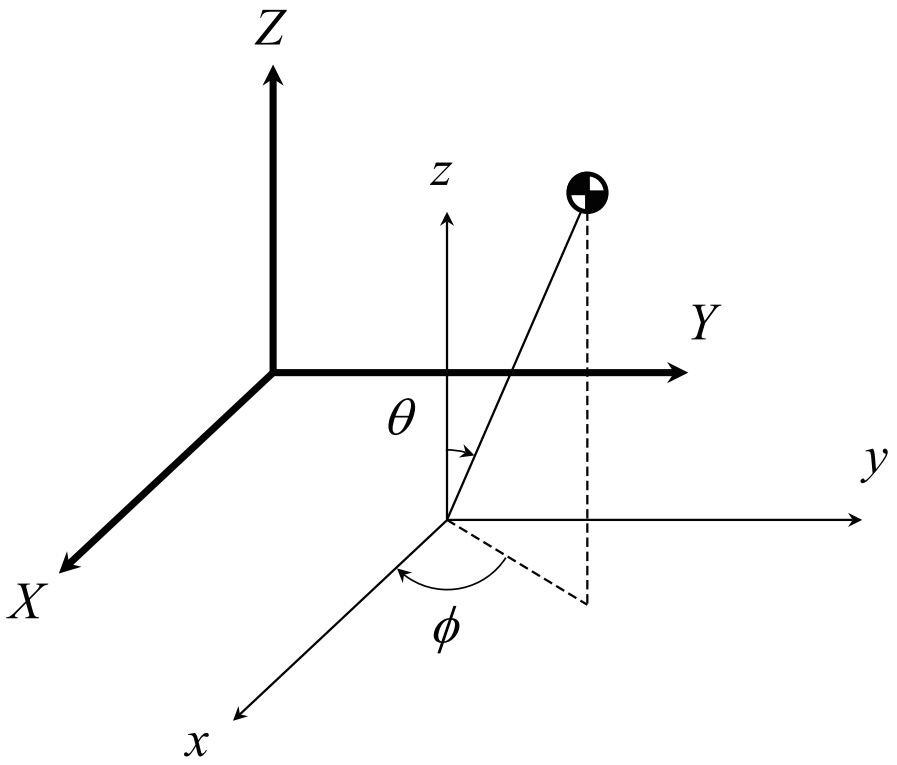

Figure 5.5: Absolute coordinate and bearing coordinate.

Single support phase model

In the single support phase, the user is modeled by a inverted pendulum, whose dynamics is described by

$$\ddot{r} - \dot{\phi} r \sin^2\theta - \dot{\theta}^2 r + g\cos\theta = f/m \tag{5.5}$$

where f consists of f_1 (reactive force) and f_2 (the force from the robot). f_2 is represented as:

$$f_2 = -f_x \sin\theta\cos\phi - f_y \sin\theta\sin\phi - f_z\cos\theta \tag{5.6}$$

where f_x, f_y, f_z are forces measured by the force sensor.

The value of r is almost a constant during walking. Based on this assumption f_1 is described by:

$$f_1 = -\frac{m(x\dot{y} - \dot{x}y)}{r(x^2+y^2)} - \frac{mr(x\dot{x}+y\dot{y})^2}{(r^2-x^2-y^2)(x^2+y^2)} + \frac{f_x x + f_y y + (f_z+mg)\sqrt{r^2-x^2-y^2}}{r} \tag{5.7}$$

Therefore, the dynamics of COG is given by

$$\begin{aligned} m\ddot{x} &= \frac{f_1 x}{r} - f_x \\ m\ddot{y} &= \frac{f_1 y}{r} - f_y \end{aligned} \tag{5.8}$$

5.3 Static Tip-Over Stability Analysis for the Cane Robot (*Prototype IV*)

As a care-nursing device, the cane robot was designed to assist the elderly in both indoor and outdoor environments. Therefore the size and weight of cane robot should be minimized. But in that case, there is high risk that the cane robot would be pushed over by the user. In this paper a constrained nonlinear multivariable algorithm was designed to optimize the stable posture of cane robot. By controlling the posture of stick, the maximums sufferable torque moment which lead to cane robot falling over can be increased.

In this section, we discuss how to ensure the stability of cane robot while the cane robot assists the elderly walking. The cane robot differs from other walker-type robot is that the former has a high mobility, and the latter has a robust stability. In our previous study, a fall detection and prevention scheme was proposed for the user walking security. But the stability of cane robot was be subjected to the small size and light weight. To improve the robust stability, a universal joint that driven by two DC motors was designed and installed in the omni-directional base connected with the aluminum stick. The posture of stick can be controlled by the universal joint. A constrained nonlinear multivariable algorithm was applied to optimize the stability posture of cane robot. By controlling the tilt angle of stick, the cane robot can prevent the user from falling over.

As we mentioned above, the ability of avoiding cane robot to fall over was restricted by the small size and light weight. Therefore, in this paper the main work is focused on improving the robust stability of robot. The optimal posture of cane robot $[\alpha_u, \beta_u]$ can be calculated by specified constraint conditions for robust stability of cane robot which is discussed in next section. The $[\alpha_u, \beta_u]$ denoted the posture of universal joint was shown

in **Fig. 5.6**. Two DC motors were used to control the angle of joint, and the controllable range of both joints is ±25°.

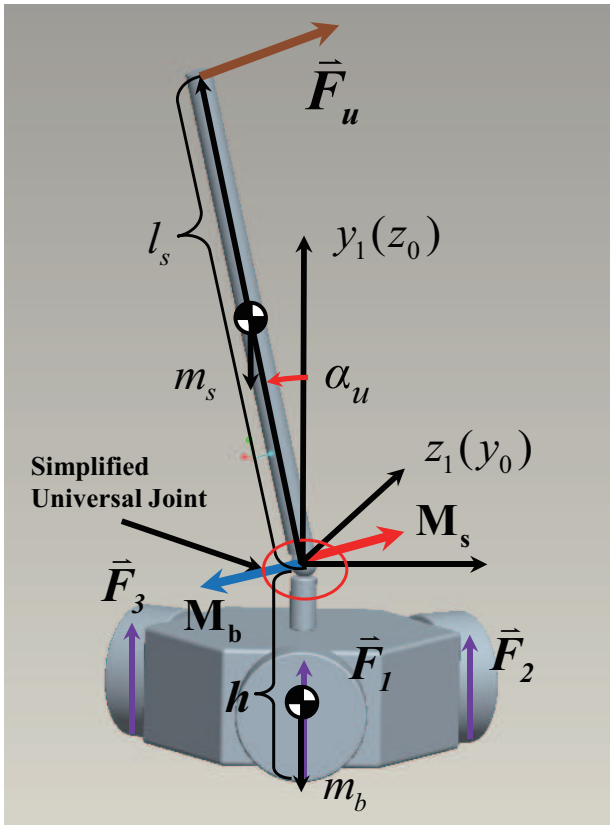

Figure 5.6: Definition of cane robot coordinate system {1}

5.3.1 Real-time Posture and Motion Control

Firstly, the stability status of cane robot was defined as that while the cane robot moving or stopping, the three omni-directional wheels must contact with ground. If the human user pushed the cane robot strongly, one or two wheels will space from ground, and finally results in the cane robot falling over. In that case, the cane robot will lose the support for assisting the elderly walking or avoiding falling over.

In case of emergency that the human user is going to fall over, the cane robot will rotate along the user and move to the position in the direction of user falling down. As soon as the robot moved to the specified position, all the three omni-directional wheels of cane robot will be broken and secure the users balance. As mentioned above, the cane robot has a defect on stability due to the limitation of small size and light weight. In this section, the

specified constraint conditions for improving robust stability of cane robot were proposed and discussed.

Coordinate Systems Definition

To describe the posture of iCane, three coordinate systems are defined. The origin points of all the coordinate systems are coincident with the universal joint. System {0} is the inertial frame. System {1} is attached to the omni-directional base and rotate with the yaw motion α about axis z_0. Start with the frame coincident with system {1}. System {2} can be obtained by firstly rotating {1} about x_1 by an angle γ, then about y_2 by an angle β. Note that system {2} is attached to the metal stick and axes x_1 and y_1 are coaxial with the two motors of universal joint.

Accordingly, the rotation matrices are then given by

$$ {}^{0}_{1}\mathbf{R} = \mathbf{R_Z}(\alpha) = \begin{bmatrix} c\alpha & -s\alpha & 0 \\ s\alpha & c\alpha & 0 \\ 0 & 0 & 1 \end{bmatrix} \tag{5.9} $$

$$ {}^{1}_{2}\mathbf{R} = \mathbf{R_Y}(\beta)\mathbf{R_X}(\gamma) = \begin{bmatrix} c\beta & s\beta \cdot s\gamma & s\beta \cdot c\gamma \\ 0 & c\gamma & -s\gamma \\ -s\beta & c\beta \cdot s\gamma & c\beta \cdot c\gamma \end{bmatrix} \tag{5.10} $$

It is obvious that the posture of iCane can be determined if the rotation angles α, β and γ are fixed

In **Fig. 5.7**, $[\alpha, \beta, \gamma]$ denotes the rotation angles of stick about each axis in coordinate {0}:

α angle of stick rotated about z_0(yaw)

β angle of stick rotated about y_0(pitch)

γ angle of stick rotated about x_0(roll)

l_s is the length of stick, and $\vec{l}_s$ is the end position vector of stick. According to the Euler equation, the end position of stick was calculated by **Eq. 5.11**.

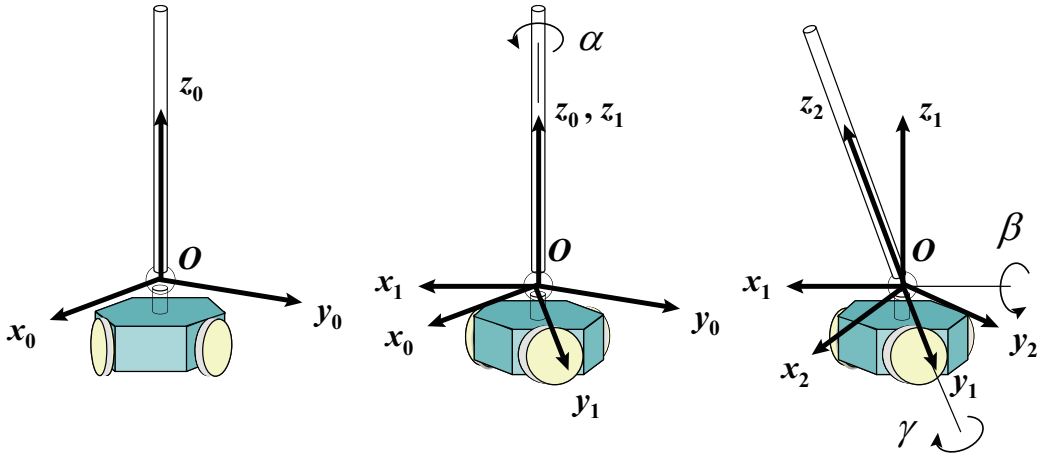

Figure 5.7: Coordinate systems definition.

$$\vec{l}_s = {}^0_1\mathbf{R}_z(\alpha) \cdot {}^1_2\mathbf{R} \cdot \begin{bmatrix} 0 & 0 & -l_s \end{bmatrix}^{\mathbf{T}}$$

$$= \begin{bmatrix} c\alpha \cdot c\beta & c\alpha \cdot s\beta \cdot s\gamma - s\alpha \cdot c\gamma & c\alpha \cdot s\beta \cdot c\gamma - s\alpha \cdot s\gamma \\ s\alpha \cdot c\beta & s\alpha \cdot s\beta \cdot s\gamma + c\alpha \cdot c\gamma & s\alpha \cdot s\beta \cdot c\gamma - c\alpha \cdot s\gamma \\ -s\beta & c\beta \cdot s\gamma & c\beta \cdot c\gamma \end{bmatrix} \cdot \begin{bmatrix} 0 \\ 0 \\ -l_s \end{bmatrix} \tag{5.11}$$

$\vec{l}_1, \vec{l}_2, \vec{l}_3$ indicates vector of contact point of each omni-directional wheels. r is the radius of omni-directional mobile base, h denotes the height from the universal joint to the ground. $\mathbf{G_s}$ are $\mathbf{G_b}$ the mass of stick and mobile robot base.

$$\vec{l}_1 = \begin{bmatrix} 0 & -r\cos(\pi/6) & h \end{bmatrix}$$

$$\vec{l}_2 = \begin{bmatrix} r\cos(\pi/6)^2 & r\cos(\pi/6)/2 & h \end{bmatrix}$$

$$\vec{l}_3 = \begin{bmatrix} -r\cos(\pi/6)^2 & r\cos(\pi/6)/2 & h \end{bmatrix}$$

Static Force Analysis for Stability of Cane Robot

The maximums sufferable thrust acted on cane robot was shown in inequality **Eq.** 5.12, the right part of inequality denotes the generated torque moment by the mass of cane

robot and left part is the torque moment which is generated by user's thrust, in the case of without using the universal joint:

$$\begin{aligned} l_s \left|\vec{F}_u\right| cos\theta_H &\leq l_R m_{all} sin\theta_R \\ \Rightarrow \left|\vec{F}_u\right| &\leq \frac{l_R m_{all} sin\theta_R}{l_s cos\theta_H} \end{aligned} \tag{5.12}$$

$\left|\vec{F}_u\right|$ denotes the maximums sufferable thrust. By changing the tilt angle of the stick a_u, the moment length can be extended to $l_s \cos\theta'_H$, and the maximums thrust can be increased to $\left|\vec{F}_u^{\,o}\right|$ as shown in inequality (**5.13**).

$$\begin{aligned} l_s \left|\vec{F}_u^{\,o}\right| cos\theta'_H &\leq l_R m \sin\theta_R \\ \Rightarrow \left|\vec{F}_u^{\,o}\right| &\leq \frac{l_R m \sin\theta_R}{l_s \cos\theta'_H} \end{aligned} \tag{5.13}$$

Optimal Posture of iCane for Fall Prevention

The force analysis of iCane is illustrated in **Fig. 5.8**. The length of metal stick is l_s. The height of universal joint is h. Three contact points between the omni-wheels and the ground are denoted by P_1, P_2 and P_3. The user exerts the contact force at the end of stick, denoted by point P_u.

Accordingly, the interactive forces at points P_1, P_2 and P_3 and P_u are denoted by $\mathbf{F}_1$, $\mathbf{F}_2$, $\mathbf{F}_3$ and $\mathbf{F}_u$. The gravities of the metal stick and the omni-directional base are $\mathbf{G}_s$ and $\mathbf{F}_b$, respectively. $\mathbf{M}_s$ and $\mathbf{M}_b$ are the moments exerted at point O by the stick and the base.

If the static balance of iCane is kept, the following equations are hold according to Newton-Euler rules:

$$\begin{aligned} \mathbf{F_1} + \mathbf{F_2} + \mathbf{F_3} + \mathbf{F_u} + \mathbf{G_s} + \mathbf{G_b} &= 0 \\ \mathbf{M_s} + \mathbf{M_b} &= 0 \end{aligned} \tag{5.14}$$

where the two moments satisfy

$$\begin{aligned} \mathbf{M_b} &= \overrightarrow{P_1O} \times \mathbf{F_1} + \overrightarrow{P_2O} \times \mathbf{F_2} + \overrightarrow{P_3O} \times \mathbf{F_3} \\ \mathbf{M_s} &= \overrightarrow{P_uO} \times \mathbf{F_u} + \tfrac{1}{2}\overrightarrow{P_uO} \times \mathbf{G_s} \end{aligned} \tag{5.15}$$

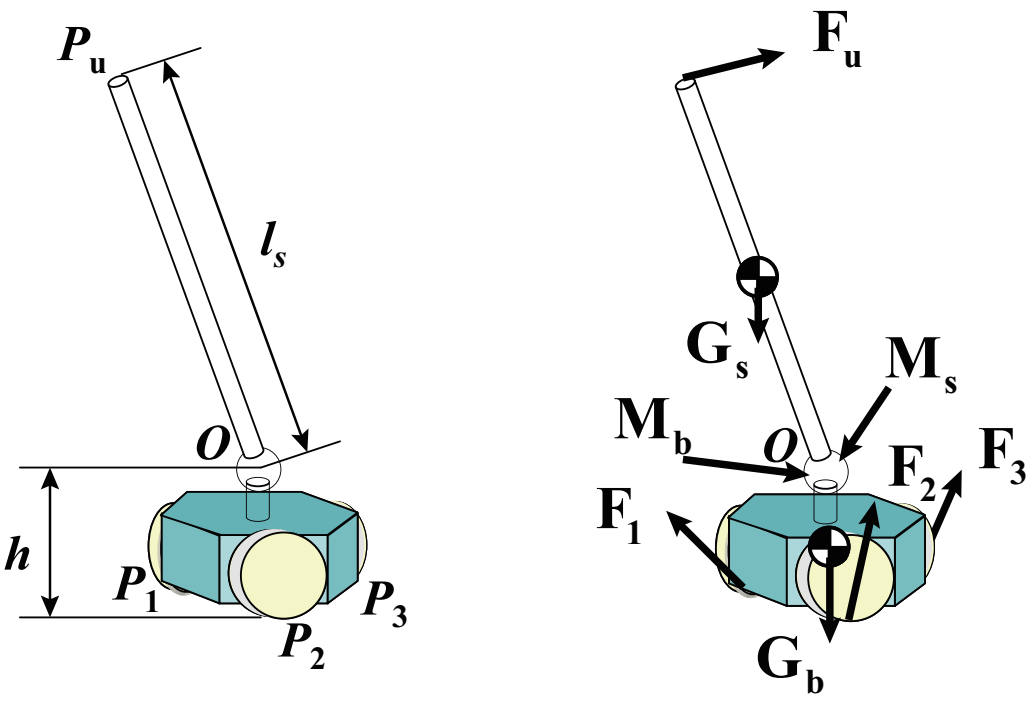

Figure 5.8: Force analysis of intelligent cane robot.

Because the rim of an omni-wheel consists of many passive rollers, the contact force $\mathbf{F_i}(\mathbf{i} = 1,\ 2 \text{ or } 3)$ has no component along the rotation axis of the i-th wheel. Thus, we have the following constraints of each contact force $\mathbf{F_i}$:

$$\mathbf{F_i} \cdot \vec{n}_i = 0, i = 1, 2, 3 \tag{5.16}$$

where the unit vector $\vec{n}_i$ is given by

$$\vec{n}_1 = \begin{bmatrix} 0 \\ 1 \\ 0 \end{bmatrix}_1, \vec{n}_2 = \begin{bmatrix} -\cos(\pi/6) \\ -0.5 \\ 0 \end{bmatrix}_1, \vec{n}_3 = \begin{bmatrix} \cos(\pi/6) \\ -0.5 \\ 0 \end{bmatrix}_1 \tag{5.17}$$

In addition, if iCane can keep still on the ground, all the contact forces between three wheels and the ground should be no less than zero. That is, we have another constraint condition:

$$f_{zi} \geq 0, i = 1, 2, 3 \tag{5.18}$$

where the three contact forces are described by

$$\mathbf{F_1} = \begin{bmatrix} f_{x1} \\ f_{y1} \\ f_{z1} \end{bmatrix}_0, \mathbf{F_2} = \begin{bmatrix} f_{x2} \\ f_{y2} \\ f_{z2} \end{bmatrix}_0, \mathbf{F_3} = \begin{bmatrix} f_{x3} \\ f_{y3} \\ f_{z3} \end{bmatrix}_0 \tag{5.19}$$

In order to prevent the user from falling down due to stumbling or false step, the iCane should adjust its posture in time when these emergencies occur. In a suitable posture, it can sustain the thrust of user as big as possible. Theoretically, we can define this suitable posture as follows.

Definition 1. (Optimal Posture for Fall Prevention)

Assume that the direction of user thrust $\mathbf{F_u}$ is known. $(\alpha^*, \beta^*, \gamma^*)$ is referred to as the optimal posture of iCane for fall prevention if it is the solution of the following optimization problem:

$$\begin{aligned} &\arg\max_{\alpha^*,\beta^*,\gamma^*} \|\mathbf{F_u}\|, s.t. \\ &\begin{cases} \mathbf{F_1} + \mathbf{F_2} + \mathbf{F_3} + \mathbf{F_u} + \mathbf{G_s} + \mathbf{G_b} = 0 \\ \overrightarrow{P_1O} \times \mathbf{F_1} + \overrightarrow{P_2O} \times \mathbf{F_2} + \overrightarrow{P_3O} \times \mathbf{F_3} + \overrightarrow{P_uO} \times \mathbf{F_u} + \frac{1}{2}\overrightarrow{P_uO} \times \mathbf{G_s} = 0 \\ \mathbf{F_i}\cdot = 0, f_{zi} \geq 0, i = 1, 2, 3 \\ \leq \alpha \leq \bar{\alpha}, \leq \beta \leq \bar{\beta}, \leq \gamma \leq \bar{\gamma} \end{cases} \end{aligned} \tag{5.20}$$

For one omni-directional wheel, it can move in two directions, one is the active direction which be marked in red(see **Fig. 5.9**-(B)). The active one can be controlled by motor, but the passive direction which marked in blue in **Fig. 5.9**, cannot be controlled directly. l is the radius of omni-robot $\vec{N}_1, \vec{N}_3, \vec{N}_3$ indicate the position vector of each wheel that extends from the center of omni-robot (5.21). ${}^0_1\mathbf{R}(\alpha)$ is the Euler angle that the stick rotated α about z-axis (5.9). In passive direction of each wheel, the friction is equal zero as shown in (5.22).

$$\begin{aligned} \vec{N}_1 &= \begin{bmatrix} 0 & -l & 0 \end{bmatrix} \\ \vec{N}_2 &= \begin{bmatrix} -\cos(\pi/6) & -\sin(\pi/6) & 0 \end{bmatrix} \\ \vec{N}_3 &= \begin{bmatrix} \cos(\pi/6) & -\sin(\pi/6) & 0 \end{bmatrix} \end{aligned} \tag{5.21}$$

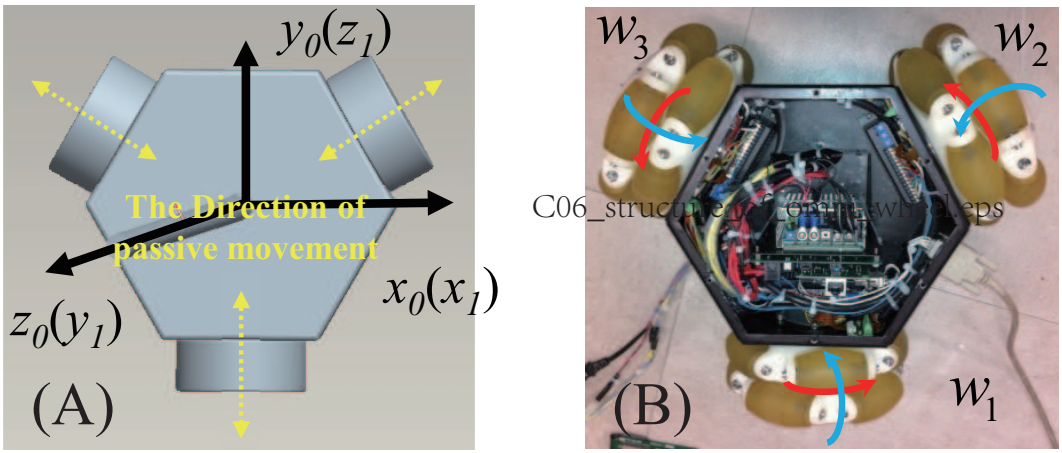

Figure 5.9: Structure of omni-wheel robot.

$$\begin{bmatrix} \vec{\mathbf{F}} & 0 & 0 \\ 0 & \vec{\mathbf{F}}_{\mathbf{2}} & 0 \\ 0 & 0 & \vec{\mathbf{F}}_{\mathbf{3}} \end{bmatrix} \cdot \begin{bmatrix} {}^{0}_{1}\mathbf{R} \cdot \vec{N}_1 \\ {}^{0}_{1}\mathbf{R} \cdot \vec{N}_2 \\ {}^{0}_{1}\mathbf{R} \cdot \vec{N}_3 \end{bmatrix} = \begin{bmatrix} 0 \\ 0 \\ 0 \end{bmatrix} \tag{5.22}$$

5.3.2 Simulation for maximum tolerant thrust

To optimize the posture of cane robot for gaining robust stability, a minimum of a constrained nonlinear multivariable function in MATLAB toolbox was used. It is generally referred to as constrained nonlinear optimization or nonlinear programming. Given an initial thrust vector $\vec{\mathbf{F}}_{\mathbf{u}}$, then the maximum thrust $\left|\vec{\mathbf{F}}_{\mathbf{u}}\right|$ and the posture of stick $\begin{bmatrix} \alpha_u & \beta_u \end{bmatrix}$ will be calculated by follow constraint conditions:

$$\begin{gathered} \min_{x} f(x) \\ Subject\ \ to \\ Aeq(x) = beq \\ lb \leq x \leq ub \end{gathered} \tag{5.23}$$

$$x = \begin{bmatrix} \vec{\mathbf{F}}_{\mathbf{1}} & \vec{\mathbf{F}}_{\mathbf{2}} & \vec{\mathbf{F}}_{\mathbf{3}} & \alpha & \beta & \gamma & \left|\vec{\mathbf{F}}_{\mathbf{u}}\right| \end{bmatrix} \tag{5.24}$$

$$beq = \begin{bmatrix} 0 & 0 & (\mathbf{G_s}+\mathbf{G_b})\, g \end{bmatrix} \tag{5.25}$$

$$Aeq = \begin{bmatrix} 1 & 0 & 0 & 1 & 0 & 0 & 1 & 0 & 0 & 0 & 0 & 0 & m \\ 0 & 1 & 0 & 0 & 1 & 0 & 0 & 1 & 0 & 0 & 0 & 0 & n \\ 0 & 0 & 1 & 0 & 0 & 1 & 0 & 0 & 1 & 0 & 0 & 0 & p \end{bmatrix} \tag{5.26}$$

Because the cane robot was with a three-point-contact was different when the cane robot was pushed in different direction. As shown in **Fig. 5.10**, in the case I, the moment arm l_a^1 is longer than l_a^2 in case II. The simulation result is shown in **Fig. 5.11**. And the experimental result of maximums thrust and posture of stick was shown as vectors x^1 and x^2 which denote the result in case I and case II including the generated force of each omni-directional wheel $\begin{bmatrix} \vec{\mathbf{F}}_1 & \vec{\mathbf{F}}_2 & \vec{\mathbf{F}}_3 \end{bmatrix}$, optimized posture of stick $\begin{bmatrix} \alpha & \beta & \gamma \end{bmatrix}$ and the maximums thrust is $\left|\vec{\mathbf{F}}_\mathbf{u}\right|$.

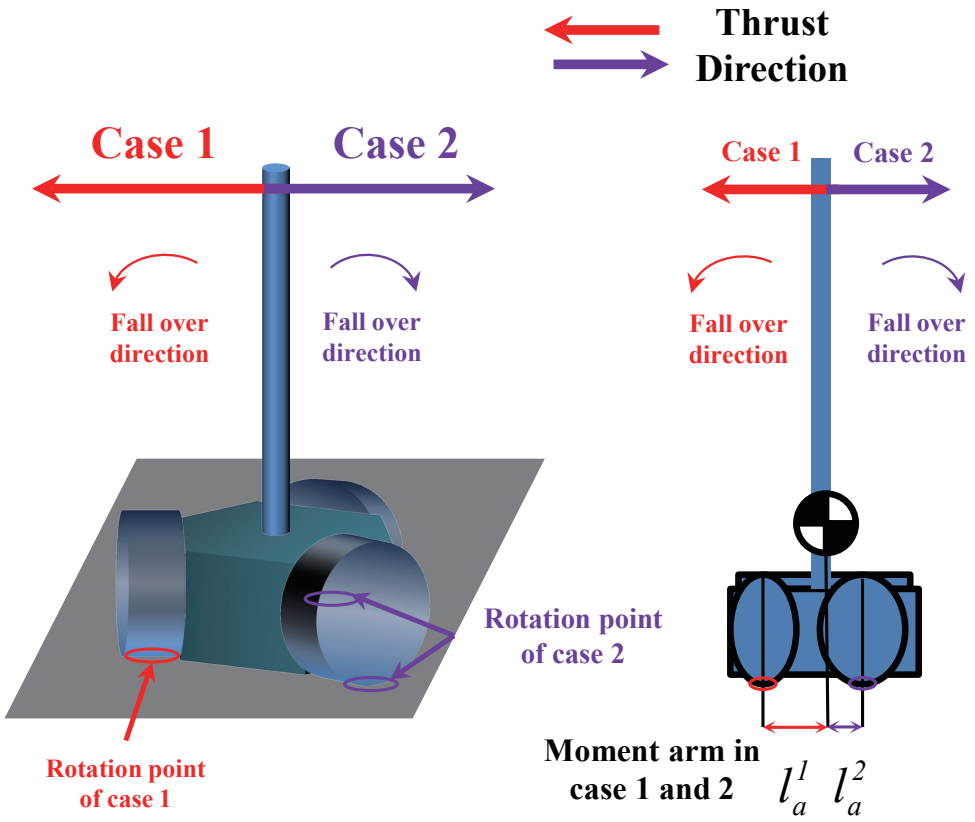

Figure 5.10: Fall direction of cane robot.

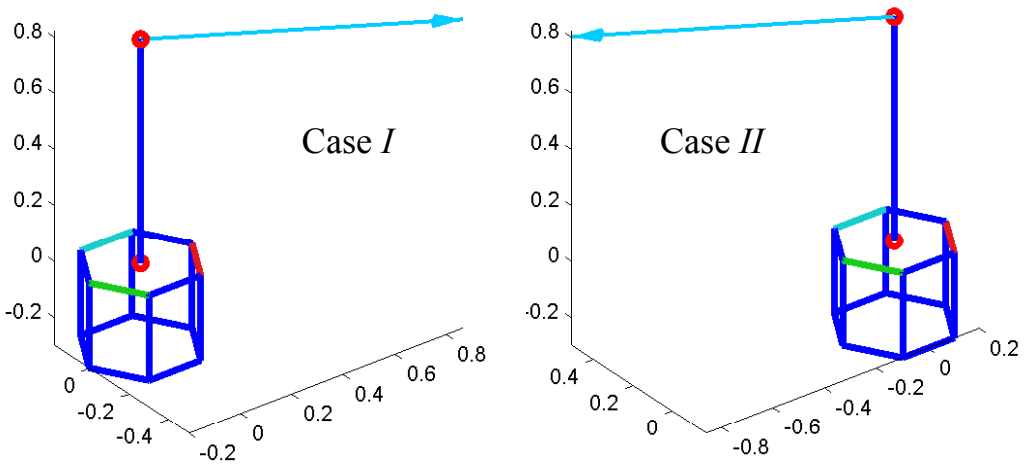

Figure 5.11: The simulation result of case *I* and case *II*.

$$x^1 = \left[\begin{vmatrix} -33.4608 \\ -19.3186 \\ -0.0000 \end{vmatrix}, \begin{vmatrix} -33.4608 \\ 19.3186 \\ 0.000 \end{vmatrix}, \begin{vmatrix} -0.000 \\ 0.000 \\ 200.900 \end{vmatrix}, \begin{vmatrix} 0.5236 \\ -0.4363 \\ -0.2393 \end{vmatrix}, 66.9217\right] \tag{5.27}$$

$$x^2 = \left[\begin{vmatrix} 13.53780 \\ -12.269 \\ -119.08 \end{vmatrix}, \begin{vmatrix} -5.6137 \\ -25.9945 \\ 81.8146 \end{vmatrix}, \begin{vmatrix} -7.9242 \\ -2.5463 \\ 0.0000 \end{vmatrix}, \begin{vmatrix} -7.7363 \\ 0.4363 \\ 0.4363 \end{vmatrix}, 40.8102\right] \tag{5.28}$$

The experimental results (as shown in Fig. 10) on pushing cane robot in the direction of case 1 and case 2 confirmed the accuracy of simulation results.

Experimental Result

To verify the effectiveness of our proposed approach that how to enhance the stability of cane robot several simulations and experiments were performed in different situations.

***Experiment Setting*:**

The parameters of cane robot were set as follow: Mass of stick $\mathbf{G_s}$ = 1kg, mass of omni-directional robot base $\mathbf{F_b}$ = 20kg, radius of omni-wheel robot r=0.2m, the height of universal joint h = 0.3m, the length of stick l_s = 1.2m.

***Experiment on universal joint implemented or not*:**

Fig.11 has shown the comparative experimental results on the case of implementing universal joint and without using it. According to the results, it can be known that in

the case of controlling the angle of universal joint the maximums thrust can be increased obviously. In other words, by optimizing the posture of stick the stability of cane robot can be enhanced.

Summary

In this section, a mechatronics device called universal joint which driven by two DC motors was designed to gain robust stability for cane robot. A constrained nonlinear multivariable algorithm was used to optimize the posture of cane robot. By controlling the posture of stick, the thrust in which the cane robot can suffers without going to fall over can be reduced obviously. The effectiveness of proposed fall prevention algorithms is confirmed through experiments.

5.4 Fall and Overturn Prevention Control for Human-Cane Robotic System (*Prototype V*)

In this section, a concept for enhancing the safety of human-cane robotic system is proposed to guarantee that both the human and cane robot can move without falling. For preventing the human subject from falling, the angle of human body and the acceleration of center of gravity(COG) should be less than some threshold. Although in a human-in-the-loop system, the human subject is regarded a uncontrollable object. However, while the user is falling over, the cane robot can move to a appropriately position and support the user for balance. As the prerequisite condition that the cane robot support the human balance, the stability of cane robot should be ensured firstly. According Newton-Euler Law, a dynamic model is proposed to present the stability of human-cane robotic system. A impedance control are used to achieve position, posture and force control of iCane for fall prevention. The simulation and experimental results show the performance of fall prevention by using iCane.

5.4.1 Introduction

As many countries step into the aging society rapidly, more and more elders suffer from deficits of motor function or disability of the limbs, which are usually caused by neurological problems, lack of muscle strength and so on. In addition, the growing elderly population causes the shortage of young people for nursing care. Therefore, there is a great need to develop rehabilitation robots that can partially replace the nurses and the therapists.

So far, many researchers have developed various intelligent walkers comprising active or passive wheels and supporting frame, including the applications for the upper limb, for the lower limb and for the assisting or training of the whole body.

Because of the problem of population aging, more and more researches raise concern about rehabilitation robot developing in these years. To improve the walking ability of the elderly, the walker-type rehabilitation robot has become a popular research topic. There has been many intelligent walker-type robots comprising active or passive wheels and supporting frame. Kotani et al. proposed the Hitomi system to help the blind in outdoor environment. Fujie et al. developed a power-assisted walker for physical support during walking. The Care-O-bot and Nurse-bot are developed as personal service robots for elderly and disables. Yu et al. proposed the Personal Aid for Mobility and Monitoring (PAMM) system to provide mobility assistance and user health status monitoring. Hirata et al proposed a new intelligent walker based on passive robotics to assist the elderly, handicapped people and the blind.

There are still many deficiencies in the present walker systems. First, many walkers are designed for the indoor environment. Second, most of them are big in size and/or heavy in weight. Many elders and patients are not so weak that they have to be nursed carefully. Nevertheless, sufficient support, like a cane or stick, is necessary to help them take a walk outside, which enables them to realize high-quality lives or accelerate the rehabilitation. In these cases, an intelligent cane system may be more useful than walkers due to its flexibility and handiness. In the living environment including the narrow space, the cane system is expected to be movable in omni-directions. Most of researchers are proposed for walker systems but cane systems, which are much smaller in size. Recently, commercial Omni-wheels are applied in the area of walker systems. The problem that slender rollers of omni-wheels have limited load capacities is partly solved by the modern technology.

Many functions are proposed to assist the elderly walking, sit-to-stand, navigation, etc. Recognizing the user walking intention plays an important role in the motion control of our cane robot. To quantitatively describe the users walking intention, a concept called intentional direction ITD is proposed in our previous work. Recognizing the user walking intention plays an important role in the motion control of our cane robot. To quantitatively describe the users walking intention, a concept called "intentional direction ITD is proposed. Recognizing the user walking intention plays an important role in the motion control of our cane robot.

The Functionality and stability are both important issues for a nursing robot. As one of the prime task, many researchers pay much attention to the safety and dependability of

the nursing-care robot. The degeneration of the balance control system in the elderly and in many pathologies has forced researchers and clinicians to understand more about how the system works and how to quantify its status at any point in time. Therefore, many works about human balance and posture control was published in the past several decades. By analyzing the human walking dynamics model, the optimal posture control for human balance was discussed by D A Winer et al. A tripod walking robot give us some inspiration that the human-cane robotic system can be considered as a three legs robot. Conghui Liang et al proposed a novel tripod walking robot, by controlling a balance mechanism, the COG can be adjusted during walking for balance.

In this study a 2D inverted pendulum model is used to describe the human-cane system stability. A fall detection method was proposed based on sensor fusion in our previous work. While human subject is falling over, the cane robot will stop and break the wheels for support the user balance. As a precondition of fall prevention by using cane robot, the stability of cane robot must be ensured. Therefore, a dynamic stability constraint condition is proposed. The impedance control is use optimal the position and posture of cane robot.

Main idea:

- Regard the required human input as disturbance, this input should ensure the fall prevention.
- Study the tip-over prevention control method of Intelligent Cane. (If we think the cane robot as a mobile manipulator, some stability criteria including ZMP, force-angle, support force can be applied).

Control objectives:

- The angle of human body should be less than some threshold(fall prevention).
- The cane robot should be stable(tip-over prevention).

Challenges:

- The interaction torque τ_h and force F_h cannot be controlled directly(unpredictable).
- It is difficult to model the dynamics human motion.

Assumptions:

- The human body is considered as a rigid stick

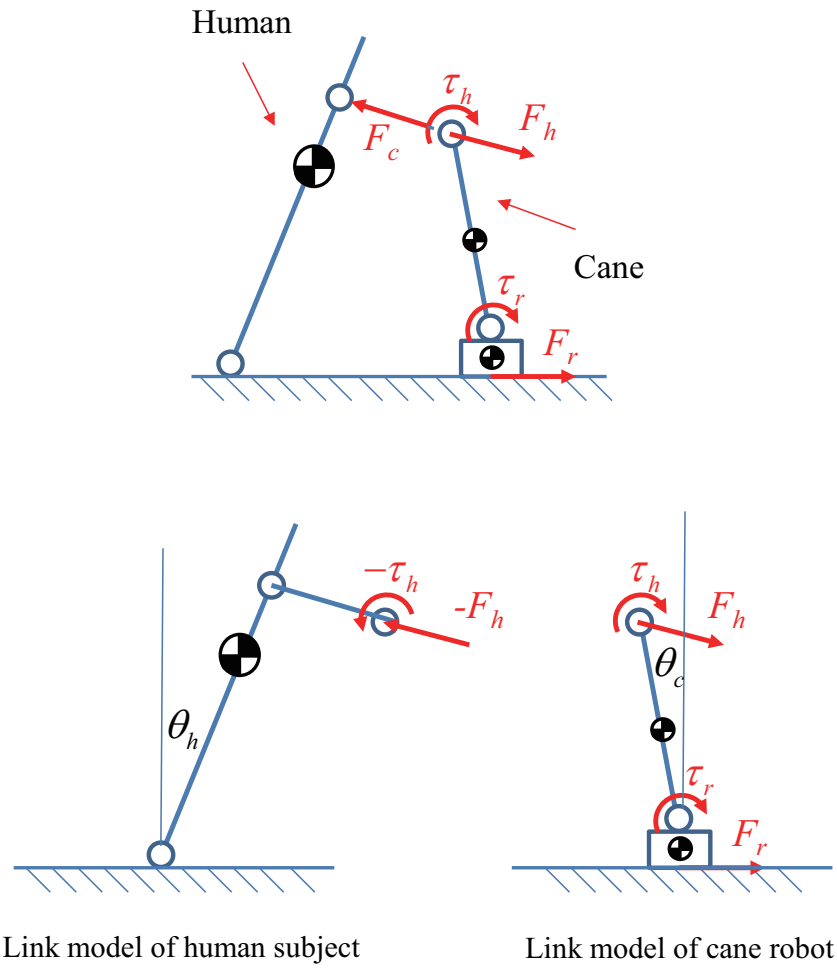

Figure 5.12: Simplified link model of human-cane robotic system.

- The users supporting foot does not move in horizontal direction
- The falling direction of human and the bending direction of stick are in same plane (3D→2D)

5.4.2 Dynamic Model of Human-Cane Robotic System

Dynamics Analysis of Human-Cane Robotics System

By analysing the Dynamics model of cane system(**Fig. 5.13**), we can know the motion of cane robot in both horizontal and vertical direction as following equations:

The motion of stick in the horizontal direction is shown as **Eq. 5.29**.

$$m_1 \frac{d^2}{dt^2}\left(x + \frac{l}{2}\sin\theta_c\right) = H + F_{hx} \tag{5.29}$$

The **Eq. 5.30** is the motion of mobile base horizontally.

$$m_2\ddot{x} = F_r - H - c\dot{x} \tag{5.30}$$

The cane robot is assumed that moving on the ground, so the base of cane robot does not move in the vertical direction. The universal joint control the posture of stick, it moves in both horizontal and vertical direction. The **Eq. 5.31** denotes the motion of stick vertically.

$$m_1 \frac{d^2}{dt^2}\left(\frac{l}{2}\cos\theta_c\right) = V - m_1 g + F_{hz} \tag{5.31}$$

Considering with the rotation of cane robot system, the base does not rotate in {1}. The universal joint control the stick rotate as shown in **Eq. 5.32**

$$I\ddot{\theta}_c = \frac{l}{2}\sin\theta_c \cdot (V - F_{hz}) - \frac{l}{2}\cos\theta_c \cdot (H - F_{hx}) + \tau_r + \tau_h \tag{5.32}$$

The state variable is:

$$\mathbf{x} = \begin{pmatrix} x_1 & x_2 & x_3 & x_4 \end{pmatrix}^T = \begin{pmatrix} x & \dot{x} & \theta_c & \dot{\theta}_c \end{pmatrix}^T \tag{5.33}$$

The dynamic model can be calculated as following steps:

(5.29)+(5.30):

$$(m_1 + m_2)\,\ddot{x} + \frac{m_1 l}{2}\cos\theta_c \cdot \ddot{\theta}_c = \frac{m_1 l}{2}\sin\theta_c \cdot \dot{\theta}_c^2 - d\dot{x} + F_r + F_{hx} \tag{5.34}$$

(5.29)→

$$H = m_1 \frac{d^2}{dt^2}\left(x + \frac{l}{2}\sin\theta_c\right) - F_{hx} = m_1 \frac{d}{dt}\left(\dot{x} + \frac{l}{2}\cos\theta_c \cdot \dot{\theta}_c\right) - F_{hx}$$
$$= m_1\left(\ddot{x} + \frac{l}{2}\cos\theta_c \cdot \ddot{\theta}_c - \frac{l}{2}\sin\theta_c \cdot \dot{\theta}_c^2\right) - F_{hx} \tag{5.35}$$

(5.31)→

$$V = m_1 \frac{d^2}{dt^2}\left(\frac{l}{2}\cos\theta_c\right) + m_1 g - F_{hz} = -m_1 \frac{d}{dt}\left(\frac{l}{2}\sin\theta_c \cdot \dot{\theta}_c\right) + m_1 g - F_{hz}$$
$$= -m_1\left(\frac{l}{2}\sin\theta_c \cdot \ddot{\theta}_c + \frac{l}{2}\cos\theta_c \cdot \dot{\theta}_c^2\right) + m_1 g - F_{hz} \tag{5.36}$$
$$= -\frac{m_1 l}{2}\sin\theta_c \cdot \ddot{\theta}_c - \frac{m_1 l}{2}\cos\theta_c \cdot \dot{\theta}_c^2 + m_1 g - F_{hz}$$

substitute (5.35),(5.36) into (5.32):

$$I\ddot{\theta}_c = \frac{l}{2}\sin\theta_c \cdot \left(-\frac{m_1 l}{2}\sin\theta_c \cdot \ddot{\theta}_c - \frac{m_1 l}{2}\cos\theta_c \cdot \dot{\theta}_c^2 + m_1 g - 2F_{hz}\right)$$
$$-\frac{l}{2}\cos\theta_c \cdot \left(m_1\left(\ddot{x} + \frac{l}{2}\cos\theta_c \cdot \ddot{\theta}_c - \frac{l}{2}\sin\theta_c \cdot \dot{\theta}_c^2\right) - 2F_{hx}\right) + \tau_r + \tau_h$$
$$= -\frac{m_1 l}{2}\cos\theta_c \cdot \ddot{x} - \frac{m_1 l^2}{4} \cdot \ddot{\theta}_c + \frac{m_1 g l}{2}\sin\theta_c - l\sin\theta_c \cdot F_{hz} + l\cos\theta_c \cdot F_{hx} + \tau_r + \tau_h$$
$$\Rightarrow$$
$$\frac{m_1 l}{2}\cos\theta_c \cdot \ddot{x} + \left(I + \tfrac{m_1 l^2}{4}\right) \cdot \ddot{\theta}_c = \frac{m_1 g l}{2}\sin\theta_c - l\sin\theta_c \cdot F_{hz} + l\cos\theta_c \cdot F_{hx} + \tau_r + \tau_h \tag{5.37}$$

To combine the (5.34) and (5.37)

$$\begin{cases} (m_1+m_2)\,\ddot{x}+\dfrac{m_1 l}{2}\cos\theta_c\cdot\ddot{\theta}_c=\dfrac{m_1 l}{2}\sin\theta_c\cdot\dot{\theta}_c^2-d\dot{x}+F_r+F_{hx} \\ \dfrac{m_1 l}{2}\cos\theta_c\cdot\ddot{x}+\left(I+\dfrac{m_1 l^2}{4}\right)\cdot\ddot{\theta}_c=\dfrac{m_1 g l}{2}\sin\theta_c-l\sin\theta_c\cdot F_{hz}+l\cos\theta_c\cdot F_{hx}+\tau_r+\tau_h \end{cases}$$

$$\Rightarrow$$

$$\begin{bmatrix} m_1+m_2 & \dfrac{m_1 l}{2}\cos\theta_c \\ \dfrac{m_1 l}{2}\cos\theta_c & I+\dfrac{m_1 l^2}{4} \end{bmatrix}\begin{bmatrix}\ddot{x}\\ \ddot{\theta}_c\end{bmatrix}=\begin{bmatrix}\dfrac{m_1 l}{2}\sin\theta_c\cdot\dot{\theta}_c^2-d\dot{x}\\ \dfrac{m_1 g l}{2}\sin\theta_c\end{bmatrix}+\begin{bmatrix}F_r+F_{hx}\\ -l\sin\theta_c\cdot F_{hz}+l\cos\theta_c\cdot F_{hx}+\tau_r+\tau_h\end{bmatrix} \tag{5.38}$$

Then

$$\begin{bmatrix}\ddot{x}\\ \ddot{\theta}_c\end{bmatrix}=\frac{1}{\Delta}\begin{bmatrix} I+\dfrac{m_1 l^2}{4} & -\dfrac{m_1 l}{2}\cos\theta_c \\ -\dfrac{m_1 l}{2}\cos\theta_c & m_1+m_2\end{bmatrix}\begin{bmatrix}\dfrac{m_1 l}{2}\sin\theta_c\cdot\dot{\theta}_c^2-d\dot{x}\\ \dfrac{m_1 g l}{2}\sin\theta_c\end{bmatrix}$$
$$+\frac{1}{\Delta}\begin{bmatrix} I+\dfrac{m_1 l^2}{4} & -\dfrac{m_1 l}{2}\cos\theta_c \\ -\dfrac{m_1 l}{2}\cos\theta_c & m_1+m_2\end{bmatrix}\begin{bmatrix}F_r+F_{hx}\\ -l\sin\theta_c\cdot F_{hz}+l\cos\theta_c\cdot F_{hx}+\tau_r+\tau_h\end{bmatrix} \tag{5.39}$$

Where $\Delta=(m_1+m_2)\left(I+\dfrac{m_1 l^2}{4}\right)-\dfrac{(m_1 l)^2}{4}(\cos\theta_c)^2$

The final nonlinear model is that:

$$\begin{bmatrix}\ddot{x}\\ \ddot{\theta}_c\end{bmatrix}=\frac{1}{\Delta}\begin{bmatrix}\left(I+\dfrac{m_1 l^2}{4}\right)\dfrac{m_1 l}{2}\sin\theta_c\cdot\dot{\theta}_c^2-\left(I+\dfrac{m_1 l^2}{4}\right)d\dot{x}-\dfrac{(m_1 l)^2 g}{4}\sin\theta_c\cos\theta_c\\ -\dfrac{(m_1 l)^2}{4}\cos\theta_c\sin\theta_c\cdot\dot{\theta}_c^2+\dfrac{m_1 l}{2}\cos\theta_c d\dot{x}+\dfrac{m_1(m_1+m_2)gl}{2}\sin\theta_c\end{bmatrix}$$
$$+\frac{1}{\Delta}\begin{bmatrix}\left(I+\dfrac{m_1 l^2}{4}\right)(F_r+F_{hx})-\dfrac{m_1 l}{2}\cos\theta_c\,(-l\sin\theta_c\cdot F_{hz}+l\cos\theta_c\cdot F_{hx}+\tau_r+\tau_h)\\ -\dfrac{m_1 l}{2}\cos\theta_c\,(F_r+F_{hx})+(m_1+m_2)\,(-l\sin\theta_c\cdot F_{hz}+l\cos\theta_c\cdot F_{hx}+\tau_r+\tau_h)\end{bmatrix} \tag{5.40}$$

To prevent the falling down of user, the optimal posture of cane robot is bending its stick toward the opposite direction of falling down. In the fall prevention motion control procedure, the whole system can be described by a 2D dynamical model (see **Fig. 5.14**). G_h, G_1 and G_2 are used to denote the center of gravities (COG) of human, stick and the

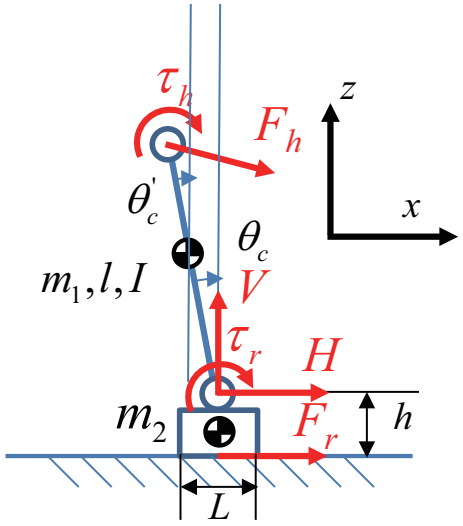

Figure 5.13: Model and dynamics analysis of human-cane robotic system.

mobile base, respectively. The masses of stick and mobile base are denoted by m_1 and m_2. l and I are the length and moment of inertia of stick. The height of stick joint is h. F is the driven force from active omni-wheels. τ_1 is the torque of motor mounted at the stick joint. Two coordinate system are defined for dynamical modeling procedure. System {1} is the reference coordinate frame. During the falling down, the distance from the end of stick to the point O (supporting foot position) is almost a constant. Thus, another polar coordinate system {2} is defined to conveniently describe the trajectory of human robot contact point.

To derive the dynamical model, the generalized coordinates of cane robot is given by $q = \begin{bmatrix} x_2 \ \theta_1 \end{bmatrix}^T$. Using the Lagrange formulation, the dynamic model of cane system can be easily obtained as follows:

$$M(q)\ddot{q} + C(q,\dot{q})\dot{q} + G(q) = U - J^T F_h \tag{5.41}$$

where matrices M, C and G are given in the appendix. U is the generalized force vector satisfying $U = \begin{bmatrix} F_r \ \tau_1 \end{bmatrix}^T$. F is the interaction force exerted at point P and can be represented as $F_h = \begin{bmatrix} F_\rho \ F_\alpha \end{bmatrix}^T$ in system {2}. J is the Jacobian matrix satisfying

$$X = f(q), \dot{X} = J(q) \cdot \dot{q} \tag{5.42}$$

where X denotes the human-robot contact point P in polar system {2}. The detail of f and J are also given as follow:

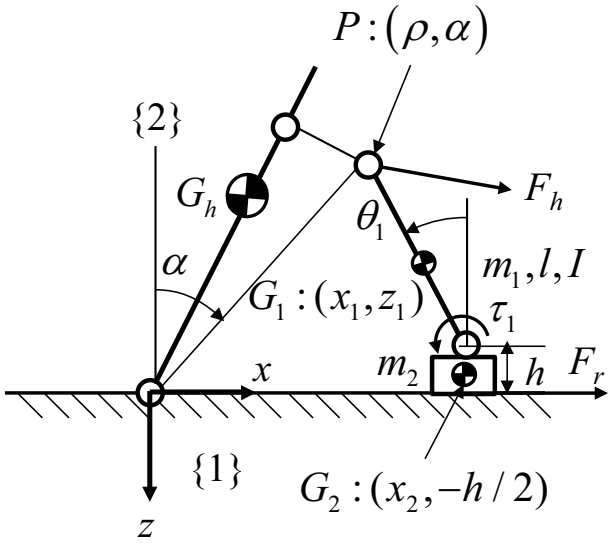

Figure 5.14: The human-cane robot system..

$M(q)$ is the Inertia matrix of cane robot.(**Eq. 5.43**)

$$M(q) = \begin{bmatrix} \frac{m_1 l^2}{4} + I & -\frac{m_1 l \cos(\theta_1)}{2} \\ -\frac{m_1 l \cos(\theta_1)}{2} & m_1 + m_2 \end{bmatrix} \tag{5.43}$$

$C(q, \dot{q})$ is the centrifugal force of cane system.(**Eq. 5.44**)

$$C(q, \dot{q}) = \begin{bmatrix} 0 & 0 \\ \frac{m_1 l \sin(\theta_1)\dot{\theta}_1}{2} & d \end{bmatrix} \tag{5.44}$$

And the $G(q)$ is the gravity terms.(**Eq. 5.45**)

$$G(q) = \begin{bmatrix} \frac{m_1 g l \sin(\theta_1)}{2} & 0 \end{bmatrix} \tag{5.45}$$

The X denotes the human-robot contact point P in polar system $\{2\}$.(**Eq. 5.46**)

$$X = \begin{bmatrix} \rho \\ \alpha \end{bmatrix} = f(q) = \begin{bmatrix} (x_2 - l\sin\theta_1)^2 + (h + l\cos\theta_1)^2 \\ \tan^{-1}\left(\frac{x_2 - l\sin\theta_1}{h + l\cos\theta_1}\right) \end{bmatrix} \tag{5.46}$$

$J(q)$ is the Jacobian matrix.(**Eq. 5.47**)

$$J(q) = \begin{bmatrix} -\dfrac{hl\sin\theta_1 + lx_2\cos\theta_1}{\sqrt{(x_2 - l\sin\theta_1)^2 + (h + l\cos\theta_1)^2}} & \dfrac{x_2 - l\sin\theta_1}{\sqrt{(x_2 - l\sin\theta_1)^2 + (h + l\cos\theta_1)^2}} \\ \dfrac{l^2 + hl\cos\theta_1 - lx_2\sin\theta_1}{h^2 + 2hl\cos\theta_1 + l^2 - 2lx_2\sin\theta_1 + {x_2}^2} & \dfrac{h + l\cos\theta_1}{h^2 + 2hl\cos\theta_1 + l^2 - 2lx_2\sin\theta_1 + {x_2}^2} \end{bmatrix} \tag{5.47}$$

Eq. 5.29 + **Eq. 5.30** and then we can get the system of equations

5.4.3 Fall and Overturn Prevention Impedance Control

When the falling emergency occurs due to stumbling, the human can be modeled as an inverted pendulum. Therefore, the distance from the end of stick to the supporting foot can be seen as a constant during natural falling. The cane robot is supposed to prevent both the falling of user and the overturn of itself. The motion controller of cane robot is needed to satisfy the following requirements:

- The cane robot should be controlled to provide sufficient supporting force to hold the user.
- The cane robot should be controlled to an optimal posture which can guarantee it will not be overturned.
- The cane robot must be configured for safe, stable and compliant motion in contact with the user.

The optimal posture problem of cane robot has been addressed in our previous work. To meet the abovementioned requirements, we assume the impedance control strategy with sufficiently large desired supporting force F_d and desired optimal cane robot posture X_d. A typical fall prevention procedure is shown in Fig. **5.15**. Assume the initial distance between support foot and robot is x_{20} and the optimal posture of robot is bending the stick with angle θ_1^*. The initial and desired human-robot contact point are denoted by P_0 and P_1 respectively. Then the relationship between α_0 and α_1 can be easily obtained from kinematic model(**Eq. 5.41**).

The desired contact dynamic behavior is described by

$$F_d - F = K_d\left(X_d - X\right) + B_d\left(\dot{X}_d - \dot{X}\right) + M_d\left(\ddot{X}_d - \ddot{X}\right) \tag{5.48}$$

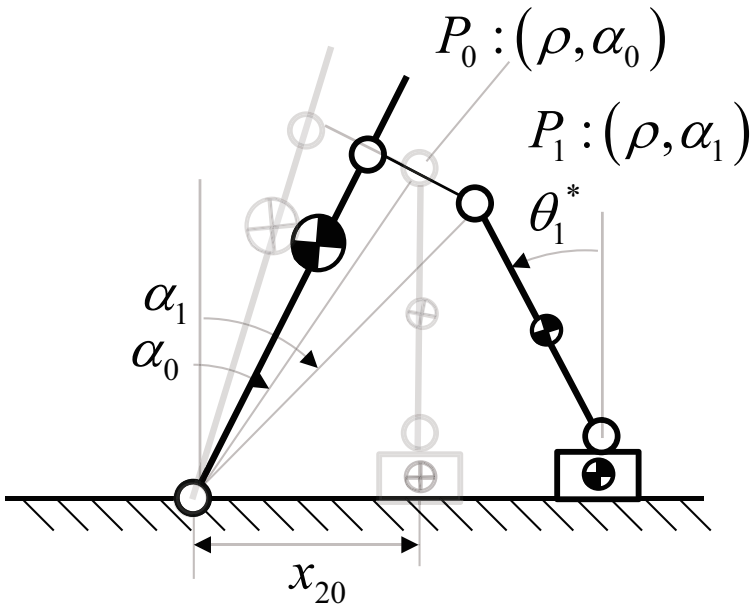

Figure 5.15: The fall prevention procedure.

where K_d, B_d and M_d are desired stiffness, damping and inertia matrices. The impedance control law is given by

$$U = J^T \left[K_p \left(X_d - X \right) + K_v \left(\dot{X}_d - \dot{X} \right) + F_d \left(K_f + I \right) - K_f F \right] + G \tag{5.49}$$

For system (1) with impedance control law **Eq. 5.49**, the following stability condition was obtained by Mehdi:

Theorem 5.1 (Stability of Impedance Control) *For desired matrices K_d, B_d, M_d and if there exist diagonal matrices K_p, K_v, K_f such that the following conditions:*

$$K_p + (I + K_f)K_d > 0, K_v + (I + K_f)B_d > 0, M_d = 0 \tag{5.50}$$

or

$$K_p > 0, K_v > 0, K_f = -I \tag{5.51}$$

are satisfied, then the robotic system described by the dynamical model (**Eq. 5.41**) *and the kinematic models* (**Eq. 5.42**) *is asymptotically stable under the constrained force* (**Eq. 5.48**) *and control law* (**Eq. 5.49**).

In this study, we assume $M_d = 0$. The whole control diagram is then shown by **Fig. 5.16**.

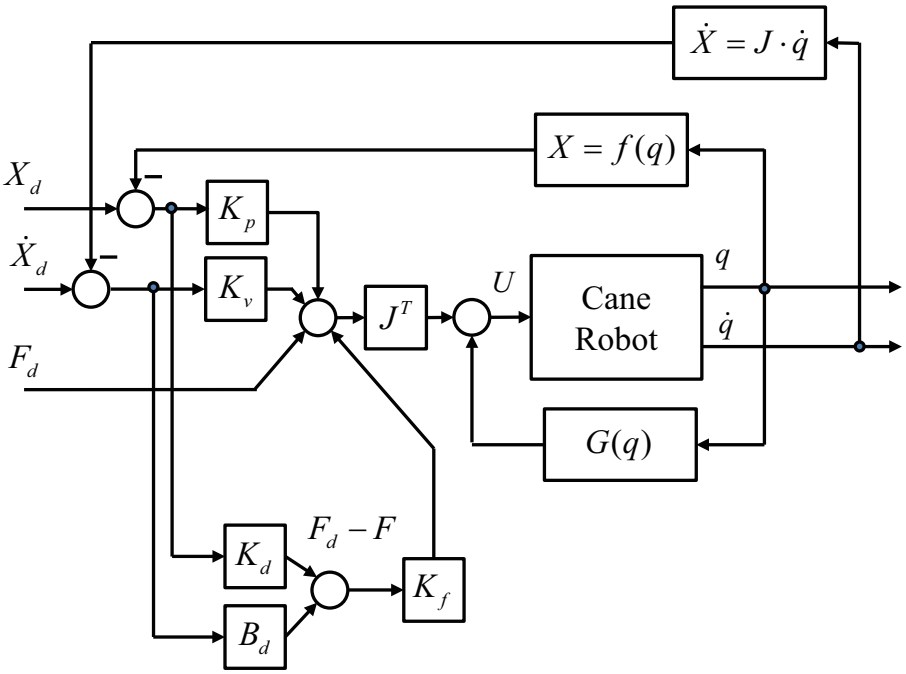

Figure 5.16: Control diagram of cane robot system.

5.4.4 Simulation and Experiment Result

To find the optimal controller gains- stiffness K_d and damping B_d, we simulated the fall prevention procedure by using the MATLAB. By adjusting the K_d and B_d, the relationship between stiffness/damping and convergence time/overshoot can be specified. Then we used the optimal gains of controller for experiments.

Simulation Result

The parameters of cane robot and the initial conditions are given as follow:

the mass, length and inertia of stick are set as m_1=1kg, l=0.8m, I=$\sqrt{m_1 \cdot l}/3$, mass of mobile base m_2=20kg, gravity g=9.8m/s^2, the distance between human and robot $x_2$0=0.6m, angle of human body θ_1=0, the system stiffness K_d=100, and the damping B_d=100.

The optimal posture and displacement of cane robot is calculated based on impedance control. The angle of human body will be affected indirectly by the supporting force from

cane robot. The **Fig. 5.17** shows 4 times simulation results with different stiffness and damping. In the simulation 1 we use the initial setting of K_d, B_d. But the overshoot and the unacceptable convergence time can not satisfy the rapid fall prevention. Therefore, we try to adjusting the system stiffness and damping to improve them. The increasing of damping coefficient can counteract the overshoot(see simulation 2); and the larger stiffness can cut down the convergence time(simulation 3). Finally, we found the optimal control gain(B_d=500, K_d=300) for the fall prevention system.

At the beginning of the falling, the human subject will push the cane robot in a large force. If the force is large enough to cause the cane robot turn over, the robot should optimize the posture of stick and control the distance between the human to counteract the falling moment. For supporting the human comfortably, the handle of cane robot should be controlled in constant position.

Experiment Result

To verify the efficiency of fall and overturn prevention control system, a 70[kg] human subject took the experiment on fall detection and prevention. The distance between the cane robot and user is limited in 0.6m just as the length of users arm. The Fig. **??** shows the result of fall prevention by using the cane robot.

5.4.5 Summary and Discussion

To improve the stability of human-cane robotic system. A impedance control method is proposed to optimize the posture and motion of cane robot. While the user is falling, the human-cane system can be described by a 2-dimension dynamical model. According the Newton-Euler law, we modeling the dynamic of human-cane robot system. The simulation results shown that when the human subject is fall, the cane robot could support him for balance effectively. In this study, we don't investigate about the finite time fall prevention strategy. In our future work, the fall procedure will be limited in a short time(about 1-2 second).

5.4.6 Summary

In this chapter, a transition motion is designed in which the multi-locomotion robot begins the brachiation motion from the ladder climbing posture. A load-allocation algorithm was proposed to cope with the unbalanced load distribution among the supporting limbs. The robot is successfully prevented from falling down from the ladder by setting a suitable

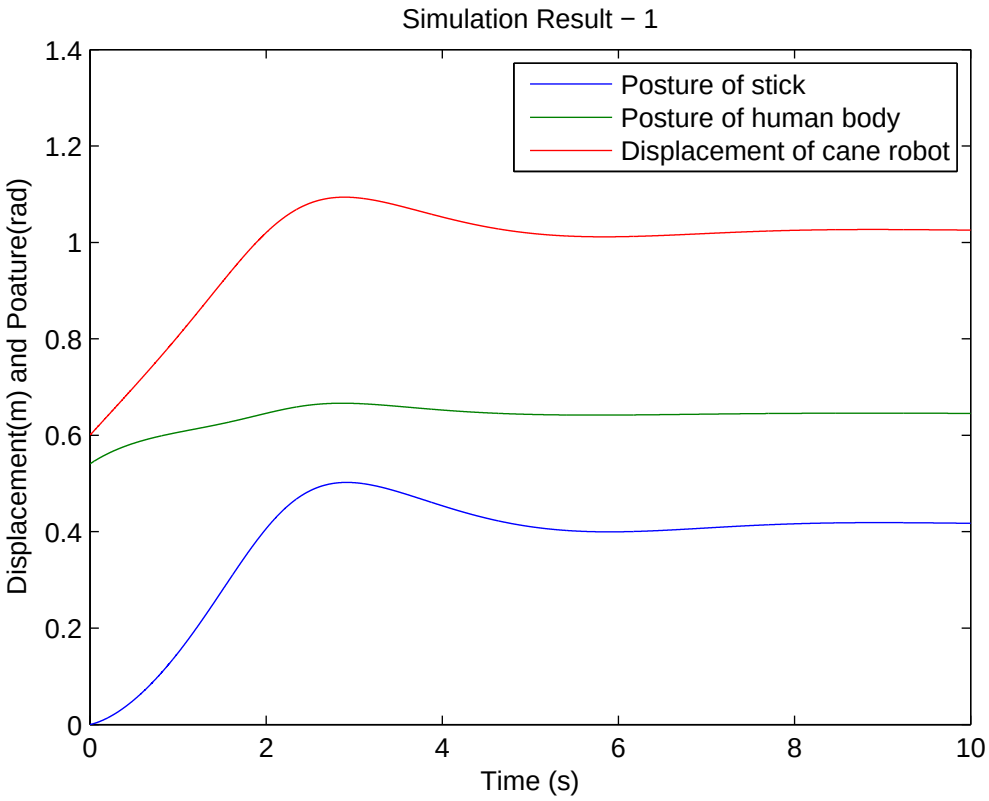
Simulation Result − 1
Posture of stick
Posture of human body
Displacement of cane robot
Displacement(m) and Poature(rad)
Time (s)
0
0.2
0.4
0.6
0.8
1
1.2
1.4
0
2
4
6
8
10

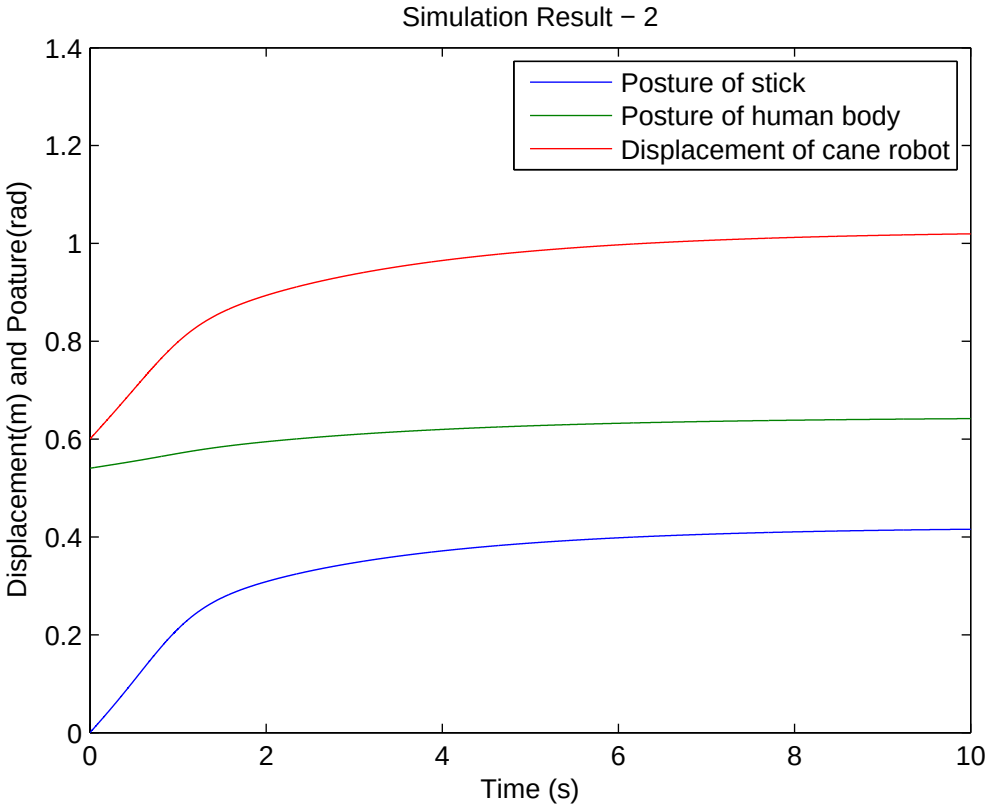
Simulation Result − 2
Posture of stick
Posture of human body
Displacement of cane robot
Displacement(m) and Poature(rad)
Time (s)
0
0.2
0.4
0.6
0.8
1
1.2
1.4
0
2
4
6
8
10

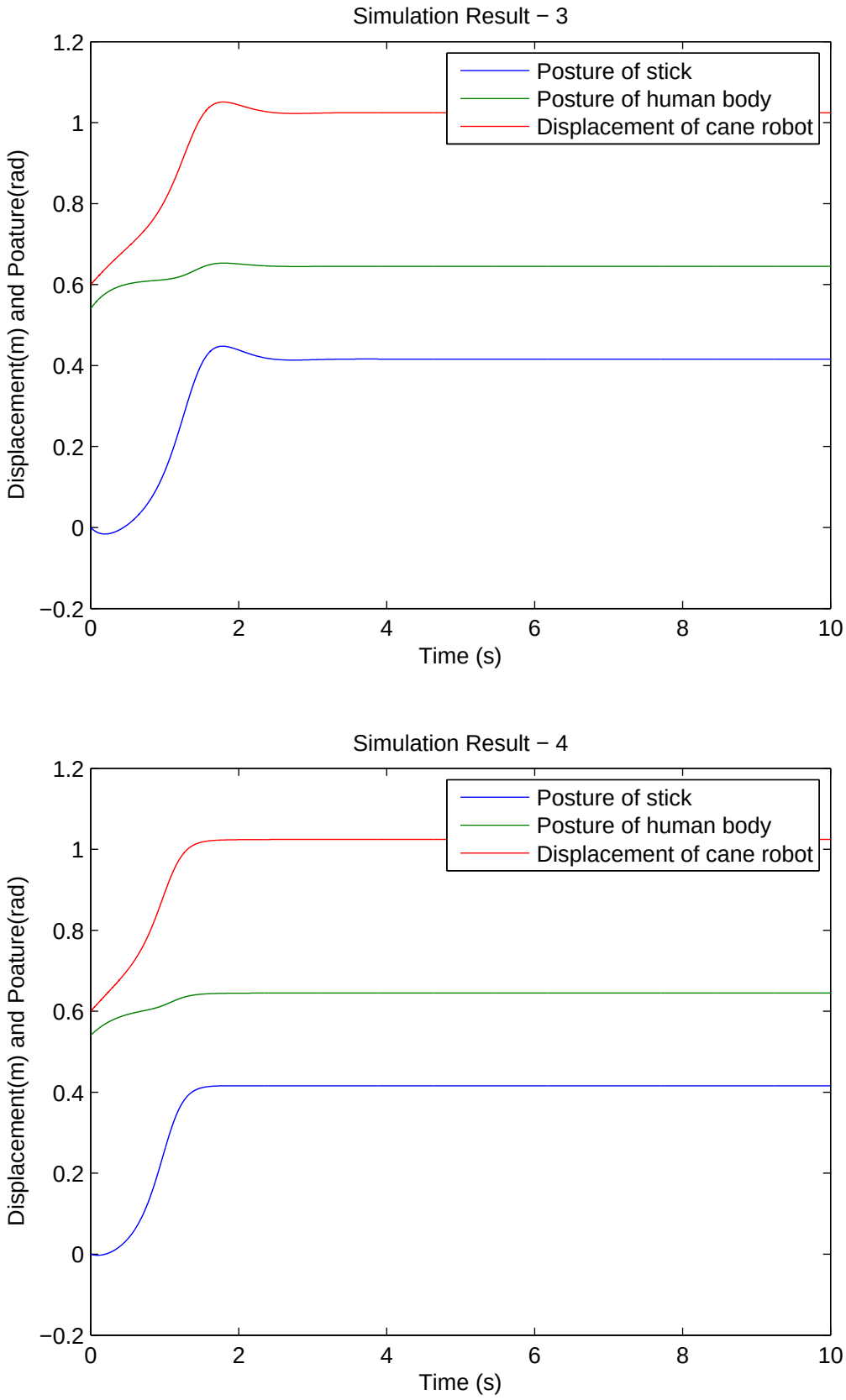

Figure 5.17: Simulation results of fall prevention.

torque at the key joint. The position errors in the initial posture are compensated by the key joint. The difference between the angle of the key joint and the expected angle is used to evaluate the position error. We confirmed that the transition motions with the load-allocation algorithm were robust and stable through the experiments with the multi-locomotion robot.

Chapter 6

Conclusion and Future Work

6.1 Conclusion

The world is facing challenges of rapid aging population. Elderly people may suffer from low levels of physical strength due to muscle weakness, which affects their motion ability significantly. Restricted movement lowers the performance of most activities of daily living (ADLs). In addition, the growing elderly population causes the shortage of young people for nursing care. Therefore, walking-aid robots find their application in the nursing and therapy field for these mobility impaired people.

In our study, an intelligent cane robot is designed for aiding the elderly and handicapped people walking. The robot consists of a stick, a group of sensor and an omni-directional basis driven by three Swedish wheels. Recognizing the user walking intention plays an important role in the motion control of our cane robot. To quantitatively describe the user's walking intention, a concept called "intentional direction (ITD)" is proposed. Both the state model and observation model of ITD are obtained by enumerating the possible walking modes and analyzing the relationship between the human-robot interaction force and the walking intention. From these two models, the users walking intention can be online inferred using Kalman filtering technique. Based on the estimated intention, a new admittance motion control scheme is proposed for the cane robot. Walking experiments aided by the cane robot on a flat ground and a slope are carried out to validate the proposed control approach. The experimental results show that the user feels more natural and comfortable when our intention based admittance control is applied.

In some cases, however the elderly can not walk uniformly because one leg suffers from muscular weakness. When the affected leg is in the support phase, the cane robot should stop to absorb more strain than the affected leg. When the healthy leg is in the

support phase, the cane robot should move forward according to ITD. In contrast to ITD, the motion of the cane robot should be controlled considering the walking pattern characteristics of the elderly to ensure safety and effectiveness. In this paper, an optimized motion control of the cane robot is proposed that is based on the characteristics gait pattern (CGP). An on-shoe load sensor was used to evaluate the reduction in muscular fatigue for the user's affected leg.

we introduce a new human fall detection method based on fusing sensory information from a vision system and a laser ranger finder (LRF). This method plays an important role in the fall-prevention for the cane robot. The human fall model is represented in a 2D space, where the distance between the head and the average leg position is a significant feature to detect the fall. The possibility distribution of this distance is estimated by using Dubois possibility theory. Fall detection is implemented by using a simple rule based on the possibility distribution. Another fall detection concept is proposed to estimate the risk of the falling based on the theory of zero moment point (ZMP) stability. An on-shoe sensor is used to measure the foot-ground reaction force and calculate the ZMP. The safety walking status is defined in the case of the ZMP is in the boundary of the support polygon. While the ZMP moving out of that boundary, the user will fall over.

In the last chapter, a concept for enhancing the safety of human-cane robotic system is proposed to guarantee that both the human and cane robot can move without falling. For preventing the human subject from falling, the angle of human body and the acceleration of center of gravity(COG) should be less than some threshold. Although in a human-in-the-loop system, the human subject is regarded a uncontrollable object. However, while the user is falling over, the cane robot can move to a appropriately position and support the user for balance. As the prerequisite condition that the cane robot support the human balance, the stability of cane robot should be ensured firstly. According Newton-Euler Law, a dynamic model is proposed to present the stability of human-cane robotic system. A impedance control are used to achieve position, posture and force control of iCane for fall prevention. The simulation and experimental results show the performance of fall prevention by using iCane.

6.2 Future Work

In our previous studies, we focus on the 'usability' and 'safety' of cane robot for aiding the elderly to walk comfortably and safely. A concept idea named "ITD" was proposed to control the cane robot, and a fall detection and prevention method was used to guarantee

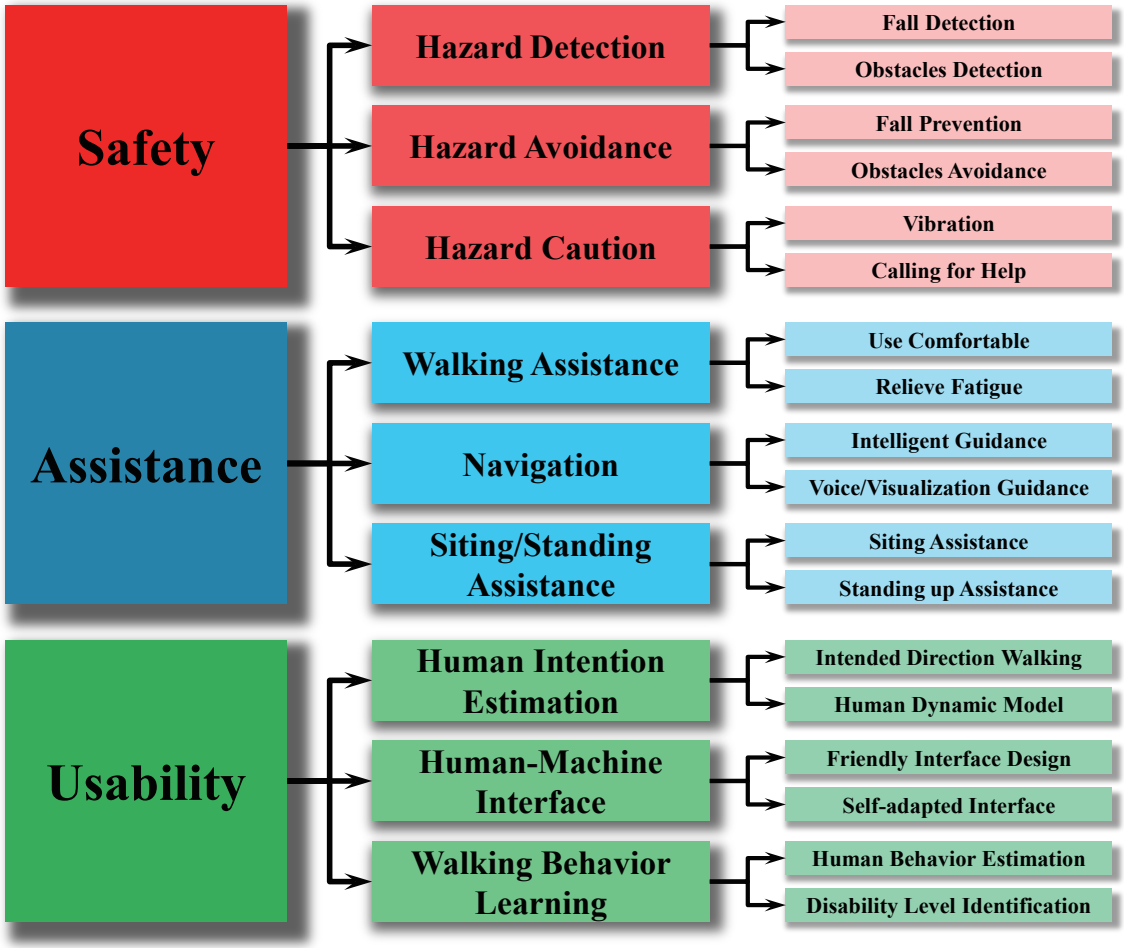

Figure 6.1: Research contents for the intelligent cane robot

the safety for both human subject and cane robot.

for the future research, we would like to accomplish the 'safety'; the hazard detection i.e. the potential risk in the environment should be investigated. The dangers including two sides, the inner and the external; the inner risk means the fall over risk of human subject and the tip-over risk of cane robot which we discussed above. By using the laser rangefinder which is fixed on the base of cane robot, the obstacles can be detected e.g. walls, steps or some moving object closing to the user.

The cane robot does not only can aid the elderly walking, but also have numbers of helpful functions. By using a smartphone, the cane robot can also play an important role in the navigation. In our future works, the function of standing up and sitting down assistance will be realized.

Bibliography

[1] D. E. Bloom, A. Boersch-Supan, P. McGee, and A. Seike, "Population aging: facts, challenges, and responses," *Benefits and Compensation International*, vol. 41, no. 1, p. 22, 2011.

[2] U. N. D. of Economic, *World population prospects: The 2004 Revision: Volume I: comprehensive tables*. United Nations Publications, 2006, no. 244-246.

[3] T.-S. Kuan, J.-Y. Tsou, and F.-C. Su, "Hemiplegic gait of stroke patients: the effect of using a cane," *Archives of physical medicine and rehabilitation*, vol. 80, no. 7, pp. 777–784, 1999.

[4] H. Hoenig, D. H. Taylor Jr, and F. A. Sloan, "Does assistive technology substitute for personal assistance among the disabled elderly?" *American Journal of Public Health*, vol. 93, no. 2, pp. 330–337, 2003.

[5] B. M. Joyce and R. L. Kirby, "Canes, crutches and walkers," *Am Fam Physician*, vol. 43, no. 2, pp. 535–542, 1991.

[6] F. W. Van Hook, D. Demonbreun, and B. D. Weiss, "Ambulatory devices for chronic gait disorders in the elderly," *American family physician*, vol. 67, no. 8, pp. 1717–1724, 2003.

[7] J. A. Ashton-Miller, M. W. Yeh, J. K. Richardson, and T. Galloway, "A cane reduces loss of balance in patients with peripheral neuropathy: results from a challenging unipedal balance test," *Archives of physical medicine and rehabilitation*, vol. 77, no. 5, pp. 446–452, 1996.

[8] W. C. Mann, D. Hurren, M. Tomita, and B. Charvat, "An analysis of problems with walkers encountered by elderly persons," *Physical & Occupational Therapy in Geriatrics*, vol. 13, no. 1-2, pp. 1–23, 1995.

[9] U. Sonn and G. Grimby, "Assistive devices in an elderly population studied at 70 and 76 years of age," *Disability & Rehabilitation*, vol. 16, no. 2, pp. 85–92, 1994.

[10] M. N. Sawka, R. Glaser, L. L. Laubach, O. Al-Samkari, and A. G. Suryaprasad, "Wheelchair exercise performance of the young, middle-aged, and elderly," *Journal of Applied Physiology*, vol. 50, no. 4, pp. 824–828, 1981.

[11] J. Hunter, "Energy costs of wheelchair propulsion by elderly and disabled people," *International Journal of Rehabilitation Research*, vol. 10, pp. 50–53, 1987.

[12] I. Moon, M. Lee, J. Ryu, and M. Mun, "Intelligent robotic wheelchair with emg-, gesture-, and voice-based interfaces," in *Intelligent Robots and Systems, 2003.(IROS 2003). Proceedings. 2003 IEEE/RSJ International Conference on*, vol. 4. IEEE, 2003, pp. 3453–3458.

[13] B. R. Kotajarvi, M. B. Sabick, K.-N. An, K. D. Zhao, K. R. Kaufman, and J. R. Basford, "The effect of seat position on wheelchair propulsion biomechanics," *Journal of rehabilitation research and development*, vol. 41, no. 3B, pp. 403–414, 2004.

[14] S. P. Levine, D. A. Bell, L. A. Jaros, R. C. Simpson, Y. Koren, and J. Borenstein, "The navchair assistive wheelchair navigation system," *Rehabilitation Engineering, IEEE Transactions on*, vol. 7, no. 4, pp. 443–451, 1999.

[15] E. Prassler, J. Scholz, and P. Fiorini, "A robotics wheelchair for crowded public environment," *Robotics & Automation Magazine, IEEE*, vol. 8, no. 1, pp. 38–45, 2001.

[16] H. Bateni, E. Heung, J. Zettel, W. E. Mcllroy, and B. E. Maki, "Can use of walkers or canes impede lateral compensatory stepping movements?" *Gait & posture*, vol. 20, no. 1, pp. 74–83, 2004.

[17] L. Kosover, "Physical rehabilitation device," Jan. 14 1958, uS Patent 2,819,755.

[18] M. Visintin and H. Barbeau, "The effects of parallel bars, body weight support and speed on the modulation of the locomotor pattern of spastic paretic gait. a preliminary communication," *Spinal Cord*, vol. 32, no. 8, pp. 540–553, 1994.

[19] I. Miyai, Y. Fujimoto, H. Yamamoto, Y. Ueda, T. Saito, S. Nozaki, and J. Kang, "Long-term effect of body weight–supported treadmill training in parkinson's disease: A randomized controlled trial," *Archives of physical medicine and rehabilitation*, vol. 83, no. 10, pp. 1370–1373, 2002.

[20] A. M. Moseley, A. Stark, I. D. Cameron, and A. Pollock, "Treadmill training and body weight support for walking after stroke," *Stroke*, vol. 34, no. 12, pp. 3006–3006, 2003.

[21] S. Hesse, B. Helm, J. Krajnik, M. Gregoric, and K. H. Mauritz, "Treadmill training with partial body weight support: influence of body weight release on the gait of hemiparetic patients," *Neurorehabilitation and Neural Repair*, vol. 11, no. 1, pp. 15–20, 1997.

[22] S. Hesse, C. Bertelt, M. Jahnke, A. Schaffrin, P. Baake, M. Malezic, and K. Mauritz, "Treadmill training with partial body weight support compared with physiotherapy in nonambulatory hemiparetic patients," *Stroke*, vol. 26, no. 6, pp. 976–981, 1995.

[23] H. Schmidt, C. Werner, R. Bernhardt, S. Hesse, and J. Krüger, "Gait rehabilitation machines based on programmable footplates," *Journal of neuroengineering and rehabilitation*, vol. 4, no. 1, p. 2, 2007.

[24] H. Ikeuchi, S. Arakane, K. Ohnishi, K. Imado, Y. Saito, and H. Miyagawa, "The development of gait training system for computer-aided rehabilitation," in *Computers helping people with special needs*. Springer, 2002, pp. 228–235.

[25] J. Kawamura, T. Ide, S. Hayashi, H. Ono, and T. Honda, "Automatic suspension device for gait training," *Prosthetics and Orthotics International*, vol. 17, no. 2, pp. 120–125, 1993.

[26] M. Peshkin, D. A. Brown, J. J. Santos-Munné, A. Makhlin, E. Lewis, J. E. Colgate, J. Patton, and D. Schwandt, "Kineassist: A robotic overground gait and balance training device," in *Rehabilitation Robotics, 2005. ICORR 2005. 9th International Conference on*. IEEE, 2005, pp. 241–246.

[27] G. Lacey and K. M. Dawson-Howe, "Autonomous guide for the blind," *The European Context for Assistive Technology, IOS Press, Amsterdam*, pp. 294–297, 1995.

[28] T. Takeuchi, Y. Nagai, and N. Enomoto, "Fuzzy control of a mobile robot for obstacle avoidance," *Information Sciences*, vol. 45, no. 2, pp. 231–248, 1988.

[29] J. Hine and A. Nooralahiyan, "Improving mobility and independence for elderly, blind and visually impaired people," *Improving the Quality of Life for the European Citizen: Technology for Inclusive Design and Equality*, vol. 4, p. 283, 1998.

[30] B. Graf, "Reactive navigation of an intelligent robotic walking aid," in *Robot and Human Interactive Communication, 2001. Proceedings. 10th IEEE International Workshop on*. IEEE, 2001, pp. 353–358.

[31] P. Aigner and B. McCarragher, "Shared control framework applied to a robotic aid for the blind," *Control Systems, IEEE*, vol. 19, no. 2, pp. 40–46, 1999.

[32] G. Lacey and K. M. Dawson-Howe, "The application of robotics to a mobility aid for the elderly blind," *Robotics and Autonomous Systems*, vol. 23, no. 4, pp. 245–252, 1998.

[33] J. Borenstein and I. Ulrich, "The guidecane-a computerized travel aid for the active guidance of blind pedestrians," in *Robotics and Automation, 1997. Proceedings., 1997 IEEE International Conference on*, vol. 2. IEEE, 1997, pp. 1283–1288.

[34] M. Sinn and P. Poupart, "Smart walkers!: enhancing the mobility of the elderly," in *The 10th International Conference on Autonomous Agents and Multiagent Systems-Volume 3*. International Foundation for Autonomous Agents and Multiagent Systems, 2011, pp. 1133–1134.

[35] H. M. Shim, J. G. Ryu, O. S. Kwon, E. H. Lee, H. K. Min, and S. H. Hong, "Development of the walking assistant robot for the elderly," in *World Congress on Medical Physics and Biomedical Engineering 2006*. Springer, 2007, pp. 3003–3006.

[36] M. Spenko, H. Yu, and S. Dubowsky, "Robotic personal aids for mobility and monitoring for the elderly," *Neural Systems and Rehabilitation Engineering, IEEE Transactions on*, vol. 14, no. 3, pp. 344–351, 2006.

[37] G. Wasson, P. Sheth, C. Huang, and M. Alwan, "Intelligent mobility aids for the elderly," in *Eldercare Technology for Clinical Practitioners*. Springer, 2008, pp. 53–76.

[38] M. Lan, A. Nahapetian, A. Vahdatpour, L. Au, W. Kaiser, and M. Sarrafzadeh, "Smartfall: an automatic fall detection system based on subsequence matching for the smartcane," in *Proceedings of the Fourth International Conference on Body Area Networks*. ICST (Institute for Computer Sciences, Social-Informatics and Telecommunications Engineering), 2009, p. 8.

[39] X. Zhang, X. Wei, and J. Zhang, "Detecting system design of tactile sensor for the elderly-assistant & walking-assistant robot," *Key Engineering Materials*, vol. 455, pp. 37–41, 2011.

[40] H. Yu, M. Spenko, and S. Dubowsky, "An adaptive shared control system for an intelligent mobility aid for the elderly," *Autonomous Robots*, vol. 15, no. 1, pp. 53–66, 2003.

[41] C. Ye, "Navigating a portable robotic device by a 3d imaging sensor," in *Sensors, 2010 IEEE*. IEEE, 2010, pp. 1005–1010.

[42] E. Cividanes, "Smart lower power obstacle avoidance device," *Development*, vol. 41, no. 3B, pp. 429–442, 2004.

[43] A. Frizera, R. Ceres, J. Pons, E. Rocon, and R. Raya, "A platform to study human-machine biomechanical interaction during gait," *Challenges for Assistive Technology: AAATE 2007*, vol. 20, p. 398, 2007.

[44] R. Ceres, J. Pons, L. Calderón, D. Mesonero-Romanos, A. Jiménez, F. Sánchez, P. Abizanda, B. Saro, and G. Bonivardo, "Andador activo para la rehabilitación y el mantenimiento de la movilidad natural," in *Actas del III Congreso Iberoamericano sobre Tecnologıas de Apoyo para la Discapacidad-IBERDISCAP 2004*, 2004.

[45] G. S. Wasson, J. P. Gunderson, S. Graves, and R. A. Felder, "Effective shared control in cooperative mobility aids." in *FLAIRS Conference*, 2001, pp. 509–513.

[46] U. Borgolte, "A novel mobility aid for independent daily living of elderly people," in *Proceedings 5th European Conference for the Advancement of Assistive Technology (AAATE)*, 1999, pp. 267–271.

[47] E. Einbinder and T. Horrom, "Smart walker: A tool for promoting mobility in elderly adults." *Journal of rehabilitation research and development*, vol. 47, no. 9, p. xiii, 2010.

[48] Y. Hirata, A. Hara, and K. Kosuge, "Motion control of passive intelligent walker using servo brakes," *Robotics, IEEE Transactions on*, vol. 23, no. 5, pp. 981–990, 2007.

[49] ——, "Motion control of passive-type walking support system based on environment information," in *Robotics and Automation, 2005. ICRA 2005. Proceedings of the 2005 IEEE International Conference on.* IEEE, 2005, pp. 2921–2926.

[50] ——, "Passive-type intelligent walking support system," in *Intelligent Robots and Systems, 2004.(IROS 2004). Proceedings. 2004 IEEE/RSJ International Conference on*, vol. 4. IEEE, pp. 3871–3876.

[51] Y. Hirata and K. Kosuge, "Human support systems based on passive robotics." World Scientific, 2012, p. 341.

[52] Y. Hirata, A. Muraki, and K. Kosuge, "Motion control of intelligent walker based on renew of estimation parameters for user state," in *Intelligent Robots and Systems, 2006 IEEE/RSJ International Conference on.* IEEE, 2006, pp. 1050–1055.

[53] ——, "Motion control of intelligent passive-type walker for fall-prevention function based on estimation of user state," in *Robotics and Automation, 2006. ICRA 2006. Proceedings 2006 IEEE International Conference on.* IEEE, 2006, pp. 3498–3503.

[54] K. Suzuki, G. Mito, H. Kawamoto, Y. Hasegawa, and Y. Sankai, "Intention-based walking support for paraplegia patients with robot suit hal," *Advanced Robotics*, vol. 21, no. 12, pp. 1441–1469, 2007.

[55] A. Tsukahara, Y. Hasegawa, and Y. Sankai, "Standing-up motion support for paraplegic patient with robot suit hal," in *Rehabilitation Robotics, 2009. ICORR 2009. IEEE International Conference on.* IEEE, 2009, pp. 211–217.

[56] T. Kawabata, H. Satoh, and Y. Sankai, "Working posture control of robot suit hal for reducing structural stress," in *Robotics and Biomimetics (ROBIO), 2009 IEEE International Conference on.* IEEE, 2009, pp. 2013–2018.

[57] A. Tsukahara, R. Kawanishi, Y. Hasegawa, and Y. Sankai, "Sit-to-stand and stand-to-sit transfer support for complete paraplegic patients with robot suit hal," *Advanced robotics*, vol. 24, no. 11, pp. 1615–1638, 2010.

[58] B. Makinson, "Research and development prototype for machine augmentation of human strength and endurance. hardiman i project," DTIC Document, Tech. Rep., 1971.

[59] R. Bogue, "Exoskeletons and robotic prosthetics: a review of recent developments," *Industrial Robot: An International Journal*, vol. 36, no. 5, pp. 421–427, 2009.

[60] S. Freivogel, J. Mehrholz, T. Husak-Sotomayor, and D. Schmalohr, "Gait training with the newly developed'lokohelp'-system is feasible for non-ambulatory patients after stroke, spinal cord and brain injury. a feasibility study," *Brain Injury*, vol. 22, no. 7-8, pp. 625–632, 2008.

[61] S. K. Banala, S. H. Kim, S. K. Agrawal, and J. P. Scholz, "Robot assisted gait training with active leg exoskeleton (alex)," *Neural Systems and Rehabilitation Engineering, IEEE Transactions on*, vol. 17, no. 1, pp. 2–8, 2009.

[62] D. Aoyagi, W. E. Ichinose, S. J. Harkema, D. J. Reinkensmeyer, and J. E. Bobrow, "A robot and control algorithm that can synchronously assist in naturalistic motion during body-weight-supported gait training following neurologic injury," *Neural Systems and Rehabilitation Engineering, IEEE Transactions on*, vol. 15, no. 3, pp. 387–400, 2007.

[63] M. Wirz, D. H. Zemon, R. Rupp, A. Scheel, G. Colombo, V. Dietz, and T. G. Hornby, "Effectiveness of automated locomotor training in patients with chronic incomplete spinal cord injury: a multicenter trial," *Archives of physical medicine and rehabilitation*, vol. 86, no. 4, pp. 672–680, 2005.

[64] J. M. Hollerbach, "Locomotion interfaces," *Handbook of virtual environments technology*, pp. 239–254, 2002.

[65] G. P. Roston and T. Peurach, "A whole body kinesthetic display device for virtual reality applications," in *Robotics and Automation, 1997. Proceedings., 1997 IEEE International Conference on*, vol. 4. IEEE, 1997, pp. 3006–3011.

[66] N. Shiozawa, S. Arima, and M. Makikawa, "Virtual walkway system and prediction of gait mode transition for the control of the gait simulator," in *Engineering in Medicine and Biology Society, 2004. IEMBS'04. 26th Annual International Conference of the IEEE*, vol. 1. IEEE, 2004, pp. 2699–2702.

[67] H. Iwata, H. Yano, and F. Nakaizumi, "Gait master: A versatile locomotion interface for uneven virtual terrain," in *Virtual Reality, 2001. Proceedings. IEEE.* IEEE, 2001, pp. 131–137.

[68] R. Boian, M. Bouzit, G. Burdea, and J. Deutsch, "Dual stewart platform mobility simulator," in *Engineering in Medicine and Biology Society, 2004. IEMBS'04. 26th Annual International Conference of the IEEE*, vol. 2. IEEE, 2004, pp. 4848–4851.

[69] H. Schmidt, S. Hesse, R. Bernhardt, and J. Krüger, "Hapticwalker—a novel haptic foot device," vol. 2, no. 2. ACM, 2005, pp. 166–180.

[70] P. Lum, D. Reinkensmeyer, R. Mahoney, W. Z. Rymer, C. Burgar *et al.*, "Robotic devices for movement therapy after stroke: current status and challenges to clinical acceptance," *Topics in stroke rehabilitation*, vol. 8, no. 4, pp. 40–53, 2002.

[71] M. Coscia, G. Galardi, V. Monaco, S. Bagnato, and S. Micera, "Evaluation of leg joint trajectories while carrying out passive manipulation by neurobike," in *Engineering in Medicine and Biology Society (EMBC), 2010 Annual International Conference of the IEEE.* IEEE, 2010, pp. 2267–2270.

[72] V. Monaco, G. Galardi, M. Coscia, D. Martelli, and S. Micera, "Design and evaluation of neurobike: A neurorehabilitative platform for bedridden post-stroke patients," 2012.

[73] V. Monaco, G. Galardi, J. H. Jung, S. Bagnato, C. Boccagni, and S. Micera, "A new robotic platform for gait rehabilitation of bedridden stroke patients," in *Rehabilitation Robotics, 2009. ICORR 2009. IEEE International Conference on.* IEEE, 2009, pp. 383–388.

[74] T. Teranishi, I. Kondo, S. Sonoda, Y. Wada, H. Miyasaka, G. Tanino, W. Narita, H. Sakurai, M. Okada, and E. Saitoh, "Validity study of the standing test for imbalance and disequilibrium (side): Is the amount of body sway in adopted postures consistent with item order?" *Gait & posture*, vol. 34, no. 3, pp. 295–299, 2011.

論 文 目 録

氏 名　　邸 霈

（発表した論文）

	論 文 題 目	公表の方法及び時期	著 者
	Ⅰ．学会誌等		
1	Robust Model-Based Online Fault Detection for Mating Process of Electric Connectors in Robotic Wiring Harness Assembly Systems	Control Systems Technology, IEEE Transactions on, vol. 18, pp. 1207-1215, 2010.	Jian HUANG Pei DI Toshio FUKUDA Takayuki MATSUNO
2	Vision-Force Guided Monitoring for Mating Connectors in Wiring Harness Assembly Systems	Journal of Robotics and Mechatronics, vol. Vol.24, No.4, pp. 666-676, 2012, February 6, 2012	Pei DI Fei Chen Hironobu SASAKI Jian HUANG Takayuki MATSUNO Toshio FUKUDA
3	Human-Walking-Intention-Based Motion Control of an OmniDIrectional-Type Cane Robot	Mechatronics, IEEE/ASME Transactions on, vol. 18, pp. 285-296, 2013.	Kohei Wakita Jian HUANG Pei DI Kosuke SEKIYAMA Toshio FUKUDA
4	Optimized Motion Control of an Intelligent Cane Robot for Easing Muscular Fatigue in the elderly during Walking	Journal of Robotics and Mechatronics, Vol.25 No.6, 2013, pp.1070-1077.	Pei DI Jian HUANG Shotaro NAKAGAWA Kosuke SEKIYAMA Toshio FUKUDA
	Ⅱ．国際会議		
1	Motion Control of Intelligent Cane Robot under Normal and Abnormal Walking Condition	RO-MAN, 2011 IEEE, 2011, pp. 497-502.	Pei DI Jian HUANG Kosuke SEKIYAMA Toshio FUKUDA
2	A Novel Fall Prevention Scheme for Intelligent Cane Robot by using a Motor Driven Universal Joint	Micro-NanoMechatronics and Human Science (MHS), 2011 International Symposium on, 2011, pp. 391-396.	Pei DI Jian HUANG Kosuke SEKIYAMA Toshio FUKUDA
3	Optimal Posture Control for Stability of Intelligent Cane Robot	RO-MAN, 2012 IEEE, 2012, pp. 725-730.	Pei DI Jian HUANG Kosuke SEKIYAMA Shan He Shotaro NAKAGAWA Fei Chen Toshio FUKUDA

論 文 目 録

氏 名　　邸 霈

（発表した論文）

	論　文　題　目	公表の方法及び時期	著　　者
4	Real Time Posture Control for Stability Improvement of Intelligent Cane Robot	Micro-NanoMechatronics and Human Science (MHS), 2012 International Symposium on, 2012, pp 346-351	Pei DI Kosuke SEKIYAMA Jian HUANG Shotaro NAKAGAWA Fei Chen Toshio FUKUDA
5	Fall Detection and Prevention in the Elderly based on the ZMP Stability Control	IEEE Workshop on Advanced Robotics and its Social Impacts (ARSO), 2013.pp.82-87	Pei DI Jian HUANG Shotaro NAKAGAWA Kosuke SEKIYAMA Toshio FUKUDA
6	Real-Time Fall and Overturn Prevention Control for Human-Cane Robotic System	International Symposium on Robotics(ISR), 2013, CD-Rom, (2003.12)	Pei DI Jian HUANG Shotaro NAKAGAWA Kosuke SEKIYAMA Toshio FUKUDA
7	Fall Detection for the Elderly using a Cane Robot based on ZMP Estimation	Micro-NanoMechatronics and Human Science (MHS), 2013. MHS 2013. International Symposium on, 2013, pp. 48-53.	Pei DI Jian HUANG Shotaro NAKAGAWA Kosuke SEKIYAMA Toshio FUKUDA
	ＩＩＩ．その他		
1	Motion Control of Omni-directional Type Cane Robot based on Human Intention	Intelligent Robots and Systems, 2008. IROS 2008. IEEE/RSJ International Conference on. IEEE, 2008, pp. 273-278.	Jian HUANG Pei DI Toshio FUKUDA Takayuki MATSUNO
2	Study of Fall Detection Using Intelligent Cane Based on Sensor Fusion	Micro-NanoMechatronics and Human Science, 2008. MHS 2008. International Symposium on. IEEE, 2008, pp. 495-500.	Jian HUANG Pei DI Kohei Wakita Toshio FUKUDA
3	Control of Intelligent Cane Robot Considering usage of Ordinary Cane	RO-MAN, 2013 IEEE, pp. 762-767.	Shotaro NAKAGAWA Pei DI Jian HUANG Kosuke SEKIYAMA Toshio FUKUDA
4	Winner of category 2a: Autonomous Micro Robot Maze Competition	17th International Micro Robot Maze Contest, 9 November, 2008	Pei DI D. KATO Zhiguo LU